UNIVERSITÀ DI PARMA

UNIVERSITA' DEGLI STUDI DI PARMA

DOTTORATO DI RICERCA IN
Scienze del Farmaco, delle Biomolecole e dei prodotti per la Salute

CICLO XXXII

Sphingosine-1-phosphate (S1P)/S1P$_1$ receptor axis in macrophages: role in atherogenesis and inflammation

Coordinatore:
Chiar.mo Prof. Marco Mor

Tutore:
Chiar.ma Prof.ssa Ilaria Zanotti

Co-Tutore:
Chiar.mo Prof. Jerzy-Roch Nofer

Dottoranda:
Dott.ssa Enrica Scalera

Anni 2016/2019

"La vie n'est facile pour aucun de nous.

Mais quoi, il faut avoir de la persévérance, et surtout de la confiance en soi.

Il faut croire que l'on est doué pour quelque chose, et que, cette chose,

il faut l'atteindre coûte que coûte."

Marie Curie

Table of Contents

Introduction

1. Sphingosine 1-phosphate (S1P)

1.1. Production and metabolism

Sphingolipids (SLs) constitute an essential class of lipids present in all eukaryotic cell membranes. Traditionally, SLs have been brought into conjunction with the modulation of the membrane formation or the energy metabolism[1]. However, over the last three decades, various studies regarding SLs metabolism suggested that some metabolites, including ceramide (Cer), sphingosine (Sph) and sphingosine-1-phosphate (S1P) play a role as bioactive signaling molecules involved in the regulation of signal transduction [2].

Sphingolipid biosynthesis is driven by common *de novo* and salvage pathways and occurs in the endoplasmic reticulum (ER)[3]. Here, *de novo* synthesis begins with the condensation of serine and palmitoyl-coA to produce 3-keto-dihydrosphingosine, catalyzed by serine palmitoyltransferase (SPT). Subsequently, several enzymatic reactions follow in order to produce ceramide, which is a hub of the SLs metabolism. This molecule is usually transported into the Golgi apparatus and it is metabolized to generate complex sphingolipids, such as the sphingomyelin (SM) and glucosylceramide (GluCer). Furthermore, Cer can be produced by a stepwise degradation of complex sphingolipids in lysosomes or by the activation of sphingomyelinase (SMase) at the plasma membrane, which metabolizes SM to ceramide[4]. Cer can be broken down by a family member of ceramidases (CDases) that promote the regeneration of sphingoid bases, among which the sphingosine can be recycled in the sphingolipid pathway or phosphorylated to generate S1P[5].

S1P is a small bioactive lipid mediator produced within the cells and classified as a lysophospholipid. Structurally, S1P is composed of one long hydrophobic chain and one phosphoric acid group. It derives from sphingosine, a backbone component of all SLs that is phosphorylated trough a reaction catalyzed by one of two known isoforms of the

sphingosine kinase (SphK-1 and SphK-2). SphK-1 is a cytoplasmic kinase, which binds to plasma membranes, endosomal vesicles and/or phagosomes. By contrast, SphK-2 is predominantly present in mitochondria and nucleus[6].

As for any signaling molecule, S1P levels are tightly regulated by its rapid formation and degradation. The sphingosine portion of S1P can be recycled through Cer after the dephosphorylation reaction carried out by S1P-specific phosphatases (SPP-1 and SPP-2) localized in ER[7] or by broad-specific lipid phosphate phosphatases known as LPPs. Alternatively, S1P can be irreversibly converted to phosphoetanolamide and hexadecenal by the activity of S1P lyase, another ER-resident enzyme [**Figure 1**]. While the S1P levels in intracellular fluids and most tissues are low, probably due to the activation of S1P lyase and phosphatase, they are high in blood and lymph[8]. In this way, the micro-molar S1P gradient of S1P between circulation and tissues is generated, which is crucial for the trafficking control of immune cells such as lymphocytes and hematopoietic progenitors cells[9].

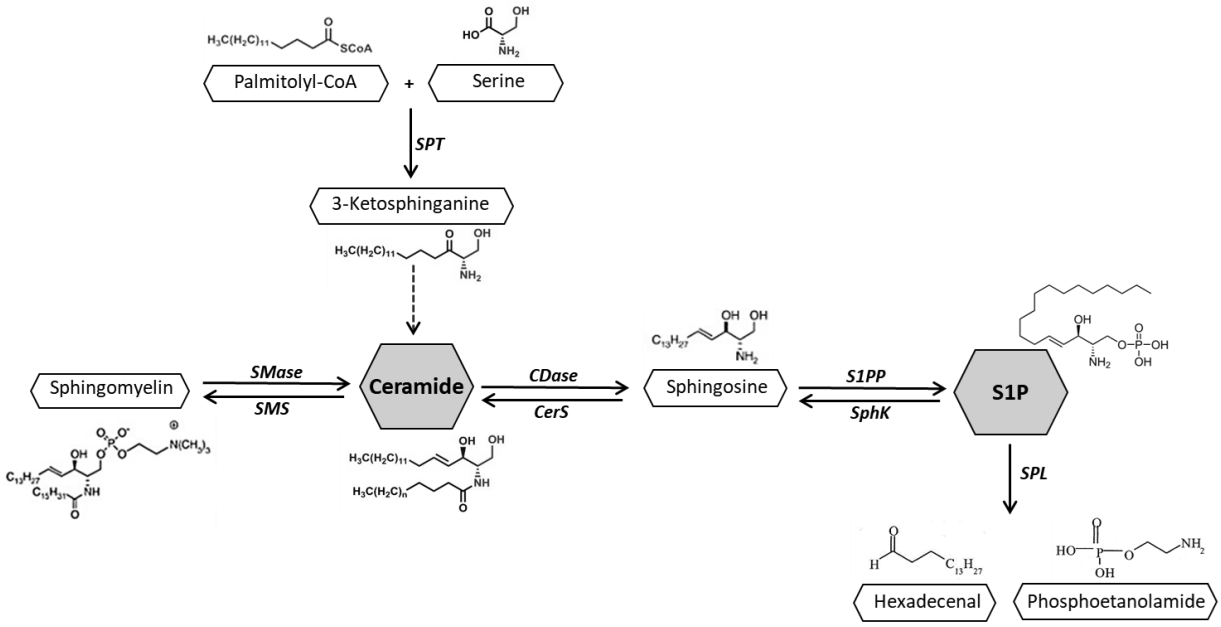

***Figure 1**: **Structure and schematic metabolism of sphingolipids**. SPT*, serin-palmitoyl-transferase; *SMase* sphingomyelinase; *SMS*, sphingomyelin synthase; *CDase*, ceramidase; *CerS*, ceramide synthase; *S1PP*, S1P-specific phosphatase; *SphK*, sphingosine kinase; *SPL*, S1P lyase.

Erythrocytes, platelets and endothelial cells represent the major S1P source to replenish the fast turnover rate in blood.[10] Cells, like macrophages and mast cells, can also contribute to produce S1P[11], albeit to lesser extent. The extracellular secretion of S1P from erythrocytes and platelets is believed to be mediated via several transporters[12]. The major facilitator superfamily transporter 2b (Mfsd2b) is an essential transporter present in erythrocytes and platelets membranes. Recent studies using Mfsbd2b-deficient hematopoietic cells demonstrated that Mfsbd2b pathway contributes approximately half of the plasma S1P pool. As a matter of fact, *Mfsbd2b*$^{-/-}$ mice presented with significantly reduced plasma S1P levels (-42-54%) as compared to WT-values, confirming that Mfsd2b actively exports S1P from blood cells[13]. Nevertheless, platelets do not seem to essentially contribute to the regulation of the circulating S1P concentrations, as mice lacking platelets do not show alterations in the plasma S1P levels[14,15]. This suggests that platelets mainly contribute to the local synthesis of S1P, likely in course of platelet activation[16]. In addition, the ATP-binding cassette (ABC) transporter family may be important for the export of S1P out of cells. This has been emphasized in experiments utilizing mast cells, which release S1P following to activation through ABCC1[11] and independently of degranulation. In concordance with these findings, it has recently been shown that the thrombin-stimulated of S1P secretion from platelets is also mediated by ABC-transporters[17,18]. Moreover, ABCA1 seems to be critical for the effective release of S1P from astrocytes[19].

By contrast, endothelial cells, which contribute approximately 30% to the plasma S1P level, express another specific S1P transporter, namely Spinster-2 (Spns2), which belongs to the Spinster-like family of transmembrane proteins and is able to regulate the energy-dependent secretion of S1P out of the cells.[20]

Due to its hydrophobic nature, S1P is preferentially bound to carrier proteins for its efficient transport and circulation [**Figure 2**]. In plasma, S1P is present at high nanomolar levels (200-

900 nmol/L) and more than the half of S1P is carried by apolipoprotein M (apo-M) in high-density lipoprotein (HDL), the rest being associated with the albumin fraction (30%) and other lipoproteins (10%), such as low-density-lipoprotein (LDL).[21] Apo-M, a small member of lipocalin protein family, is found in a subpopulation of HDL particles and it has been reported as the main S1P binding protein in blood.[22] Actually, apo-M-deficient mice present with a reduction of S1P plasma levels (≈50%), compared to wild type mice[23]. In human plasma S1P content in HDL is almost entirely restricted to the apo-M containing particles[24] constituting the HDL_3 lipoprotein subclass. The plasma apoM concentration in humans is ~0.9 μmol/L. It is speculated that apoM serves as a chaperon protecting S1P from degradation and facilitating its presentation to receptors.

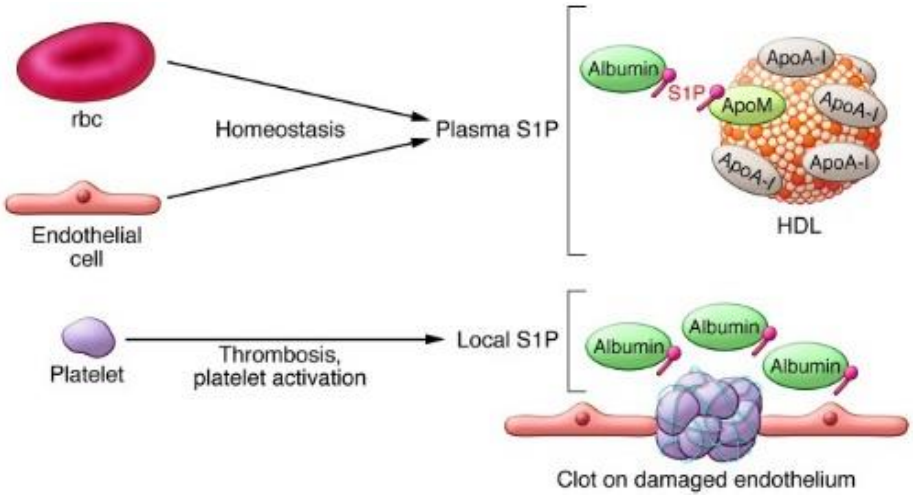

Figure 2**: **Cellular sources of plasma S1P. Endothelial cells and Erytrocytes (Rbc) release S1P, which is picked up and chaperoned by ApoM on the HDL particles and albumin. Chaperone-bound S1P interacts with S1P1 on the endothelial cells to promote vascular barrier function. When endothelial cells are damaged, platelet activation and aggregation release S1P, which leads to local release of S1P that aids in the repair of vascular injury.[6]

There is broad experimental evidence documenting that S1P influences important processes involved in the regulation of inflammation and immune responses[25]. These processes include cell growth in response to external stimuli, differentiation, survival, vascular integrity and suppression of apoptotic process. To date, several studies demonstrated the involvement of S1P in various pathological conditions including multiple sclerosis, inflammation,

atherosclerosis, diabetes and cancer. The molecular background accounting for the diverse roles assumed by S1P in various physiological processes is its dual mode of action: S1P functions not only as an intracellular second messenger, but also as an agonist of five high-affinity G protein-coupled receptors (GPCRs)[26].

1.2. Intracellular and extracellular signaling

1.2.1. Extracellular signaling

The important biological role of S1P is to act as the natural ligand of the endothelial differentiation gene (EDG) family of GPCRs, which are also known as S1P receptors (S1PRs)[27].

So far, five members, $S1P_1$(***EDG1***), $S1P_2$(***EDG5***), $S1P_3$(***EDG3***), $S1P_4$(***EDG6***) and $S1P_5$(***EDG8***), which bind only S1P and dihydro-S1P, have been identified in mammals[28]. The $S1P_{1\text{-}2\text{-}3}$ are ubiquitously expressed in tissues, with the highest levels in cardiovascular and immune systems. $S1P_4$ and $S1P_5$ have lower expression and are mainly present in the lymphatics and in the central nervous system (CNS), respectively[29]. However, among the three ubiquitous S1P receptors, only the deletion of $S1P_1$ leads to embryonic death at day 13. Actually, *S1p1*$^{-/-}$ mice present with a low amount of vascular smooth muscle cells (VSMCs), which leads to a defective vascular maturation and excessive bleeding.[30] By contrast, the deletion of $S1P_2$ and $S1P_3$ is not incompatible with the life, although the offspring is affected from deafness as well as reduced fertility.

The S1P-receptors are coupled to various G proteins classified according to their α-subunit, which leads to activation or inhibition of numerous downstream signaling pathways. In this way, S1P regulates several physiological process such as immunity,[31,32] cell proliferation, wound healing, angiogenesis[33] and vascular maturation[34], in a highly specific manner depending on the relative expression of S1PRs and G proteins. The $S1P_1$ couples exclusively

with $G\alpha_{i/o}$, whereas $S1P_2$ and $S1P_3$ couple with $G\alpha_{i/o}$, $G\alpha_q$ and $G\alpha_{12/13}$ and $S1P_{4\text{-}5}$ with $G\alpha_{i/o}$ and $G\alpha_{12/13}$.

Signaling through $G\alpha_{i/o}$ leads to the activation of several kinases, including the Ras/ERK pathway that enhances proliferation of immune cells, and the phosphatidylinositide 3-kinase (PI3K)/Akt pathway[35], which in turn prevents apoptosis and consequently increases survival of lymphocytes and other immune cells. In addition, $G\alpha_{i/o}$ activates the PI3K/Rac pathway, which is required for cytoskeletal rearrangement and cellular migration. Moreover, the interaction between $S1P_1$ and $G\alpha_i$ inhibits adenylyl cyclase, thus reducing the intracellular concentration of 3',5'-monophosphate (cAMP)[36]. Signaling through $G\alpha_q$ activates the phospholipase C (PLC)[37,38] pathway to increase intracellular Ca^{2+}, whereas the signaling through $G\alpha_{12/13}$ enhances Rho activation to inhibit Rac and, consequently, the cellmigration[39,40]. Each of these S1PRs, when activated, initiates different signaling pathways and cellular responses that are either synergistic or antagonistic **[Figure 3]**.

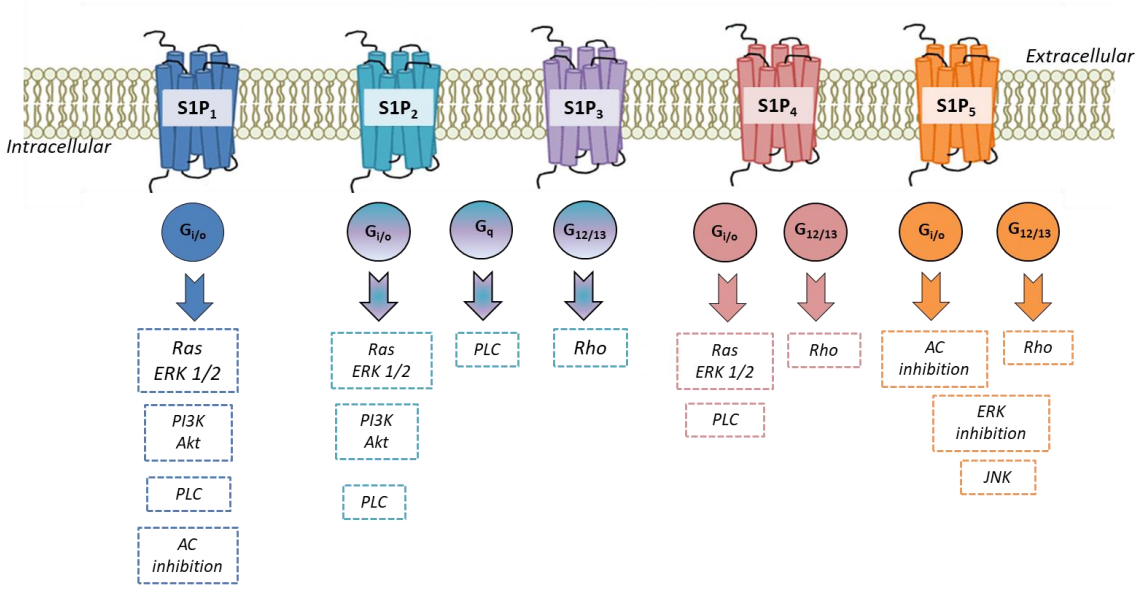

***Figure 3*: *S1PRs family and downstream pathways*.** S1P binds five G-protein coupled receptors which leads the activation or inhibition of the indicated downstream signaling pathway, depending on the coupled Gα subunits. *Abbreviations: ERK=extracellular signal-regulated kinase; PI3K=phosphatidylinositol 3-kinase; PLC=phospholipaseC;AC=Adenylyl cyclase-cyclic AMP; JNK=Jun aminoterminal kinase.[Modified from[41]].*

The S1P receptors present in the vasculature can be briefly characterized as follows:

- **$S1P_1$** is ubiquitously and abundantly expressed in tissues and it was discovered during the study of early genes implicated in endhotelial cell differentiation. Studies conducted with *S1pr1*$^{-/-}$ mouse model clarified the key role of S1P/$S1P_1$ axis in angiogenesis and vascular maturation, endhotelial barrier function and vascular tone[42]. Futhermore, acting via $S1P_1$, S1P interferes with proliferation and immune cell migration. It is expressed by lymphocytes and regulates their egress from secondary lymphoid organs and it has a role in monocytes/macrophages, regulating their recruitment to sites of inflammation. The S1P/$S1P_1$ signaling axis in T-lymphocytes plays a key role in a lymphocyte trafficking also during infection[43]. Further, $S1P_1$ is especially active in areas exposed to low shear stress, which are known to have increased susceptibility to atherosclerosis due to increased exposure time to pro-atherosclerotic molecules[44].
- **$S1P_2$** is also expressed in the endothelial cells and exerts opposite effects on the endothelial barrier as compared to $S1P_1$. It also inhibits cell migration, proliferation and disrupts cell barriers mainly through the activation of Rho GTPase[45]. Several studies elucidated critical roles of $S1P_2$ in angiogenesis and atherogenesis. Double-knock-out $S1P_2$/ApoE mice showed a significantly reduction of atherosclerotic lesion formation compared to control mice. Furthermore, these mice presented less amount of foam cells into the plaques and a higher pro-inflammatory cytokines secretion (IL-8 and IL-1β) in plasma[46]. These results suggested that $S1P_2$ may promote the recruitment of macrophages in the inflammation site, exerting pro-athero- and pro-inflammatory effects. On the contrary, the activation of $S1P_2$ inhibits the SMCs growth in arteries, promoting the expression of different genes able to modulate their differentiation. In this way, S1P may act as a negative modulator of

neointimal formation in arteries. Therefore, $S1P_2$ could produce opposite effects in atherosclerosis development, based on its expression site[47].

- **$S1P_3$** is highly expressed in spleen, kidney, intestine, heart and lung. It mediates cell chemotaxis towards S1P through Rac and PI3K activation[48]. $S1P_3$ is also important for the VEGF-induced sprouting of endothelial cells[49] and regulates coronary flow via activation of Rho in VSMCs[50]. More evidence underlying a pro-inflammatory role of $S1P_3$ was presented in a recent study demostrating that silencing of $S1P_3$ protects mice from developing severe pulonary fibrosis independently of S1P levels in the broncho-alveolar lavage fluid[51]. In addition, the putative role of this receptor in atherosclerosis process was examined in same studies, using *S1p3*$^{-/-}$. $S1P_3$ deficiency reduced the NO production and NO-dependent vasodilation, suggesting that this receptor may serve as an important target-mediator of HDL-S1P *in vivo* effects[52]. However, in double-knock-out mice $S1P_3$/ApoE, the absence of $S1P_3$ did not influence the atherosclerotic lesion size, although the recruitment of monocytes and macrophages to lesion site was reduced. Moreover, monocytes lacking $S1P_3$ presented with a reduction of migration towards inflammation sites and relative secretion of monocyte chemoattractant protein-1 (MCP-1)[53]. At the same time,$S1P_3$ deficiency promoted the neointima formation, suggesting that this receptor could exert pro- and anti-atherogenic effects in macrophages and SMCs, culminating a neutral effect on the atherosclerosis development *in vivo*.

1.2.2. Intracellular signaling

Several pieces of evidence suggested that S1P can function as a second messenger inside the cells, regulating calcium mobilization, cellular proliferation/survival and suppressing apoptosis[54,55]. The intracellular signaling functions of S1P have not been completely

clarified yet, but several effects have been attributed to its capacity to bind and modify functions of various intracellular proteins, including protein kinase C-δ (PKCδ), histone deacetylase (HDAC), prohibitin-2 (PHB2) and TNF receptor-associated factor-2 (TRAF2). The direct interaction of S1P with these intracellular targets has been confirmed in several studies. For instance, it could be demonstrated that S1P is an essential co-factor for the activation of NF-kB triggered by TNFα, which is important for inflammatory and immune processes and anti-apoptotic responses[56]. Indeed, S1P is indispensable for the polyubiquiylation of RIP1 (receptor-interacting serine/threonine-protein kinase-1) by TRAF2, an adaptor protein that binds to SphK1 and stimulates its activity. Moreover, polyubiquiylation of RIP1 prevents its interaction with pro-caspase-8, promoting consequently the inhibition of apoptosis[57].

Another intracellular S1P target, PKCδ is implicated in the endotoxin-induced activation of NF-kB, suggesting the crucial role of this lysosphingolipid in the septic shock[58].

Afterwards, another recent study revealed the role of S1P in the nucleus. SphK2, indeed, is present in the nucleus of many cell types and, through the formation of a repressor complex with histone H3 and HDACs producing S1P. S1P, through its binding with both HDAC1 and HDAC2, regulates the histone acetylation and influences the epigenetic regulation of specific target genes (c-fos, p21)[59,60].

In addition, PHB2, a protein that regulates mitochondrial function and assembly, is able to bind S1P in *vitro* and in vivo. *SphK2*$^{-/-}$ mice showed a reduction of mitochondria respiration which is directly associated with aberrant assembly and lowering activity of complex IV (cytochrome oxidase). These data suggested that the interaction of S1P with PHB2 is important for mitochondrial respiration and cytochrome-c oxidase assembly[61].

Due to the fact that S1P and ceramide are interconvertible metabolites, the "sphingolipid rheostat" concept must be placed in context of intracellular signaling. Pioneering studies *in*

vitro demonstrated the involvement of S1P in the cell proliferation induction and in the suppression of the ceramide-induced programmed cell death[62,63,64]. These studies suggested that the dynamic balance between intracellular levels of S1P and ceramide determines the growth, the survival and the death of the cells[65,66]. SphKs and SPPs, which are key regulators of the sphingolipid rheostat, exert accordingly contrary effects on growth and apoptosis by oppositely modulating intracellular S1P and Cer levels. Of course, the "sphingolipid rheostat" could also affect cell behavior ('sphingodynamics' model) by modulating the concentration of other sphingolipids as well as their localization within the cell and the activation of different enzymes and receptor subtypes[67].

1.3. S1P/S1PRs axis in human disease and pharmacological targets

As summarized above, the SphKs/S1P/S1PRs axis is implicated in many physiological processes, underling its potential role in the pathophysiology of various diseases. The study of S1PR as new promising pharmacotherapeutic targets is an emerging area of research, in particular concerning various aspects of inflammatory cell functions. For instance, the egress of T and B lymphocytes from thymus and secondary lymphoid organs to circulation is promoted by the activation of $S1P_1$. Accordingly, *FTY720* (Fingolimod), a high affinity agonist for all the S1PRs bar $S1P_2$, which promotes specific $S1P_1$ downregulation and degradation in lymphocytes, blocks lymphocytes egress and consequently induces lymphopenia[68] . Similar role has been attributed to $S1P_5$ in the regulation of natural killer cell egress from lymphoid organs[69] as well to $S1P_4$ in neutrophil trafficking[70]. Moreover, S1PRs signaling is also involved in the modulation of circulating monocytes and affects monocytes activation by TNF-α[71].

Another biological function of S1P/S1PRs axis is its ability to modulate cell migration processes by regulating chemotaxis[72,48]. S1P inhibits migration of various tumor cells and

vascular smooth muscle cells (VSMCs),[72,48] but at the same time induces chemotaxis in vascular endothelial cells[73] and T and B lymphocytes. As different cell types, including SMCs and endothelial cells (ECs), express multiple receptors subtypes, the net effect of S1P on migration likely represents the averaged outcome resulting from counteracting signals stemming from both chemoattractant ($S1P_1$ and $S1P_3$) and chemo-repellent receptors ($S1P_2$)[74]. Crucially, S1P/$S1P_1$ axis plays a key role in angiogenesis, a complex process including ECs proliferation and migration. The prominent evidence regarding the *in vivo* angiogenic activity of S1P is a defective vascular stabilization or maturation[75] observed in *$S1p_1^{-/-}$* mice[30] and in conditional $S1P_1$ deficiency in ECs. In addition, S1P regulates vascular tone by acting on either SMCs and ECs through $S1P_1$, $S1P_2$ and $S1P_3$. As a matter of fact, S1P binding to $S1P_1$ and $S1P_3$ stimulates the enzyme eNOS producing NO, which determines the relaxation of SMCs. Furthermore, S1P activates Rho and its kinase via $S1P_2$/$S1P_3$ in SMCs thus promoting the activation of myosin light chain kinase and consequently vascular contraction[76,77].

Numerous studies demonstrated that S1P promotes metastasis, tumor growth and angiogenesis[78]. The overproduction and relatively enhanced secretion of S1P from tumor cells acts in autocrine manner, through the activation of S1PRs, leading to improved tumor cell survival, growth and motility, or in a paracrine manner, promoting neo-angiogenesis and increasing the production of endothelial adhesion molecule[79]. Furthermore, S1P may control resistance of tumor cells to therapy by counteracting the pro-apoptotic effect of ceramide. Several studies suggested the pro-tumorigenic role of $S1P_1$, as a key upstream regulator of STAT-3 (signal transducer and activator of transcription-3), a transcription factor involved in tumor progression[80]. Based on these findings, the main therapeutic approach aiming to regulate the activity of S1P in cancer is based on the removal of extracellular S1P using receptor-active compounds and sphingosine kinase inhibitors[78]. A new monoclonal

antibody, *Sphingomab*, has been developed to sequester extracellular S1P. Preliminary data suggest that *Sphingomab* reduces tumor growth and improves antiangiogenic effects in mice[81,82].

Furthermore, first generation of SphKs inhibitors, such as *Safingol*, are in clinical development, mainly in phase 1 clinical trials. Other promising SphK1-specific inhibitors such as the *SK1-I*, which inhibits the growth of acute myelogenous leukemia and glioblastoma in xenografts, and, the *SK1-II* which enhances the sensitivity of non-small cell lung cancer to chemotherapy, are also under development. The latter inhibitor promotes also the degradation of proteosomal Sphk1 and inhibits the estrogen receptor-stimulated transcriptional activity in human breast cancer cells[83].

In addition to the role in tumorigenesis and angiogenesis, S1P plays a prominent role in inflammatory diseases. In fact, S1P is able to mimic TNF-α in the NF-kB-mediated activation of endothelial cells. Several studies also showed that S1P promotes the production of cyclooxygenase-2 and prostaglandin-E2 (PGE-2) in response to TNF-α[84]. In addition, it has been suggested that SphK1 is a pro-inflammatory mediator in LPS, TNF-α and IL-β signalling[85]. The involvement of S1P/S1P receptors axis in inflammation is confirmed by its key roles in different autoimmune diseases, including rheumatoid arthritis (RA), inflammatory bowel disease (IBD) and multiple sclerosis. In fact multiple sclerosis and RA patients showed high levels of S1P, respectively observed in the cerebrospinal fluid[86] and in synovial liquid[87]. Based on these evidences, several S1P modulators are currently in pre-clinical or clinical steps of drug development, in addition to *FTY720*, which has been approved some years ago for multiple sclerosis patients treatment.[88] These compounds act either as SphKs-inhibitors or as specific S1P receptors agonists and antagonists, such as *Ozanimod* [89,90], *Siponimod* [91] and *KRP-203*[92], or as S1P-lyase inhibitor as *LX3305*[93].

2. Atherosclerosis and inflammation

2.1. Atherosclerosis: an overview

Atherosclerosis is the main pathophysiological cause of coronary artery disease (CAD), peripheral artery disease (PAD) and ischemic stroke (IHD). It is defined a lipid-driven, multifactorial and chronic disease, which affects large and medium-sized elastic and musculature arteries (aorta, iliac artery, carotid, coronary and cerebral arteries), promoting the development of lesions within the arterial wall. The formation of these atheromatous plaques is a consequence of an inflammatory process and ultimately leads to the sudden obstruction of blood flow[94]. The atheroma is characterized by accumulation of macrophages engorged with cholesterol crystals, called foam cells, T-lymphocytes and fibrous elements in the arteries, which protrude in the vessel lumen, causing partial or complete occlusion. Connective tissue production by fibroblasts and deposition of calcium in the lesion cause sclerosis or hardening of the arteries. Rupture of vulnerable plaque can lead to the acute clinical complications of myocardial infarction (MI), stroke and ischemia of the heart or brain[95]. For many years, it was believed that atherosclerosis was a result of the passive accumulation of lipids, in particular cholesterol, in the arterial wall. Over past decades, epidemiological studies have revealed several risk factors associated with atherosclerotic progression, which were classified into two main groups: **non-modifiable** and **modifiable** risk factors. The former includes age, race, ethnicity and genetic factors (family history), whereas the latter comprise two subgroups:

- behavioral risk factors such as unhealthy diet, physical inactivity and tobacco smoking;
- metabolic disorders including hypertension, obesity, diabetes mellitus, and dyslipidemia.

These subgroups of risk factors are strongly linked to each other because the long-term exposure to one or more of behavioral risk factors leads to metabolic alterations[96].

More recently, several inflammatory biomarkers have been associated with the increased cardiovascular risk suggesting that inflammation plays a prominent role in the pathogenesis of atherosclerosis[97]. Patients presenting with higher levels of acute phase proteins C-reactive protein (CRP) or fibrinogen[98], showed an increased incidence morbidity and mortality related to CVD[99]. Moreover, several studies suggested that other circulating pro-inflammatory mediators in addition to CRP have been related to an increased risk of CVD. These include among others serum amyloid A (SAA), soluble intercellular adhesion molecule type-1 (sICAM), selectins (such as P-selectin) as well as cytokines and chemokines (TNF-α, IL-6, IL-8, MCP-1)[100].

Currently, growing epidemiological evidences suggest that atherosclerosis is not an unavoidable degenerative consequence of ageing, but rather a chronic inflammatory condition that can be converted into an acute clinical event through plaque rupture and thrombosis[101].

2.2. Current theories regarding the development of atherosclerotic lesions

As mentioned above, the development of atherosclerotic lesion in the arterial wall, known as "atherogenesis", begins in the *tunica intima*, a layer comprehending the luminal endothelium and the underlying connective tissue. The intima consists of a monolayer of endothelial cells (EC) and few smooth muscle cells (SMCs) and acts as a semipermeable barrier separating arterial wall from circulating blood. An internal elastic lamina separates the intima from *tunica media*, an ordered structure of contractile SMCs layered within elastic fibers and collagen. Finally, an outer layer of loose connective tissue, called *adventitia*, encircles the media. It consists mainly of nerves, lymphatic vessels, fibers, fibroblasts and mast cells. Notably, the healthy intima is avascular and thus dependent on the adventitial lymphatics and blood vessels[102,103].

The early stages of atherogenesis commence when the functional injury to the intimal endothelial barrier is induced by various factors, such as noxious substances or altered hemodynamic forces[104]. As response to this dysfunction, ECs produce inflammatory mediators including cytokines and promote increased expression of leukocytes adhesion molecules on the arterial endothelium, such as intracellular adhesion molecule-1 (ICAM-1), vascular cell adhesion molecule-1 (VCAM-1), as well as selectins P- and E. Moreover, this process involves a decreased ECs ability to release nitric oxide (NO), and additional substances that cooperate to prevent adhesion of immune cells such as monocytes and T-cells to the endothelium[105]. Consequently, T-cells and monocytes are recruited from the blood circulation to the vessel intima. In addition, plasma lipoproteins, mainly apoB-rich lipoprotein such as low-density lipoproteins (LDLs) and remnants of very low density lipoproteins (VLDLs) start to accumulate at the site of atherosclerosis-prone regions[106,107]. Once infiltrated into the tunica intima of the vessel wall, monocytes differentiate into

macrophages and cholesterol-containing lipoproteins undergo different modifications, including oxidation and glycosylation, which alter their properties and trigger pro-inflammatory responses. Within the intima, oxidized LDLs, following the fragmentation of the apo-protein part (apoB), lose the capacity to interact with the conventionally endocytic LDL-receptor (LDLR). They are rather recognized by macrophages scavenger receptors, such as CD36 and SR-AI, which are not able to limit the internalization of lipids within the cells[108,109]. This leads to lipid overhang, which triggers fatty streaks formation. Moreover, oxLDL upregulate the expression of arginase I (Arg-1) in the intima of endothelial cells, blocking in this way the synthesis of NO, a potent vasodilator with anti-atherogenic properties[110]. The accumulated mononuclear phagocytes ingest ox-LDL and became cholesterol-laden foam cells, which aggregate to form the early atherosclerotic plaque, named "fatty streaks". Lesion macrophages display a reduced migration ability, which compromises their capacity to exit from the inflamed plaque and to resolve the ongoing inflammation in the vessel wall. In fact, the apoptosis follows in macrophages-rich region of early lesions, but the mechanisms of their death are partly still unknown[111]. Several studies showed that in this context, the apoptosis process is related with smaller plaque progression and lesion size. In fact, apoptotic cells are effectively eliminated by adjoining macrophages in early lesions and therefore the lesion would have scarce inflammatory and post-apoptotic necrotic cells, as well as more efferocytes-derived anti-inflammatory mediators[112,113]. This concept was confirmed in a recent study where, using *C1qa*$^{-/-}$*Ldlr*$^{-/-}$ mice, the appearance of apoptotic macrophages in early lesions increased dramatically targeting the efferocytosis mediator complement component 1q(C1q) in this animal model. This result suggests that the normal paucity of detectable apoptotic cells in early lesions is due to efficient efferocytosis[114], defined as the physiological process through which apoptotic cells are recognized and internalized by phagocytic cells, including macrophages.

On the other hand, monocytes, due to the continues migration and subsequently differentiation in macrophages, are able to promote the progression of atherosclerotic disease, leading from an early to more advanced plaques. In this pathological condition, further immune subgroups of cells and SMCs are involved in the inflammatory process.

SMCs migrate from the media layer of the arterial wall to the intima and their proliferation is stimulated by many factors such as platelet-deriver growth factor (PDGF). In the advanced plaques, activated macrophages amplify the ongoing inflammatory response trough the secretion of pro-inflammatory mediators, including cyto and chemokines, reactive oxygen species (ROS) and ECM-degrading matrix metalloproteinase (MMP). Under these conditions, lesions show marked disruption of the normal structural organization of the arterial wall. The hallmark of advanced plaque is the appearance of a large pool of extracellular lipids, named "lipid core", in the deep intima. This is accompanied by a dramatic increase in size and number of cholesterol crystals in the core areas. Many of the cholesterol-laden foam cells eventually die, causing the accumulation of necrotic debris and apoptotic bodies, which triggers the formation of a "necrotic core" in advanced plaque[115]. In fact, an important cause for this sequence of events is thought to be the apoptosis and secondary necrosis of foam cells and SMCs[116,117]. In human lesions, apoptotic cells are visible during the lipid accumulation[118] and consequently, cell death, both apoptotic and in other forms, can be detectable at the margin of the necrotic core[119]. Moreover, the presence of free apoptotic bodies inside the lesions, not associated with phagocytic cells, indicates that their impaired removal (efferocytosis), contributes to the growth of the necrotic core[120,121]. In a more advanced plaques, macrophages and foam cells are specialized in apoptotic cells clearance and scavenging in a microenvironment, where efferocytosis is compromised. In fact, when cells undergo apoptosis, they release different molecule, known as "find me" signals, which are able to recruit phagocytes. One of them is the lipid

lysophosphatidylcholine, which is formed through the caspase-3-activated phospholipase A2. Additionally, apoptotic cells could also express other set of molecules, named "find me" which are upregulated or translocated to the surface to promote to simplify interactions with phagocytes. Genetic and experimental data suggest that efferocytosis could depend on the quality of positive (eat me) and negative (find me) signals, undergoing programmed cell death. A deficiency of efferocytosis may contribute to lipid mediator imbalance as well as increased plaque necrosis, through a post-apoptotic secondary necrosis[122], and prevention of dying cell clearance[123]. In term of mechanism, the reduced efferocytosis may depend on the suppression or decreased expression of several molecules that mediated the interaction between apoptotic and phagocytic cells, including Gas6 and MFG-E8[124]. Gas6, binding TAM family of receptors (Tyro-3-Axl-MerTK), plays a crucial role in this process. In particular, it has been demonstrated that its depletion leads to the accumulation of apoptotic cells, to the extension of necrotic core and, as a consequence, to increase of the size of plaque[125]. Likewise, the two functions of LXR, that are the inflammation regulation and the ability to respond to phagocytosed lipids, are accountable to modulate macrophages responses to particular phagocytic contexts. In fact, LXR is activated by the phagocytosis of apoptotic cells, likely through the accumulation of membrane-derived cholesterol. LXR in turn is able to activate transcription of MertK[126], thereby providing positive feedback to promote further clearance, as well Abcg1 and Abca1 activation to promote efflux of the excess cholesterol[127]. Nevertheless, LXR activated in response to apoptotic cells is also able to suppress the production of inflammatory mediators. In addition, the lack of LXR promotes inflammation process and impaired efferocytosis[126].

Although growing atherosclerotic plaques may reduce the vessel volume, they often remain asymptomatic for years, which hinders the timely diagnostics of the condition. At later stages, SMCs produce extracellular matrix rich in proteoglycan, elastin and collagen that

leads to the formation of a fibrous cap between the lipid core and endothelium, which is considered to exert a protective effect against plaque rupture[128]. A reduction in clearance of apoptotic bodies promotes several process that can contribute to unstable plaque and the thrombus formation[129] [**Figure 4**].

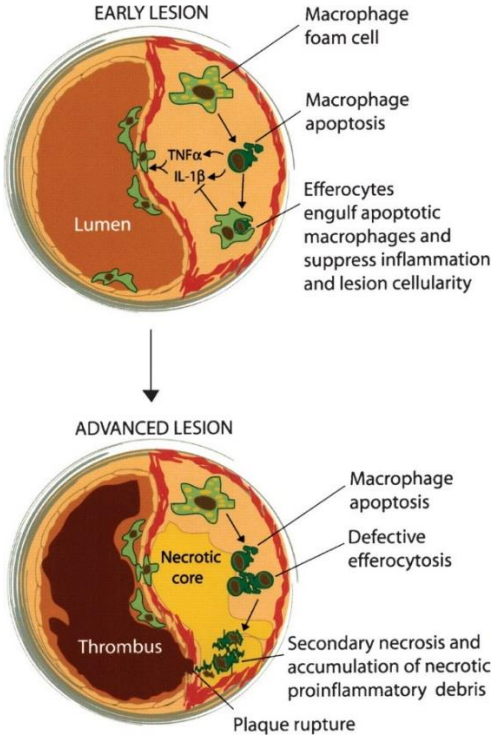

Figure 4: Schematic representation of functional consequences of macrophages apoptosis in early and advanced lesion[130].

The primary danger comes from a secondary necrosis process, through which the apoptotic cells, not removed by efferocytosis, contributes to the growth of the necrotic plaque of atheroma. The interaction of macrophages with necrotic cells amplified the inflammatory response, through higher secretion of pro-inflammatory cytokines (TNF-α, IL-12) and consequently decreased anti-inflammatory cytokines release (IL-10, TGF-β)[131].

All these processes promote an unstable plaques development, in which the fibrous cap is not well-developed and which tend to rupture thus exposing the atherosclerotically altered intima to the circulating blood[132]. Notably, the lipid content and the necrotic cell debris exert a pro-thrombotic action and contribute to the platelet adhesion and activation, which

stimulates the further recruitment of platelets to eventually form a thrombus[133,]. After that, thrombus may lead to myocardial infarction, an obstruction of blood flow in lower extremities (peripheral vascular disease) and to ischemic stroke[134]. However, the mechanisms involved in plaque rupture are still unknown, although coronary spasm is suspected. In older individuals, the calcium-mineral nodules (micro-calcification), generating after the calcification of osteoblast-like cells stimulated by TGF-β1 and 25-hydroxycholesterol[135], have been suggested as a rare cause of coronary thrombosis in highly calcified and tortious arteries. Notably, vascular calcification, as opposed to bone formation, appears to be triggered and not inhibited by inflammation[136]. For all these reasons, in research and clinical practice, it is important to characterize atherosclerosis and consequently the individual plaques for a few measurable characteristics that convey the status of the disease and risk of progression. Several variables can be used as end points for clinical trials and some terms have been adopted to characterize the severity and prognosis of atherosclerotic plaques. The plaque vulnerability describes the short-term risk of developing symptomatic thrombosis[137], the activity may refer to one of different process that characterize the progression, whereas the burden explains the extent of disease[138].

2.3. Key cells in atherosclerosis: monocytes recruitment versus macrophages proliferation

Several studies demonstrated that the areas of intimal thickening harbor a dynamic population of innate and adaptive immune cells, including macrophages and dendritic cells. This implies that a continuous recruitment of immune cells to the lesion area amplifies the first step of inflammatory reaction and alter the metabolism of the resident arterial wall cells[139].

The adhesion of leukocytes on the endothelial surface represents a multistep process, which involves capture, selectin-dependent rolling and activation by endothelial chemokines, firm adhesion mediated by integrins and finally trans-endothelial migration[140]. In response to different stimuli mentioned above, ECs expresses P-, L- and E-selectins trough which leukocytes could adhere to the endothelium, via its ligand P-selectin glycoprotein ligand 1 (PSGL-1). Further on, leukocytes, in particular monocytes, can perform a firm adhesion through the interaction between different cell adhesion molecules (CAMs) and the corresponding leukocytes cell membrane proteins. In particular, VCAM-1 interacts with very late antigen-4 (VLA_4)[141] and ICAM-1 binds lymphocytes function-associated antigen-1 (LFA-1)[142]. Finally, the migration of leukocytes (*diapedesis*) into the intimal space is mediated by the interaction between different chemokines, such as IL-8, RANTES and CXCL1, and their receptors, CCR2, CCR5 and CX_3CR1[143]. In *Apoe*$^{-/-}$ mice, for example, the inhibition of these pathways generated a protective effect, reducing atherosclerotic plaque growth[144]. Once reaching atherosclerotic plaques, macrophage-colony stimulating factor (M-CSF) and additional endothelial cell-derived cytokines, promote monocytes differentiation into tissue macrophages[116].

2.3.1. Monocyte subsets in atherosclerosis

Monocytes are the most abundant cell population among immune cells present in atherosclerotic plaques. They have a pivotal role in the pathogenesis of atherosclerosis, especially because they give rise to tissue macrophages, which are non-stop accumulating in atheroma or sites prone for atherosclerotic lesion formation[145]. There are two different subsets of monocytes, which are traditionally distinguished based on their surface markers and migratory properties[146]. Pro-inflammatory Ly6C^{high} (lymphocyte antigen 6 complex) monocytes, known as *classical monocytes*, are able to be recruited and efficiently infiltrate

the sites of inflammation because they express more functional PSGL-1 than Ly6C^{low} monocytes[147]. They are characterized by CCR2^{+}CX3CR1^{low} antigen expression pattern in mice and CD14^{high} or CD14^{+}CD16^{+} in humans, and they used both of these receptors to enter atherosclerotic lesions[148]. Ly6C^{high} monocytes are also believed to give rise to the classically activated, pro-inflammatory M1-like macrophage phenotype. On the other hand, CCR2^{low}CX3CR1^{high} monocytes in mice or CD14^{dim} monocytes in humans, are known as Ly6C^{low} or *nonclassical monocyte*s that patrol blood vessels in homeostatic conditions and are responsible for the resolution of inflammation. In the sites of inflammation, they turn into alternatively activated, anti-inflammatory M2-like macrophages[149]. During hypercholesterolemia, the numbers of Ly6C^{high} monocytes increase, whereas nonclassical monocytes population remains unchanged[147]. Importantly, Ly6C^{high} monocytes recruited to injured myocardium or allergic skin are able to give rise to M2-macrophaes phenotype[150,151] thus challenging the paradigm that these cells are the sole precursors of M1-macrophages. The recent study demonstrated that the infiltration of Ly6C^{high} monocytes into atherosclerotic plaque and their differentiation of M2-macrophages is a pre-requisite for the effective plaque regression[152].

2.3.2. Macrophage subsets in atherosclerosis

Macrophages are the prominent cellular contributors to the early plaque development and play pivotal roles at all stages of its progression[153]. In mice with the M-CSF deficiency resulting in the impaired differentiation of monocytes into macrophages, the atherosclerotic development is delayed[154]. Several studies demonstrated that the inflammatory phenotype of macrophages influences the atherosclerotic plaque stability[155]. Macrophages subtypes are divided into classically activated pro-inflammatory M1 and alternatively activated anti-inflammatory M2 macrophages[156]. The former are most often triggered by Toll like receptors

ligand (TLR) and interferon-γ (IFN-γ), a cytokine produced by T-helper lymphocytes (Th1), which were both identified in the plaque shoulder regions. M1-macrophages generated in this process are able to secrete pro-atherogenic cytokines, such as IL-1β, IL-6 and TNF-α[157], largely responsible for the potentiation of inflammatory response and finally the lesion destabilization[158,159]. This has been clearly demonstrated in mice deficient in TNF-α or IL-1β that showed a reduced progression of atherosclerotic lesions and a decreased VCAM-1 and MCP-1 expression leading to attenuated monocyte recruitment into the atherosclerotic lesion area[160,161]. On the other hand, the M2-macrophages are induced in response of several Th2-lymphocytes cytokines, such as IL-4, IL-5, IL-13 and TGF-β[162]. When activated, these macrophage subtype secretes anti-inflammatory cyto/chemokines such as IL-10, IL-1RA, and CCL17,CCL22 and CCL24[163]. M2-macrophages are associated with the resolution of acute inflammation, tissue repair and, during a chronic condition like atherosclerosis, produce lesion stabilization. Moreover, these cells display a high phagocytic activity and are able to express several scavenger receptors[164]. To date, through different *in vitro* studies, the M2-macrophages are sub-classified into four different subtypes, based on gene expression pattern and activation stimuli. For instance, M2a macrophages, induced by IL-13 and IL-4, express high levels of CD206 and secrete IL-1RA. M2b macrophages can be induced by TLR signaling and IL-1R ligands and produce high amounts of both pro- and anti-inflammatory cytokines (IL-10, IL-6, TNF-α)[165]. M2c cells, promoted by IL-10, have a strong anti-inflammatory properties trough the production and secretion of TGF-β, IL-10 and PTX3[166]. Moreover, this subtype cells showed a high expression of MerTK and for this reason, they are considered as a professional efferocytes[167]. The last M2-subtype macrophages, named M2d, present a low expression of CD206 and a suppression of Dectin-1. In contrast, these cells express high levels of IL-10, VEGF and iNOS, low level of TNF-

α and mildly elevated levels of Arg-1. These macrophages play a key role in tumor progression and atherosclerotic plaque growth, through their angiogenic properties[168].

In addition, four additional macrophages phenotypes were specifically identified in human atherosclerotic plaque, namely M(Hb)-, Mhem-, Mox- and M4-macrophages[169]. M(Hb)-macrophages are present in the hemorrhagic sites of human atherosclerotic plaque and they play a role in hemoglobin clearance process. They exert several anti-inflammatory properties, increasing IL-10 secretion, reducing ROS production and inducing cholesterol efflux. M(Hb)-macrophages are $CD163^+$ $CD206^+$ and present a resistance to foam cell formation[170].

Macrophages give rise to Mhem-phenotype upon exposure to heme and they are also able to reduce levels of oxidative stress and lipid accumulation. Moreover, they are resistant to foam cells formation through ATF-1 signaling, which promotes LXR-β and induces other genes implicated in cholesterol efflux, such as ABCA1 and LXR-α[171,172].

The accumulation of phospholipids oxidation products in atherosclerotic lesion leads to a development of Mox-macrophages. This process affects the expression of redox regulatory genes, in particular the transcription factor Nrf2[173]. Moreover, Mox-macrophages are characterized by a reduction of chemotactic and phagocytic capacities, but they produce some inflammatory cytokines like COX-2 and IL-1β[174].

Finally, M4-macrophages are induced by exposure to CXCL4[175] and they completely lack phagocytic capacities and show a pro-inflammatory phenotype similar to M1 macrophages. The presence of M4-macrophages within the intima and the media is significantly associated with plaque instability[176].

2.4. HDLs and their role in atherosclerosis

HDLs are a heterogeneous class of lipoproteins particles characterized by a small size (diameter: 12nm), high density (>1.063 g/ml) and the highest amount of proteins (called apolipo-proteins). Several epidemiologic studies revealed that HDLs are an important protecting factor against CVD in humans, as demonstrated by an inverse relationship between HDL-cholesterol (HDL-C) levels and cardiovascular morbidity[177]. Indeed, HDLs play a pivotal role in reverse cholesterol transport (RCT), a physiological mechanism allowing the un-esterified cholesterol to be transported from the peripheral tissues to the liver for the excretion with bile[178]. The first step of RCT consists in a cholesterol efflux from plaque to plasma lipoproteins, mediated by macrophages presents in atheroma[179]. Cholesterol efflux is dependent on cholesterol amount in macrophages, on the expression of cholesterol transporters and on different lipid composition of HDL. In addition, atheroprotective effects is partly modulated by the other biological activities of HDLs, that are independent from the RCT, such as countervailing the oxidation of LDL, inhibition of inflammation, platelet activation, apoptosis of ECs and thrombosis, which may also aid to prevent atherosclerosis[180].

Recent clinical trials targeting HDL cholesterol failed to show clinical benefits in term of cardiovascular risk reduction, suggesting that other HDL components instead of cholesterol may account for anti-atherogenic effects attributed to these lipoproteins[179]. Overall these functions are carried out by a direct interaction of HDL particle or its components, including Apo-AI or S1P, with receptors (such as ABCA1, SR-BI, $S1P_1$, $S1P_2$, $S1P_3$) localized on the cell surface followed by generation of intracellular signals[181]. Several studies demonstrated the HDL's ability to bind to plasma membrane and to generate a number of signaling cascades to promote among others cholesterol efflux process. More specifically, apoA-I binds to ABCA1 and activates phosphatidylcholine lipases, which activate PKC promoting

the mobilization of cellular cholesterol from intracellular stores to the plasma membrane. Additional HDL-induced signaling pathways which play a role in an increase of cholesterol and lipid efflux are represented by protein kinase A (PKA)[182], cell division control protein 42 (Cdc42)[183] and Janus kinases-2 (JAK2) cascades. HDL-induced cell signaling trough ABCA1 suppresses anti-inflammatory M1 macrophages activation and promotes M2 macrophages phenotype and relative anti-inflammatory cytokines secretion trough JAK2 and STAT3 activation[184]. Moreover, in the last years it was demonstrated that the apoA-I:JAK2:ABCA1 axis was able to suppress the endothelial cells inflammation through the activation of COX-2, which promotes an increase of PGI_2 levels[185]. Additionally, HDL was demonstrated to exerts endothelial protective effects through the activation of additional signaling pathways. The PI3K/Akt pathway triggered through the $S1P_1$[186], SR-B1 and $S1P_3$,[187] may be involved in the inhibition of TNF-α-dependent activation of endothelial cells, leading to the decreased expression of adhesion molecules on the endothelial surface[188]. Recently, an high expression of VCAM-1 and ICAM-1 has been discovered in SR-B1 deficient *Ldlr*$^{-/-}$ mice on the coronary artery endothelium, suggesting the key role of SR-B1 signaling pathway into the regulation of adhesion molecules expression in vivo[189]. HDL particles also carry microRNAs, among which miR-223 is highly related to inflammation. It has been demonstrated that anti-inflammatory property of HDL can be attributes in part to its ability to transfer miR-233 to endothelial cells to target and inhibit ICAM-1 mRNA[190].

Furthermore, several studies showed HDL ability to protect endothelial cells from apoptosis induced by ox-LDL of growth factor deprivation[191,192]. Through the PI3K/Akt activation and phosphorylation of Bcl-2 protein, HDL inhibits different cell events implicated in the activation of mitochondria-dependent apoptosis, including caspase-3 and -9 activation, cytochrome C release and a stimulation of cytoplasm Ca^{2+} production[52].

Several studies *in vivo* and *in vitro* suggested that anti-inflammatory effects of HDL could be related to its content of lysosphingolipids, including S1P. For instance, HDL-associated S1P reduced the expression of VCAM-1 and ICAM-1 in response to TNF-α. In this way, the penetration of monocytes and lymphocytes across endothelial barrier could be reduced[193,194]. Moreover, in macrophages, HDL-S1P attenuated the pro-inflammatory signaling of toll-like receptor-2 (TLR2) and this was accomplished, through the reduction of cytokine production and secretion[195]. Furthermore, HDL-associated lysosphingolipid prevented endothelial apoptosis and promoted endothelial proliferation and migration[52,187]. Recent studies demonstrated that the amplification of S1PRs mediated signaling, through the administration of FTY720 or KRP-203, reduces pro-inflammatory macrophage activation in mice. Moreover, this amplification promoted a reduction of pro-inflammatory cytokines secretion in plasma, including IL-6, TNF-α and IFN-γ, facilitating, in this way, the development of M2 macrophage phenotype[196,197]. Nonetheless, HDL-mediated atherosclerotic protection is largely associated with potent anti-inflammatory effects exerted by these lipoproteins[198].

2.5. S1P/S1PRs axis and atherosclerosis

As extensively explained in the previous chapter, HDL is a macromolecular complex that comprises several components, which could directly account for its atheroprotective potential. In the last decades, *in vitro* and *in vivo* studies identified several anti-atherosclerotic effects modulated by HDL-associated S1P and dependent on the S1P receptor and the cell type involved[199]. $S1P_{1-3}$ are abundantly expressed in cardiovascular system and could play a role in the pathogenesis of atherosclerosis. In fact, HDL/apoM-bound S1P has been found to exert protective effects in the vasculature and low S1P levels have been reported in patients with coronary artery disease and myocardial infarction[200,201]. However, several studies regarding the role of S1P in the atherosclerotic process in animal models, led

to controversial results. For instance, administration of FTY720 or KRP-203 in *Ldlr*$^{-/-}$ or *ApoE*$^{-/-}$ mice led to a reduction of atherosclerotic lesion size[202,203]. Consistent with these results, the amount of pro-inflammatory cytokines in these mice decreased in response of TLR4 and TLR3 stimulation, indicating the suppression of the M1 macrophages phenotype[204]. In addition, KRP-203-treatment reduced T-cells activation in peripheral organs, with a simultaneous lowering of pro-inflammatory cytokines in the blood as well as in the aortic wall[197]. Likewise, high levels of endogenous S1P, obtained through the depletion of SKII and S1P-lyase in hematopoietic cells, reduced atherosclerosis in *Ldlr*$^{-/-}$ mice[205,206]. Conversely, the deletion of $S1P_1$ in endothelial cells or macrophages enhanced plaque development in *Ldlr*$^{-/-}$ or *ApoE*$^{-/-}$[207].

HDL-S1P is able to stimulate migration and survival of endothelial cells through the activation of $S1P_{1-3}$ signalling[208]. At the same time, $S1P_{1-3}$ activation stimulate eNOS release, NO production which causing vasodilation[209,210]. Furthermore, in *S1P$_3$/ApoE* double knock-out mice, presented a reduction of monocytes/macrophages amount in the atherosclerotic lesions[53]. However, the absence of $S1P_3$ enhanced the SMCs content and neointima formation in a mouse model of carotid artery ligation[211].

Aim

Epidemiological studies unequivocally point to HDL as the potent plasma-born atheroprotective factor in humans[212]. Its anti-atherogenic potential is attributed to the capacity of cholesterol transport from peripheral macrophages to liver, with the subsequent excretion and thereby the reduction of cholesterol depositions in atherosclerotic lesions. In addition to mediating lipid efflux, HDL also acts on macrophages and T-cells as an anti-inflammatory factor[213,214]. For instance, HDL was shown to reduce NF-kB activation and pro-inflammatory cytokines (TNFα, IL-6) production in macrophages exposed to TLR-2 and -4 agonists and these effects were at least in part attributed to the HDL-mediated cholesterol efflux and the resulting reduction of cholesterol in plasma membranes[215,216].

HDL is composed of different proteins and lipid species exerting potentially atheroprotective effects. Several pieces of evidence suggest that some of the potentially anti-atherogenic constituents of HDL belong to the family of lysosphingolipids characterized by the absence of an acyl group at the sphingosine backbone nitrogen[217,218,219]. Recent studies indicate that HDL-associated lysosphingolipids actively contribute to the anti-inflammatory effects of HDL, among others preventing endothelial apoptosis[52] and the generation of reactive oxygen species[211], promoting vasodilation and stimulating endothelial proliferation and migration[187,209]. In addition, S1P, the most prominent biologically active lysosphingolipid present in HDL correlates with HDL-C in a concentration range in which HDL effectively protects against atherosclerosis. Conversely, a decreased HDL-bound S1P levels were noted in patients with coronary artery disease and myocardial infarction[220,201].

Current evidence supporting the notion that S1P, acting as a constituent of HDL, exerts anti-atherogenic effects derives primarily from experiments *in vitro*, whereas findings in animal models of atherosclerosis are scares and partly discrepant[42]. In particular, the use of pharmacological agonists for amplification of S1P signaling is hampered by poorly defined side effects[206,243]. In addition, several investigations suggest that S1P exert an anti-

inflammatory effect in macrophages, for example by preventing macrophage activation or promoting the secretion of anti-inflammatory cytokines[221]. However, the evidence regarding anti-atherogenic effects of HDL-associated S1P in macrophages remains controversial. More specific approaches focusing in the endogenous S1P signaling are necessary to demonstrate *in vivo* beneficial effects of this sphingolipid on atherosclerosis and inflammation and to delineate the role of macrophages. Nevertheless, the S1P receptor subtype mediating the atheroprotective effects of S1P and the underlying molecular mechanisms remain enigmatic.

Therefore, the aim of this study was to provide more insights of the impact of S1P/$S1P_1$-receptor axis in atherosclerotic disease, using $S1P_1$ knock-in transgenic mouse model capable to overexpress this receptor in macrophages and/or monocytes (*S1p1-LysMCre* or *S1p1-F4/80Cre*).

To this purpose, several *in vivo* analysis have been conducted in order to get insights into molecular mechanisms underlying anti-atherogenic effect of $S1P_1$ receptor. Multiple *in vitro* experimental approaches were used to understand the effect of S1P signaling on the known atherosclerosis relevant functions of macrophages, such as polarization, apoptosis and innate activation.

Materials and Methods

3. Animal models and experimental design

S1p1$^{f/stop/f}$ on B6 background (referred to as *S1p1-KI*) was generated by GenOway by knocking in the floxed murine *S1p1* transgene into ES cells. Briefly, the murine $S1P_1$ cDNA controlled by the synthetic CAG promoter was engineered to contain a neomycin-stop cassette between promoter and the cDNA. Hence, the $S1P_1$ cDNA is only expressed following Cre-mediated removal of the cassette. The construct was introduced into the Rosa 26 locus using the GenOway proprietary targeting vector. To achieve $S1P_1$ overexpression in monocytic cells, *S1p1*$^{f/stop/f}$ were crossed to B6.129P2-*Lyz2*$^{tm1(cre)Ifo}$/J mice (Jackson Laboratories)[222] or B6.129P2-*Adgre1*$^{tm1(cre)Kpf}$ (Klaus Pfeffer, University of Düsseldorf, Germany)[223] to yield *S1p1*$^{f/stop/f}$-*Lyz2*$^{tm1(cre)Ifo}$/J mice (referred to as *S1p1-LysMCre*) or *S1p1*$^{f/stop/f}$-*Adgre1*$^{tm1(cre)Kpf}$ (referred to as *S1p1-F4/80Cre*). Animals were maintained in individually ventilated cages under a 12-h light/12-h dark cycle with free access to water and regular chow diet (66% carbohydrate, 12% fat, 22% protein).

Female *LDL-R*$^{-/-}$ mice on a C57BL/6J background[224] were purchased from Jackson Laboratories. To induce bone marrow aplasia, *Ldl-r*$^{-/-}$ mice (6-8 week of age) were exposed to a single dose of 11-Gy total body irradiation, one day before the transplantation. Bone marrow (BM) was isolated by flushing femurs and tibias from female *S1p1-KI, S1p1-LysMCre or S1p1-F4/80Cre* mice with phosphate-buffered saline (PBS) and single-cell suspensions were prepared by passing the cells through a 70µm cell strainer. Irradiated recipients received 5.0 x 10^6 cells by intravenous injection into the tail vein. The hematological chimerism of transplanted animals was determined in genomic DNA from blood leukocytes 4 weeks after transplantation. Thereafter, animals were put on the Western diet (0.25% cholesterol, 21% fat) for 14 weeks. At the end of the treatment, mice were sacrificed by cervical dislocation under anesthesia and tissues were collected for further

analysis. All animal experiments were approved by government authorities in charge of animal protection (LANUV).

4. Histology and Lesion Atherosclerotic Analysis

Atherosclerosis in the aortic root and brachiocephalic artery (BCA) was determined in a blinded fashion[225]. In brief, aortic roots and BCAs were removed under a dissecting microscope, embedded in O.C.T. (ThermoFisher Scientific, Schwerte, Germany) and snap-frozen at -80°C. Cross sectional lesion areas at the aortic root were quantified in five oil red O-stained sections in the region beginning at the end of the aortic sinus and extending to the ascending aorta. In addition, atherosclerotic lesions luminal to the internal elastic lamina were quantified in three oil red O-stained sections per BCA. For both, aortic root and BCA, mean lesion sizes were calculated for each animal.

Macrophage content of lesions and smooth muscle cells were determined by immunohistochemistry using specific antibodies against CD68 (AbD Serotec, Germany) and alpha-actin (Abcam, AB5694-100), respectively.

Total collagen fiber content was analyzed in PicroSirius Red stained sections by polarization microscopy (Zeiss AxioObserver). Movat pentachrome staining to assess lesion quality was performed according to the manufacturer´s protocol (Morphisto, Germany).

All lesions were photographed and analyzed using AxioVision KS400 image analysis (Carl Zeiss Microscopy GmbH, Germany).

5. Isolation of monocytes and macrophages

Monocytes were isolated from mice peripheral blood using EasySep mouse monocyte isolation kit (StemCell Technologies, Köln, Germany) according to the protocol provided by the manufacturer. Briefly, erythrocytes were lysed as described above and remaining white blood cells (1 x 10^8/mL) were resuspended in 0.5 mL PBS containing fetal bovine serum (FBS, 2%, v/v) and 1 mmol/L EDTA. Sample was equilibrated with rat serum, transferred to a polystyrene tube and incubated for 5 min at 4°C with a selection cocktail. Thereafter, RapidSpheres^{TM} were added to the sample for 3 min, the tube was placed in the magnetic separation device (StemCells Technologies), and the suspension enriched in monocytes was decanted, washed in PBS, and used for further analysis. The monocyte content of the isolated cells fraction was controlled by FACS and exceeded 94% in each isolation.

Peritoneal leukocytes were isolated by peritoneal lavage with ice-cold PBS as described previously[202,196]. Cells were suspended in DMEM containing FBS (10.0 % v/v) and 2 mmol/L glutamine and were either used for flow cytometry or seeded in a 12- 24- or 96-well cell culture plate at a required density. After 2h, non-adherent cells were removed and remaining macrophages were harvested and analyzed or used for further experiments.

6. Evaluation of apoptosis and efferocytosis in *vivo* and in *vitro*

6.1 *In vivo* analysis: lesion apoptosis and efferocytosis quantitation

Apoptosis and efferocytosis in the aortic root cryosections were analyzed by confocal immunofluorescence microscopy. Serial 10 μm thick proximal aortic cryosections were stained with TUNEL (Tdt-Mediated dUTP Nick end Labeling) using the TMR red detection kit (Roche) according to the manufacturer instructions. Briefly, sections were fixed with 2% diluted neutral buffered formalin solution, permeabilized with a fresh prepared buffer containing Triton X-100 (0.1% v/v) in sodium citrate (0.1% w/v) and stained with TUNEL TMR red for 1 h at 37°C. Subsequently, sections were blocked with BSA solution (1.0 % v/v in PBS) and then incubated with anti-mouse MOMA-2 rat antibody (1:100 (v/v), Santa Cruz Biotechnology, Heidelberg, Germany), overnight at 4°C. After washing, sections were incubated with goat anti rat IgG DyLight 488 (1:300 (v/v), Novus Biologicals, Centennial, CO) for 1 h at room temperature and protected from light. Slides were mounted with 4′,6-diamidino-2-phenylindole (DAPI) containing mounting media for nuclear counterstaining. Images were acquired using the Leica TCS SP2 confocal microscope (Leica, Wetzlar, Germany), and then processed by at least two different operators using Fiji open-source image processing software[226]. The TUNEL positive nuclei were quantitated and normalized to the lesion area. In lesions where the TUNEL stain was condensed, fragmented, and/or faded, the average area of healthy DAPI-stained nuclei was used as reference to quantitate TUNEL positive signals. The free versus macrophage-associated TUNEL stain in the same sections were quantitated as described[121,227] and accordingly expressed. TUNEL positive nuclei were counted as free when they were not associated with or in close proximity to viable macrophages that were detected as clearly MOMA-2 stained macrophage cytoplasm surrounding a DAPI-stained nucleus.

6.2 *In vitro* analysis

6.2.1 Flow cytometry assessment of apoptosis and efferocytosis

Annexin binding was used as an indicator of macrophage apoptosis. Peritoneal macrophages isolated as described above and seeded in a 24-well plate at a density of 2.5 x 10^5 cells/mL were incubated in DMEM supplemented with FBS (10.0 % v/v) and exposed for 24 h to thapsigargin (0.5 µmol/L) and fucoidan (25 µg/mL) or AcLDL (100 µg/mL) and ACAT inhibitor Sandoz 58-035 (10.0 µg/mL). For determination of the Annexin V binding macrophages were detached from plate by scraping and re-suspended in a buffer containing NaCl (140 mmol/L), Hepes (10 mmol/L) and $CaCl_2$ (2.5 mmol/L). Annexin V-FITC (Bender Med-Systems Diagnostics, Vienna, Austria) was added for 30 min at room temperature according to the supplier instruction. Flow cytometric measurements of Annexin V binding were performed on CyFlow Space flow cytometer (Sysmex Partec).

Necrotic cells were detected by counterstaining with propidium iodide (PI). For the assessment of efferocytosis, RAW 264.7 murine macrophages were seeded onto 6 well plate at the density 1 x 10^6 cells/well. Adherent cells were labelled with calcein-AM (1.0 µmol/L, BioLegend) for 30 min and washed twice with PBS to remove dye excess. Apoptotic cells were generated by incubating RAW 264.7 cells with staurosporine (10.0 µmol/L) in serum-free DMEM for 16 - 18 hours. Under these conditions the efficiency of apoptosis exceeded 90% as tested by Annexin-V staining. Apoptotic cells were collected by scraping, washed in PBS, and re-suspended in serum-free DMEM (1 x 10^6 cells/mL).

Peritoneal macrophages were isolated as described above, seeded on 12-well plate at density of 0.5 x 10^6 cells/well, and starved overnight in DMEM containing 0.1% (v/v) FBS. Afterwards, cells were washed with PBS and overlayed with apoptotic RAW 264.7 cells at ratio 1:1 (cell/cell). After incubation for 30 minutes at 37°C, the medium was removed, peritoneal macrophages rinsed twice with ice cold PBS and collected by scraping. The

labelling with the APC-conjugated antibody against F4/80 was performed as described above. The fraction of F4/80$^+$ efferocytotic (calcein-positive) cells was assessed by flow cytometry (CyFlow Space).

6.2.2. Fluorimetric assays for caspases 3 and 12

Peritoneal macrophages exposed to thapsigargin or Ac-LDL were re-suspended in a hypotonic cell lysis buffer, subjected to three freeze/thaw cycles, and centrifuged. Caspase activities were measured in the supernatant, according to the manufacturer protocols, using Ac-DEVD-AFC, LEHD-AFC and ATAD-AFC (380(ex)/500(em) nm), as substrates for caspases-3, -9 and -12, respectively (all from BioVision, Milpitas, CA). Fluorescence was determined using a LS70 spectral fluorimeter (PerkinElmer, Rodgau, Germany). Data were expressed as relative fluorescence units (RFU) adjusted for the sample protein content.

7. Analysis of gene expression by real-time quantitative RT-PCR or microarray and pathway analysis

Total RNA was isolated from peritoneal macrophages or monocytes using Trizol reagent (ThermoFisher Scientific) according to manufacturer protocol. RNA was eluted in RNAse free water and quantified using BioPhotometer (Eppendorf, Hamburg, Germany). The entire cDNA was synthesized from 1.0 µg of total RNA using RevertAid H Minus First Strand cDNA Synthesis Kit (ThermoFisher Scientific). PCR products were detected using ABI7900ht sequence detection system (Applied Biosystems, Darmstadt, Germany) in a 384-well format, using SYBR™ Green PCR master mix (ThermoFisher Scientific). PCR primer sequences are shown in **Table 1**.

Relative gene expression was calculated by applying the $2^{-\Delta\Delta Ct}$ method. Briefly, the threshold cycle number (Ct) of target genes was subtracted from the Ct of GAPDH ($Ct_{housekeeping}$) and raised to the 2nd power of this difference.

Gene	Forward (5'-3')	Reverse (5'-3')
S1p1r	TTCCATCTGCTGCTTCATCATCC	GGTCCGAGAGGGCTAGGTTG
Abca1	GGACATGCACAAGGTCCTGA	CAGAAAATCCTGGAGCTTCAAA
Lxrα	AGGAGTGTCGATTCGCAAA	CTCTTCTTGCCGCTTCAGTTT
Abcg1	CTGAAAAGAATGGGTGTTGG	ACCTGGACAGGAAAGAATCC
ApoE	GTTTCGGAAGGAGCTGACTG	TGTGTGACTTGGGAGCTCTG
Il-5	CTGGCCTCAAACTGGTAATG	TGAGGGGGAGGGAGTATAAC
Arg-1	CGATTCACCTGAGCTTTGAT	AAGCCAAGGTTAAAGCCACT
Pu.1	CCTACATGCCCCGGATGTGC	TGCTGTCCTTCATGTCGCCG
Irf8	AGACCATGTTCCGTATCCCCT	CACAGCGTAACCTCGTCTTCC
Klf4	TCAAGTTCCCAGCAAGTCAG	AAACTTCCAGTCACCCCTTG
Lgmn	TGCTACCAGGAGGCTGTAAC	TTGTCCATGGCCATCTCTAT
Axl-1	GAAGGTCAGCTCAATCAGGA	GTCAGAGCCCTGAAAACAGA
MertK	CGCCAAGGCCGCATT	TCGGTCCGCCAGGCT
Egr1	ACAGCAGTCCCATCTACTCG	CTCCCTGTTGTTGTGGAAAC
C/ebpα	GCGGGAACGCAACAACATC	GTCACTGGTCAACTCCAGCAC
Hmox-1	TGATGGCTTCCTTGTACCAT	CTCGTGGAGACGCTTTACAT
Cd163	GCAAAAACTGGCAGTGGG	GTCAAAATCACAGACGGAGC
Fizz	CCAATCCAGCTAACTATCCCTCC	ACCCAGTAGCAGTCATCCCA
Bcl-6	CACACCCGTCCATCATTGAA	TGTCCTCACGGTGCCTTTTT
Mafb	GAGCGAGCAGAGTTTCAGTC	AGCTTGCTGCTACCTTCTCA
Ym-1	CCAGCAGAAGCTCTCCAGAAGCA	TGGTAGGAAGATCCCAGCTGTACG
Gapdh	CTGGAGAAACCTGCCAAGTA	TGTTGCTGTAGCCGTATTCA
Ccr2	ATTCTCCACACCCTGTTTCG	GATTCCTGGAAGGTGGTCAA
Ccr5	ATCCTGCCTCTACTTGTC	CTCTTCTTCTCATTCCTACAG
Vla4	GTCTTCATGCTCCCAACAGC	ACTTCTGACGTGATTACAGGAAGC
Psgl-1	CTTCCTTGTGCTGCTGACCAT	TCAGGGTCCTCAAAATCGTCATC

Table 1: PCR Primer sequences

For gene expression by microarrays, the peritoneal leukocytes were isolated as described above and seeded on a 24-well plate at density 4 x 10^5 cells/mL. After 2h non-adherent cells were removed and macrophages covered with RNeasy Lysis Buffer (RLT buffer, Qiagen, Venlo, The Netherlands). RNA was isolated using RNeasy Micro kit (Qiagen) according to the instruction of the manufacturer. The concentration and purity of RNA was analyzed on BioPhotometer. RNA integrity was assessed with the Agilent 2100 Bioanalyzer (Agilent Technologies Inc., Palo Alto, California). After cRNA labeling and hybridization to the

Illumina HT-8 expression bead chips, microarrays were scanned on an iScan array scanner (Illumina, SanDiego, CA) and raw array data were processed and background-subtracted in Illumina GenomeStudio. Further analysis was performed using the Chipster open source platform[228]. Expression values were quantile normalized and log2-transformed using the Bioconductor package 'lumi' implemented in Chipster. Statistical comparison between the sample groups was done within Chipster using the empirical Bayes method[229] and the Benjamini-Hochberg (BH) multiple-testing correction of the raw p-values. FDR threshold of 5% ($q < 0.05$) was used for filtering differentially expressed genes.

The microarray data have been deposited in the ArrayExpress database at EMBL-EBI (www.ebi.ac.uk/arrayexpress) under accession number**.**

Pathway analysis[230] to identify enriched pathways and processes was performed online (www.metascape.org), using default parameters. For genes with >2-fold upregulation in S1pr1-LysMCre mice, pathway and process enrichment analysis has been carried out with the following ontology sources: GO Biological Processes, KEGG Pathway, Reactome Gene Sets and CORUM. All genes in the genome have been used as the enrichment background. Terms with a p-value < 0.01, a minimum count of 3, and an enrichment factor > 1.5 (the enrichment factor is the ratio between the observed counts and the counts expected by chance) were collected and grouped into clusters based on their membership similarities. More specifically, p-values were calculated based on the accumulative hypergeometric distribution, and q-values were calculated using the Banjamini-Hochberg procedure to account for multiple testing. Kappa scores were used as the similarity metric when performing hierachical clustering on the enriched terms, and sub-trees with a similarity of >0.3 were considered a cluster. The most statistically significant term within a cluster was chosen to represent the cluster.

For the *in silico* gene expression profiling the ImmGen consortium[231] data and browsers were used, which were developed as an open resource supported by the National Institute of Allergy and Infectious Diseases (Bethesda, MD, www.immgen.org). ImmGen Gene Skyline tool allows extracting the expression profiles of a selected gene in a group of cell types, basing on fully validated microarray datasets. We here searched for Lyz2 (lysozyme) or Emr1 (F4/80) gene expression in "Key populations" data group, or in "Stem and progenitor cells" and "Macrophages (MFs), Monocytes, Neutrophils" for specific subset evaluation. Display settings provide a bar graph with linear scale of expression on x axis and various cell populations on y axis.

8. Western Blotting

Peritoneal macrophages were collected, centrifuged, and lysed on ice in RIPA buffer supplemented with protease inhibitor (Complete, Roche). Protein concentration was estimated for each cell lysate using BCA protein assay (ThermoFisher Scientific). Following protein concentration determination, 40 µg/lane of the prepared protein samples were loaded and run on an SDS-polyacrylamide gel electrophoresis. Thereafter, proteins were transferred onto a PVDF membrane (BioRad Laboratories, München, Germany) which was then blocked 1 hours with 5% non-fat dry milk in Tris-buffered saline containing 0,1% Tween-20 (TBS-T) prior to incubations with antibodies. S1P1/EDG-1 (Novus Biologicals), p-P70S6K (Thr 389, Cell Signaling) and CHOP (9C8, Novus Biologicals) specific rabbit primary antibodies, and an anti-rabbit IgG horseradish peroxidase-conjugated (BioRad Laboratories) were used to incubate the blots. An anti-β-actin-peroxidase antibody (Sigma-Aldrich) and P70S6K (Bio-Techne) were used to visualize actin or p70s6k as a control protein. Antibody binding visualization was obtained by enhanced chemi-luminescence (Western Lightning ECL Pro, Perkin Elmer), according to the manufacturer's instructions.

9. Leukocyte differential count and immunophenotyping

Differential leukocyte count was performed on an automated hematology analyzer (XN1000, Sysmex Deutschland GmbH, Norderstedt, Germany) in a routine hospital laboratory.

Blood and peritoneal leukocytes were immunophenotyped by flow cytometry as described previously. FITC-, PE-, APC-, or APC/Cy7-labeled monoclonal antibodies against surface markers on macrophages (F4/80, MHCII, CD86, CD93, CD206, CD115, Dectin-1, MerTK, AXL-1, CD244, CD226) or monocytes (CCR2, CCR5, PSGL-1, LFA-1, VLA-4, VLA-1) were purchased from ThermoFisher Scientific or BioLegend (Fell, Germany). For each FACS staining 2 x 10^5 cells were incubated with antibody dilutions (0.25 µg for each antibody) in PBS with FBS (1.0 % v/v) for 30 minutes at 4ºC. Cells were fixed for additional 30 minutes with formaldehyde (0.5% v/v). Afterwards, cells were centrifuged for 10 minutes, washed one time in PBS and analyzed on a CyFlow Space flow cytometer (Sysmex Partec, Münster, Germany). For the surface $S1P_1$ detection leukocytes were stained with antibody against EDG1 (1:50, Biorbyt, Cambridge, UK) for 30 minutes at 4°C. After washing, cells were incubated for additional 30 minutes with a secondary antibody (donkey anti-rabbit Alexa Fluor 647, 1:60) and anti-CD11b-PE or anti-F4/80-PE to identify monocytes or macrophages, respectively. Afterwards, cells were analyzed by flow cytometry. For intracellular staining, blood monocytes or peritoneal macrophages were processed using Fix&Perm Cell Permeabilization Kit (ThermoFisher Scientific) following to recommendations of the manufacturer. Briefly, cells were stained with antibodies with CD11b-APCCy7 (for monocytes) and F4/80- APC (for peritoneal macrophages) as described above and incubated in the Fixation Medium (Medium A) for 30 min at room temperature. Thereafter, cells were washed with PBS (1x) and the Permeabilization Medium (Medium B, 2x), resuspended in 50 µl of Medium B, which included antibody against IRF8 (PE-conjugated, 0.25 µg/test, ThermoFisher Scientific) and PU1 (Alexa Fluor488-

conjugated, 0.25 µg/test, Biolegend). The labelling was carried out in room temperature in the dark for 30 minutes. Subsequently, the cells were washed, centrifuged, resuspended in PBS supplemented with FBS (1,0% v/v) and analyzed by flow cytometry as described above.

10. Cyto/chemokines determination

Cytokine (IL10, IL-4, IL-1RA, IL-5) and chemokine (CCL22) levels were quantified in mouse plasmas and supernatants of peritoneal macrophages by commercially available ELISA (Bio-Techne).

11. Flow cytometry assessment of kinase activities

Peritoneal leukocytes were isolated as described above and seeded in a 24-well plate at a density of 4,0 x 10^5 cells/mL. After removal of non-adherent cells macrophages were incubated for 0, 60 or 120 minutes in DMEM containing or not S1P (1.0 µmol/L). Subsequently, cells were fixed with pre-warmed BD Phosflow™ Lyse/Fix Buffer I (BD Biosciences, Heidelberg, Germany) for 15 minutes at 37°C. Cells were detached using cell scraper, washed, and permeabilized for 30 minutes at room temperature with BD Phosflow™ Perm/Wash Buffer I (BD Biosciences). Afterwards, cells were stained with anti-F4/80 (APC- or FITC-conjugated, 5.0 µg/mL), anti-phospho-STAT6 (Tyro 641, PE-conjugated, 0.25 µg/mL), anti-phospho-STAT3 (Tyro 705, Alexa Fluor488 -conjugated, 0.25 µg/mL, all from BioLegend) or anti-phospho-AKT (PE-conjugated, 0.25 µg/mL, Miltenyi Biotec, Bergisch Gladbach, Germany) for 30 minutes at room temperature. After washing macrophages were re-suspended in BD Phosflow™ Perm/Wash Buffer I and analyzed using CyFlow Space flow cytometer (Sysmex Partec).

12. Determination of the cellular cyclic AMP (cAMP) concentration

Quantification of intracellular cAMP was performed using a DetectX Cyclic AMP Direct EIA Kit (Arbor Assays, Ann Arbor, MI), according to the manufacturer instructions. Briefly, peritoneal macrophages were isolated as described above, seeded in a 48-well plate (4.5 x 10^6 cells/mL) and incubated with 3-isobutyl-1 methyl xanthine (IBMX, Sigma Aldrich, 0.2 mmol/L) for 30 minutes. After treatment, cells were exposed S1P (1.0 µmol/L) for additional 30 minutes. Cell media were aspirated, and cells were washed with ice-cold PBS. Adherent cells were treated directly with the sample diluent provided by the manufacturer for 10 minutes at room temperature. Cell lysates were precleared by centrifugation (600 x g, 4°C, 15 minutes) and used for EIA as suggested by the manufacturer. The optical density was determined spectrophotometrically at 450nm (FluoSTAR Optima, BMG Labtech, Ortenburg, Germany). Samples were analyzed in duplicate to ensure consistency of reading.

13. Determination of protein kinase A (PKA) activity

The PKA activity was determined using the PepTag Assay (Promega, Mannheim, Germany) according to the protocol provided by the manufacturer. Briefly, peritoneal macrophages were isolated as described above, seeded on 24-well plate at density of 1 x 10^6 cells/mL and incubated with or without S1P (1.0 µmol/L) for 2 h. The cells were washed and suspended in PKA extraction buffer containing Tris-HCl (25.0 mmol/L, pH 7.4), EDTA (0.5 mmol/L), EGTA (0.5 mmol/L), β-mercaptoethanol (10.0 mmol/L), leupeptin and aprotinin (each 1.0 µg/mL). After homogenization the lysates were precleared by centrifugation (14000 x g, 5 min, 4°C) and incubated with PKA assay buffer, PKA activator (cAMP, 1.0 µmol/L) and PKA substrate (PepTag® Peptide A, 2.0 µg) for 2h at room temperature. The reaction was

stopped by heating the probes (10 minutes, 95°C). Two forms of PKA substrate (phosphorylated and non-phosphorylated) were separated on agarose gel (0,8% (v/v) in 50.0 mmol/L Tris-HCl, pH 8,0) and visualized under UV light. The phosphorylated peptide form was excised from the gel, solubilized using the acidified gel solubilization solution provided by the manufacturer, and its amount was quantified by measuring the absorbance at 570 nm. The negative control containing the PepTag® Peptide A but no kinase was used to determine the exact molar absorptivity of the dye.

14. Cell cholesterol efflux assay

Peritoneal macrophages were seeded in 48-well plates at a density of 3,5 x 10^5 cells/mL and incubated for 24 h in DMEM containing FBS (10.0 % v/v) and 2 mmol/L glutamine. Cells were labeled with 2.0 μCi/mL [1,2-^{3}H]-cholesterol (Perkin Elmer) in DMEM containing FBS (1.0 % v/v) for 24 hours. Subsequently, cells were treated for 18 hours with 22-(R) hydroxycholesterol (22-OH, 5 μg/mL) and 9-cis retinoic acid (9cRA, 10 μmol/L) or desmosterol (50 μg/mL, Biomol, Hamburg, Germany) in DMEM containing bovine serum albumin (BSA, 2.0 % v/v) and the ACAT inhibitor Sandoz 58-035 (2.0 μg/mL) to prevent cellular accumulation of cholesteryl ester. Cholesterol efflux was induced by adding apoA-I (10.0 μg/mL) or HDL (12.5 μg/mL) for 4 hours. Afterwards, 100 μL of efflux medium was added to scintillation vials containing 4 mL of scintillation cocktail (Ultima Gold, Perkin Elmer) and counted for the radioactivity using beta scintillation spectrometer. Total cholesterol was extracted from macrophages with 0.6 ml of 2-propanol. Lipid extracts were dried under N_2, resuspended in 1 ml of toluene, and their [^{3}H]-cholesterol content was quantified by liquid scintillation counting. Cholesterol efflux was expressed as a percentage of the radioactivity released into the medium over the total radioactivity incorporated by cells.

15. Monocytes

15.1 Flow cytometry assessment of VCAM-1, ICAM-1 and P-Selectin binding on monocytes

Whole blood was anti-coagulated with EDTA, erythrocytes were lysed as described above and suspended in PBS. Cells were exposed for 4 h at 37°C to TNFα (20.0 ng/mL, PeproTech, Hamburg, Germany) and then incubated for additional 10 minutes at 37°C with 10.0 ng/mL of recombinant chimera proteins comprising human immunoglobulin Fc region and murine VCAM-1 (VCAM-1/Fc), murine ICAM-1 (ICAM-1/Fc) or murine P-selectin (P-selectin/Fc). All chimeric proteins were obtained from Bio-Techne (Wiesbaden, Germany). After washing, cells were stained with PE-conjugated antibodies against human IgG1 (BioLegend) and APC/Cy7-conjugated antibodies against CD11b (ThermoFisher Scientific). Binding of ICAM-1, V-CAM1 or P-Selectin to monocytes was assessed by flow cytometry (CyFlow Space, Sysmex Partec, Münster, Germany).

15.2 Monocyte adhesion assay

Murine endothelial cell line bEnd.5 was a generous gift of Dr. Sigrid März, Max-Planck-Institute for Molecular Medicine, Münster, and was maintained in DMEM supplemented with glutamine (2.0 %, v/v), sodium pyruvate (1.0 %, v/v), non-essential amino acids (1.0%, v/v), FBS (20.0 %, v/v), and endothelial cell growth supplement (Promocell, Heidelberg, Germany). Monocytes were isolated from mouse blood using EasySep monocyte isolation kit as described above, labeled for 30 min at 37°C with calcein-AM (1.0 µmol/L, Sigma-Aldrich), and added at a number of 10^5 cells/mL to a confluent bEnd.5 monolayer on 8-well chamber slides (ThermoFisher Scientific) for 30 min. under gentle rocking as described previously[232]. Non-adherent cells were removed thereafter by rinsing plates 3 times in PBS and the number of adherent cells was counted (>5 fields per cover slip) under fluorescence

microscope Eclipse Ti (Nikon Instruments Europe BV, Amsterdam, The Netherlands) equipped with a digital camera CoolSNAP HQ2 (Roper Scientific GmbH, Martinsried Germany).

15.3 Monocyte migration assay

Chemotaxis was analyzed as previously described [233]. Briefly, monocytes were isolated from mouse blood using EasySep isolation kit as described above and resuspended in medium at a concentration of 0.5×10^6 cells/ml. Subsequently, monocytes were placed to the upper wells of a 48-well (Boyden) chemotactic chamber (NeuroProbe, Gaithersburg, MD) and allowed to migrate towards RANTES (5.0 ng/mL) or MCP1 (10.0 ng/mL), which were added to the lower wells of the chamber. Upper and lower wells were separated by a polyethylene terephthalate (PET) membrane (pore size 5 μm, Whatman, Dassel, Germany). The cells were allowed to migrate for 90 minutes in a humidified incubator at 37°C. Adherent cells on polycarbonate membrane were fixed for 10 min using absolute ethanol and stained with Giemsa dye. The non-migrated cells from the upper side of the membrane were scraped off gently with a cotton bud. Migrated cells were quantified by counting cells in five high-power fields (20 x primary magnification) of four different wells per condition.

16. Statistical analysis

Data are presented as means ± S.D. for at least three separate experiments or as results representative of at least three repetitions. Comparisons between the means of two groups were performed with Mann-Whitney test. Comparisons between the means of multiple groups were performed with Kruskal-Wallis test or two-way ANOVA. Pairwise post-hoc comparisons were performed with Connover test or Holm-Sidak test. p values less than 0.05 were considered significant.

Results

17. S1pr1-LysMCre and S1pr1-F4/80Cre mice overexpress $S1P_1$ in monocyte/macrophage lineage

To amplify $S1P_1$ signaling in selected target cells, double transgenic mice expressing murine $S1P_1$ in the monocyte/macrophage lineage were constructed by crossing two lines. The *S1pr1-KI* line carries a transgenic cassette in the Rosa 26 locus, which harbors the murine $S1P_1$ cDNA. It is separated from the CAG promoter by a lox-Stop-lox insert (Figure 1A). *S1pr1-KI* mice were either crossed to *LysMCre* or to *F4/80Cre* mice, which express the Cre recombinase under control of the lysozyme M promoter or the F4/80 promoter, respectively. In double transgenic mice, the lox-Stop-lox insert is excised only in Cre-expressing cells, which induces cDNA expression driven by the CAG promoter. *In silico* analysis of the lysozyme M and F4/80 expression patterns using the ImmGen Skyline tool, predicted the highest activity in monocytes, macrophages and neutrophils for the lysozym M promoter and in macrophages for the F4/80 promoter, as shown in Figure 1B.

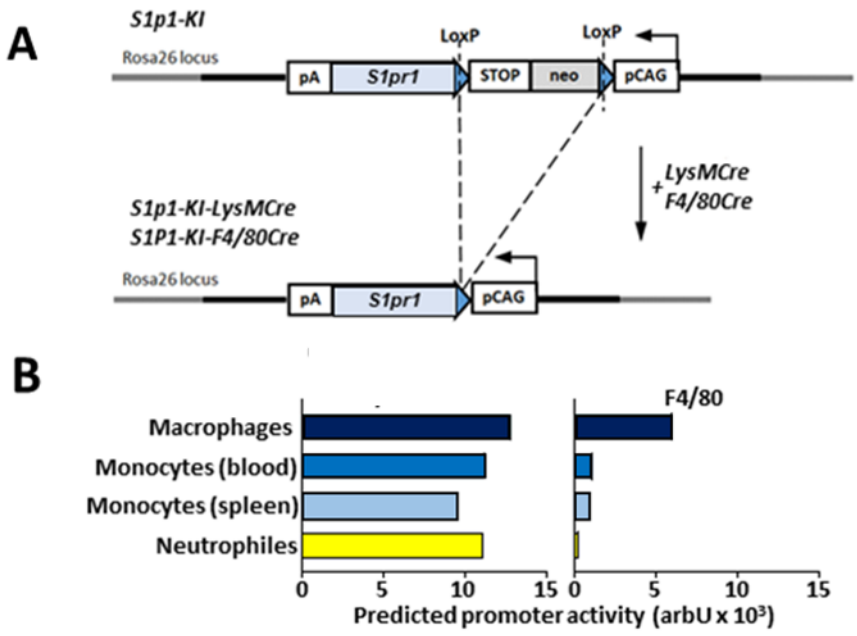

Figure 1. Generation of S1p1-LysMCre or S1p1-F4/80Cre mice and characterization of $S1P_1$ overexpressing monocytes and macrophages - **A**. Schematic representation of the targeting vector prior to (top) and following (bottom) Cre recombinatioan. The excision of a floxed blocking element activates pCAG promoter and produces S1P1 expression **B**. Predicted LysM and F4/80 promoter activities in myeloid cells as determined using the ImmGen Skyline tool.

Consistent with this prediction, enhanced $S1P_1$ expression was observed by RT-PCR and WB in *S1pr1-LysMCre* or *S1pr1-F4/80Cre* mice in peritoneal macrophages (PM), but not in spleen lymphocytes. By contrast, only *S1pr1-LysMCre* but not *S1pr1-F4/80Cre* mice showed increased $S1P_1$ expression in monocytes (Figure 2A). In addition, a 3- to 6-fold increase in $S1P_1$ expression on the macrophage cell surface was noted in both double transgenic lines (Fig. 2B).

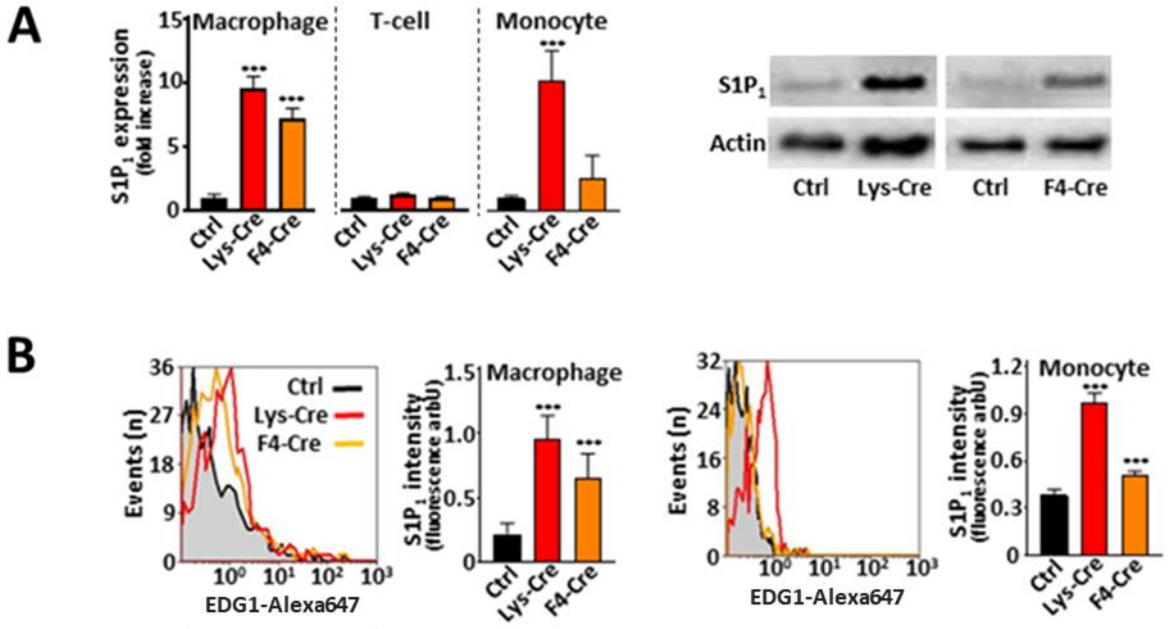

Figure 2. Characterization of S1P₁ overexpressing monocytes and macrophages - **A**. PM were collected from *S1pr1-KI* (Ctrl), *S1pr1-LysMCre* (Lys-Cre) or *S1pr1-F4/80Cre* (F4-Cre) fed Chow diet (ChD). Expression of $S1P_1$ was analyzed by qPCR, in PM, T-cell and monocytes. mRNA levels were normalized to GAPDH. Protein extracts from PM were subjected to Western Blotting with an anti-$S1P_1$ antibody. Blots were stripped and re-probed with an antibody to β-actin. Blots are representative for one experiment out of two. **B.** Cell surface staining for $S1P_1$ was analyzed by flow cytometry. Data represent means ± SD from 8 to 14 determinations. *p<0.05, **p<0.01, ***p<0.001 (Lys-Cre vs. Ctrl or F4-Cre vs. Ctrl).

18. $S1P_1$ overexpression retards atherosclerosis and alters plaque composition

Atherosclerotic lesions were quantified in *Ldl-r*$^{-/-}$ mice transplanted with BM from *S1pr1-KI, S1pr1-LysMCre* or *S1pr1-F4/80Cre* mice and placed on an atherogenic western diet for 14 weeks. Lesion areas were profoundly reduced in aortic roots (~50%) and brachiocephalic arteries (~90%) in *S1pr1-LysMCre* transplanted mice (Figure 3A and B). By contrast, they were modestly reduced in aortic roots and roughly halved in brachiocephalic arteries from *S1pr1-F4/80Cre* chimeras (Figure 3A and B). In addition, necrotic core formation was reduced in *S1pr1-LysMCre* and *S1pr1-F4/80Cre* transplanted mice (Figure 3C). Immunochemical analysis of aortic root lesions yielded an increase of CD68-positive macrophage content in *S1pr1-LysMCre* but not in *S1pr1-F4/80Cre* chimeras (Figure 3D). Conversely, the plaque collagen content as assessed by PicroSirius Red staining was lower in *S1pr1-LysMCre*- but not in *S1pr1-F4/80Cre*-transplanted mice (Figure 3E).

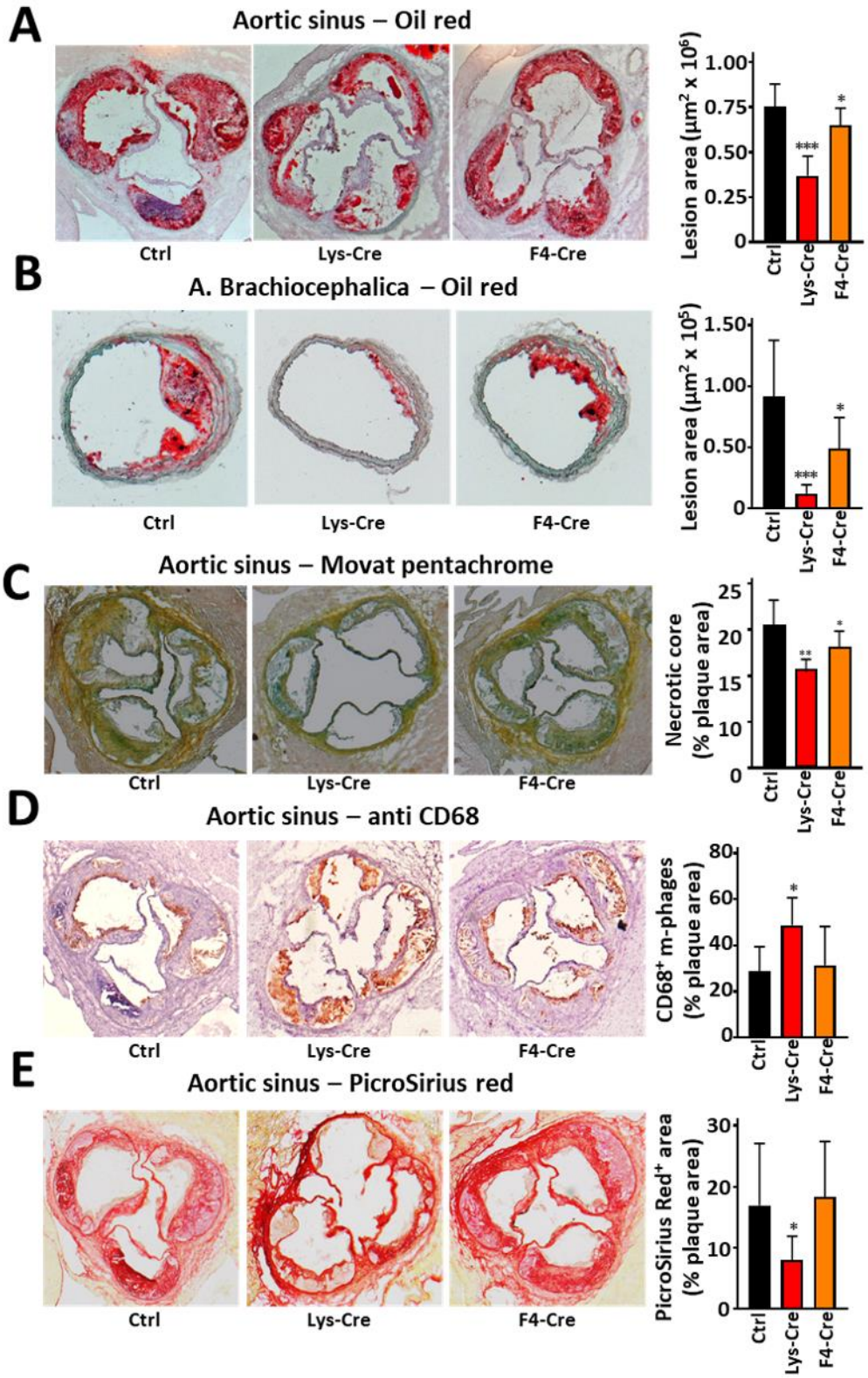

Figure 3. S1P1 overexpression in macrophages and monocytes retards atherosclerotic lesion development and alters plaque morphology in *Ldl-r*$^{-/-}$ mice - Aortic root and brachiocephalic arteries obtained from Western diet-fed LDL-R-/- mice transplanted with S1pr1-KI (Ctrl, n=11), S1pr1-LysMCre (Lys-Cre, n=10) or S1pr1-F4/80Cre (F4-Cre, n=10). **A and B**. Representative Oil Red O stainings of lesions in aortic roots (A) and brachiocephalic arteries (B) and quantification of lesion areas (bar graphs). **C to E**. Photomicrographs showing Movat pentachrome (C), CD68 (D) or PicroSirius Red (E) stainings. Bar graph shows the necrotic core extent or the macrophage or collagen content in plaques expressed as the percentage of lesion area. *p<0.05, **p<0.01, ***p<0.001 (Lys-Cre vs. Ctrl or F4-Cre vs. Ctrl).

19. $S1P_1$ overexpression in macrophages activates PU.1 and IRF8

To characterize the transcriptional response to $S1P_1$ overexpression, gene expression profiling on PM was performed using oligonucleotide microarrays. Expression levels of several genes involved in M2 macrophage polarization were significantly increased in cells from *S1pr1-LysMCre* mice (Figure 4: left graphic). These findings were corroborated in a pathway and process enrichment analysis using Metascape. Upregulated transcripts (≥2-fold) in macrophages from *S1pr1-LysMCre* mice revealed significant enrichment for M2 phenotype-associated functions, such as wound healing. Cell chemotaxis was also identified as the top scoring term in the enrichment analysis (Figure 4: right graphic).

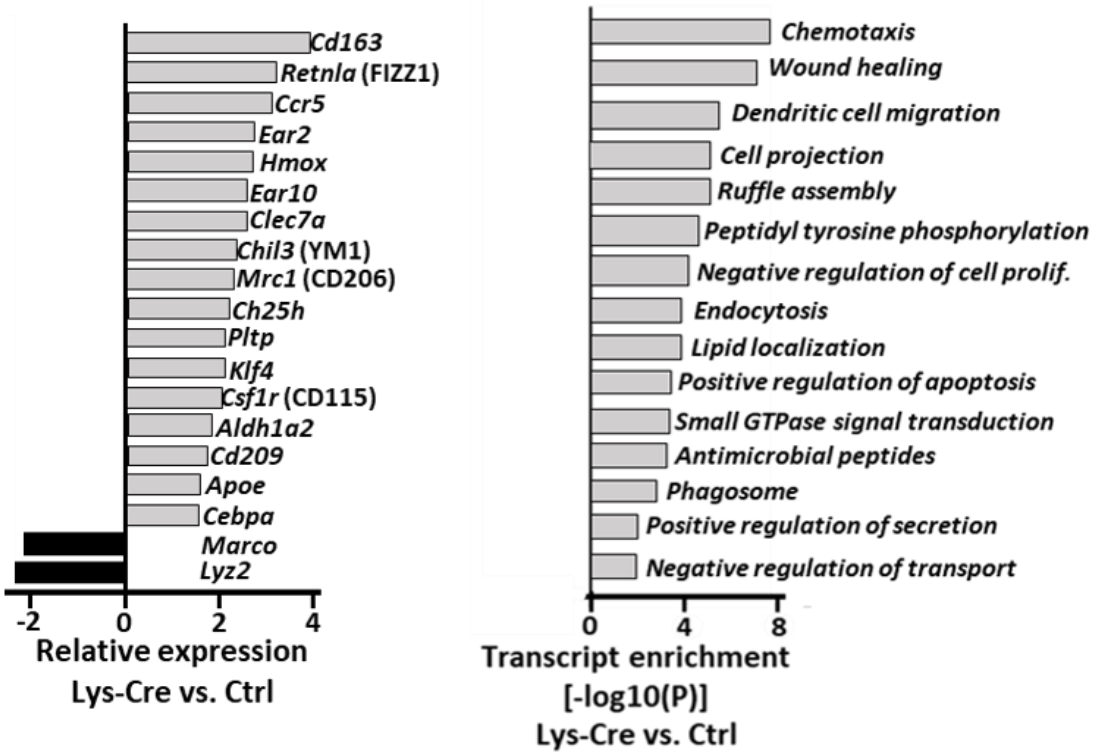

Figure 4. Gene expression in PM from Lys-Cre and Ctrl mice on ChD (n = 5 for each group) assessed with microarrays- Left graphic – gene expression pattern related to macrophage polarization. Note elevated expression of genes controlled by PU.1 and IRF8 (Csf1r, Clec7a, Klf4, Mrc1) and LXR (Pltp, Ch25h, Apoe) in Lys-Cre mice. **Right** graphic – Upregulated transcripts in Lys-Cre mice related to various cell functions.

Since these genes are directly or indirectly controlled by IRF8 and PU.1[234,235], the effect of $S1P_1$ overexpression on these two transcription factors was assessed both in mice fed ChD or WD. mRNA and protein levels of IRF8 and PU.1 were increased in PM from *S1pr1-LysMCre* and *S1pr1-F4/80Cre* mice (Fig. 5A and B). In addition, an elevated expression of several atheroprotective genes coordinately regulated by PU.1 and IRF8[236] was detected in cells overexpressing $S1P_1$ (Fig. 5C).

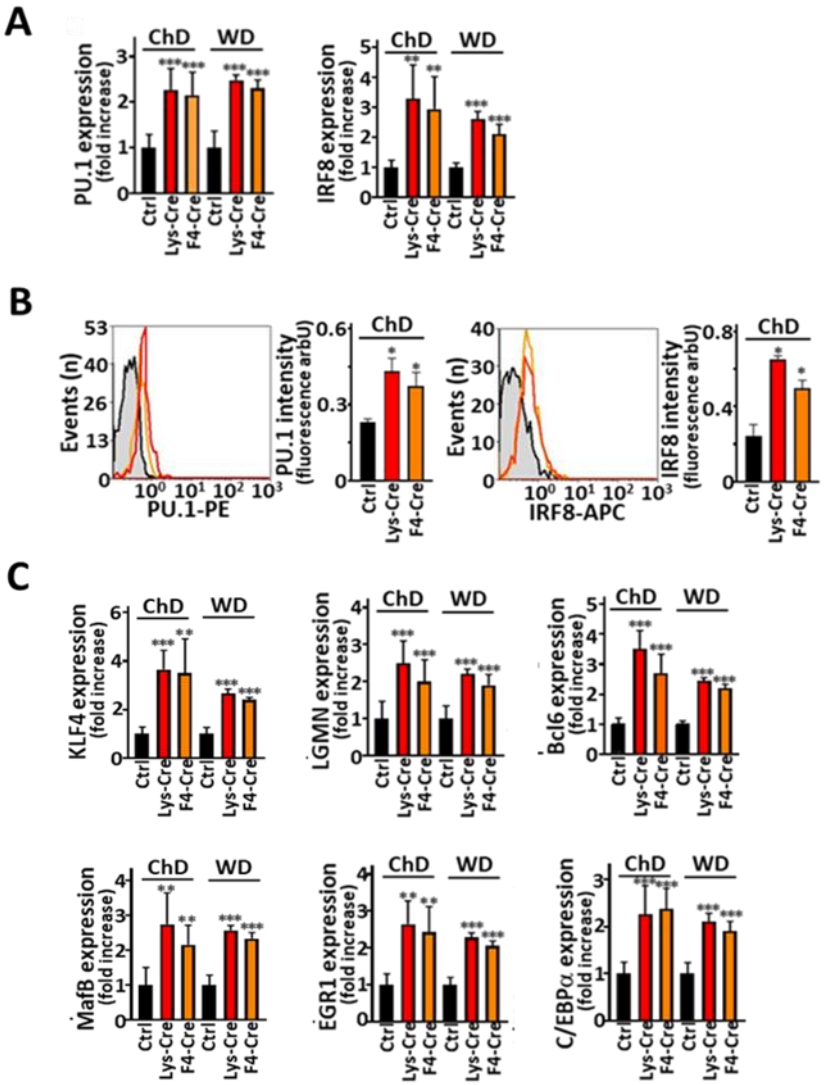

Figure 5. S1P1 overexpression in macrophages enhances expression and activation of PU.1 and IRF8 - PM were collected from either S1pr1-KI (Ctrl, n=10-12), S1pr1-LysMCre (Lys-Cre, n=9-12) or S1pr1-F4/80Cre (F4-Cre, n=10-12) fed Chow diet (ChD) or *Ldl-r*$^{-/-}$ mice transplanted with S1pr1-KI (n=10), S1pr1-LysMCre (n=9) or S1pr1-F4/80Cre (n=9) BM and fed Western diet (WD). **A**. PU.1 and IRF8 expression analyzed by qPCR. mRNA levels normalized to GAPDH and presented relative to S1pr1-KI. **B**. Intracellular staining for PU.1 and IRF8 in macrophages from mice on ChD analyzed by flow cytometry (n= 5 for each group). Bar graphs show fluorescence intensity medians. **C**. Expression of PU.1 and IRF8 signature genes analyzed by qPCR. mRNA levels were normalized and presented as described above. *p<0.05, **p<0.01, ***p<0.001 (Lys-Cre vs. Ctrl or F4-Cre vs. Ctrl).

Notably, $S1P_1$-overexpressing cells showed an increased surface presence of MHC-II and CD115 (Fig. 6A), which promoters are canonical targets of PU.1-mediated transactivation. An increased MHC-II and *CD115* mRNA expression levels were also observed in aortas from these animals (Fig. 6B).

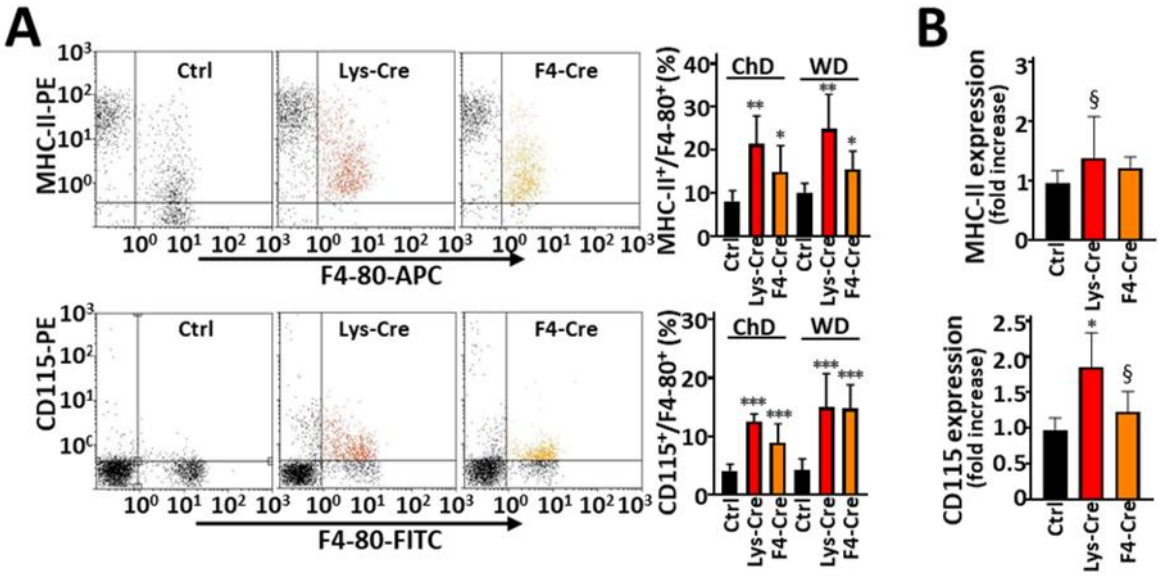

Figure 6. $S1P_1$ overexpression in macrophages enhances expression of MHCII and CD115 **-A**. Cell surface staining for CD115 and MHC-II analyzed by flow cytometry (n=10 for each group). Bar graphs represent percent $CD115^+/F4/80^+$ and $MHC\text{-}II^+/F4/80^+$ macrophages. **B**. CD115 and MHCII mRNA expression in aortas of WD-fed *Ldl-r*$^{-/-}$ mice receiving S1pr1-KI, S1pr1-LysMCre or S1pr1-F4/80Cre BM. §p<0.1, *p<0.05, **p<0.01, ***p<0.001 (Lys-Cre vs. Ctrl or F4-Cre vs. Ctrl).

20. $S1P_1$ overexpression promotes M2 phenotype in macrophages

Transcription factors Klf4 and MafB control the development of the anti-inflammatory M2 phenotype[237,238]. As expression of both was elevated in $S1P_1$-overexpressing macrophages, we next investigated M2 macrophage polarization markers in $S1P_1$-knock-in mice. The enhanced expression of prototypical M2 genes resistin-like α (*Rentla*, *Fizz1*), chitinase 3-like 3 (*Chi3l3*, *Ym1*), hemoglobin scavenger receptor (*CD163*), and heme oxygenase-1 (*HMOX1*) was detected in PM from *S1pr1-LysMCre* and *S1pr1-F4/80Cre* mice (Fig. 7).

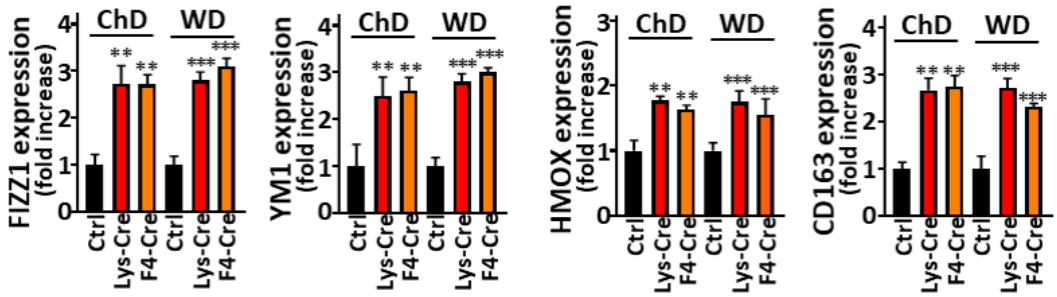

Figure 7. M2 macrophage polarization markers – PM were collected from either S1pr1-KI (Ctrl, n=10-12), S1pr1-LysMCre (Lys-Cre, n=9-12) or S1pr1-F4/80Cre (F4-Cre, n=10-12) fed Chow diet (ChD) or *Ldl-r*$^{-/-}$ mice transplanted with S1pr1-KI (n=10), S1pr1-LysMCre (n=9) or S1pr1-F4/80Cre (n=9) BM and fed Western diet (WD). Expression of M2a signature genes analyzed by qPCR. mRNA was normalized to GAPDH and presented relative to S1pr1-KI. **p<0.01, ***p<0.001 (Lys-Cre vs. Ctrl or F4-Cre vs. Ctrl).

In addition, these cells showed increased expression of the M2a subset marker mannose receptor 1 (CD206). By contrast, M1 polarization markers CD86 and CD93 were downregulated in PM overexpressing $S1P_1$ (Fig.8).

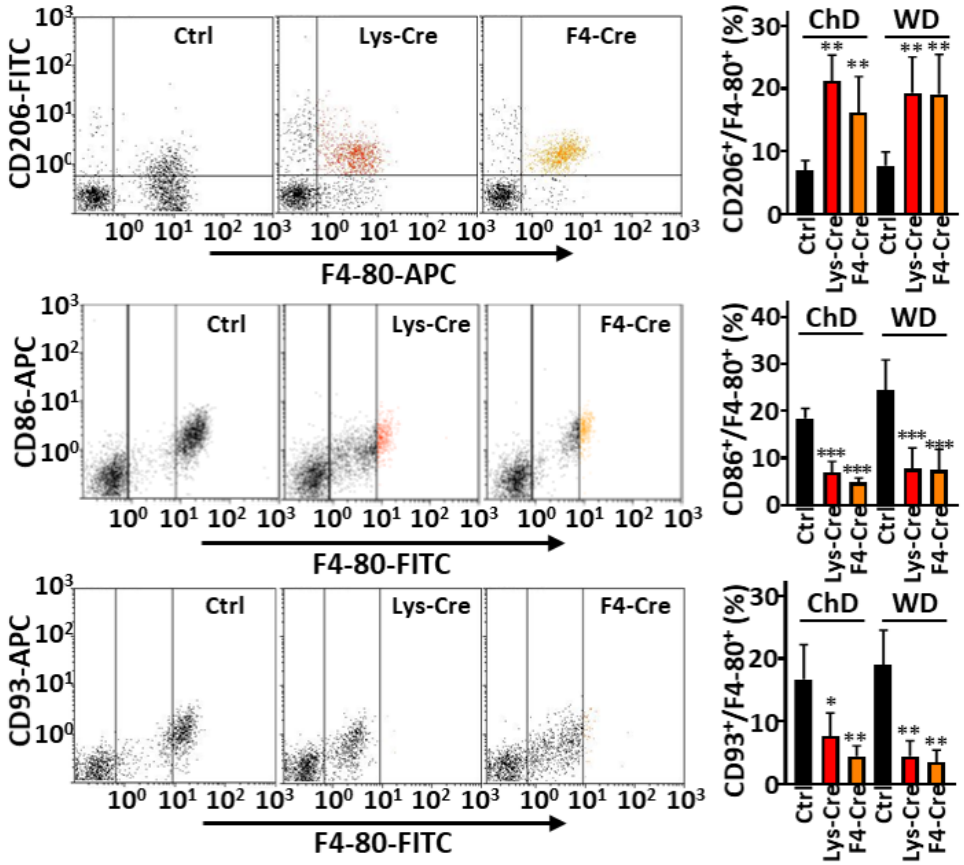

Figure 8. S1P1 overexpression in macrophages promotes M2a functional polarization– Cell surface staining for CD206 (M2a marker) and CD86 and CD93 (M1 markers) analyzed by flow cytometry. Bar graphs representing % of $CD206^+/F4/80^+$, $CD86^+/F4/80^+$ and $CD93^+/F4/80^+$ macrophages. (n=10 for each mouse group fed with different type of diet); *p<0.05, **p<0.01, ***p<0.001 (Lys-Cre vs. Ctrl or F4-Cre vs. Ctrl).

To further elucidate the functional characteristics of PM from *S1pr1-LysMCre* and *S1pr1-F4/80Cre* mice, M2 cytokines were measured in cultured macrophage supernatants. As shown in Figure 9, production of IL-10, IL-1RA and IL-4 was increased in PM from *S1pr1-LysMCre* and *S1pr1-F4/80Cre* mice both on Chow and Western diet. In parallel, an elevated plasma levels of IL-10, IL-1RA and IL-4 were detected in mice on Western diet (Fig.9).

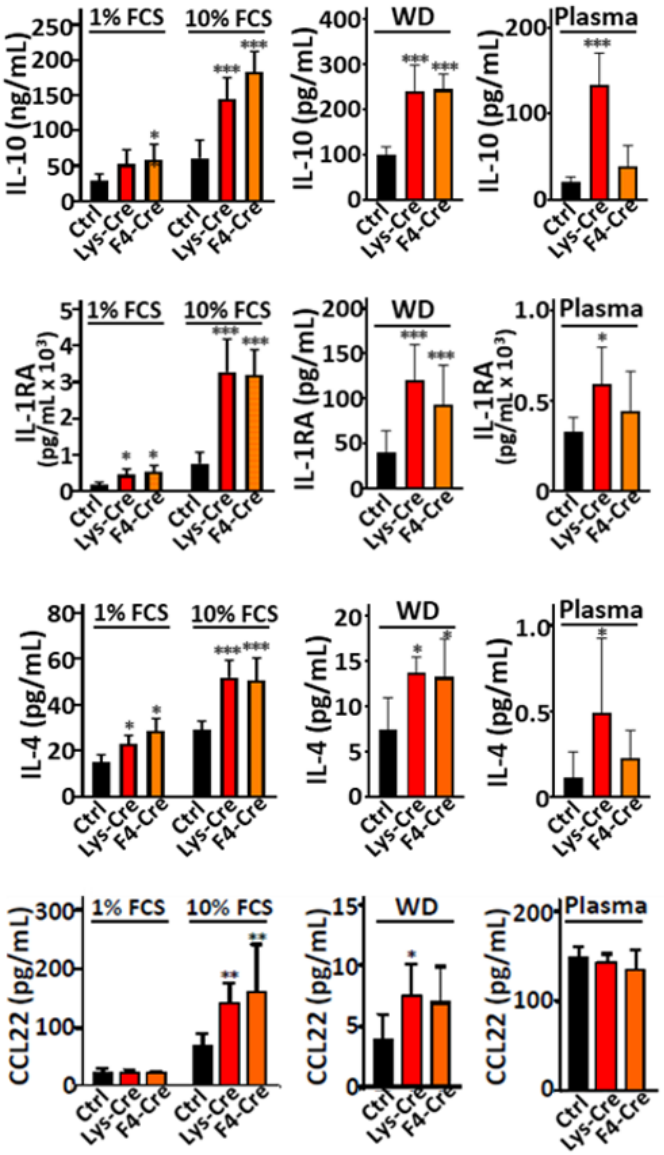

Figure 9. Anti-inflammatory M2 cytokines production– PM were incubated for 24 h in media containing 1% FCS or 10% FCS (ChD-fed mice, n=6 for each group). Cytokines in media (contained 10% FCS) and plasmas from WD-fed mice (n=10 for each group) were determined by ELISA. * - $p<0.05$, ** - $p<0.01$, *** - $p<0.001$ (Lys-Cre vs. Ctrl or F4-Cre vs. Ctrl).

Moreover, mRNA levels of M2 markers CD163 and IL-10 were increased in the aortic arch of *Ldl-r*$^{-/-}$ mice transplanted with *S1pr1-LysMCre* or *S1pr1-F4/80Cre* BM (Fig. 10).

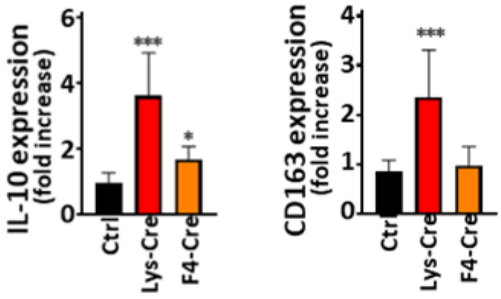

Figure 10. Expression of IL-10 and CD163 genes analyzed by qPCR. mRNA was normalized to GAPDH and presented relative to S1pr1-KI. *p<0.05, **p<0.01, ***p<0.001 (Lys-Cre vs. Ctrl or F4-Cre vs. Ctrl).

21. $S1P_1$ overexpression leads to $Ly6C^{hi}$ monocyte subset expansion

As PU.1, IRF8 and Klf4 promote the expansion of the $Ly6C^{hi}$ monocyte subset[234,235], their expression was assessed in monocytes from $S1P_1$-knock-in mice. As shown in Figure 11A, $S1P_1$-overexpressing monocytes from *S1pr1-LysMCre* mice showed increased mRNA of all three transcription factors and increased PU.1 and IRF8 protein levels (Fig.11B). Consequently, the $Ly6C^{hi}$ monocyte population was expanded in blood from *S1pr1-LysMCre* but not *S1pr1-F4/80Cre* or *S1pr1-KI* mice (Fig. 11C).

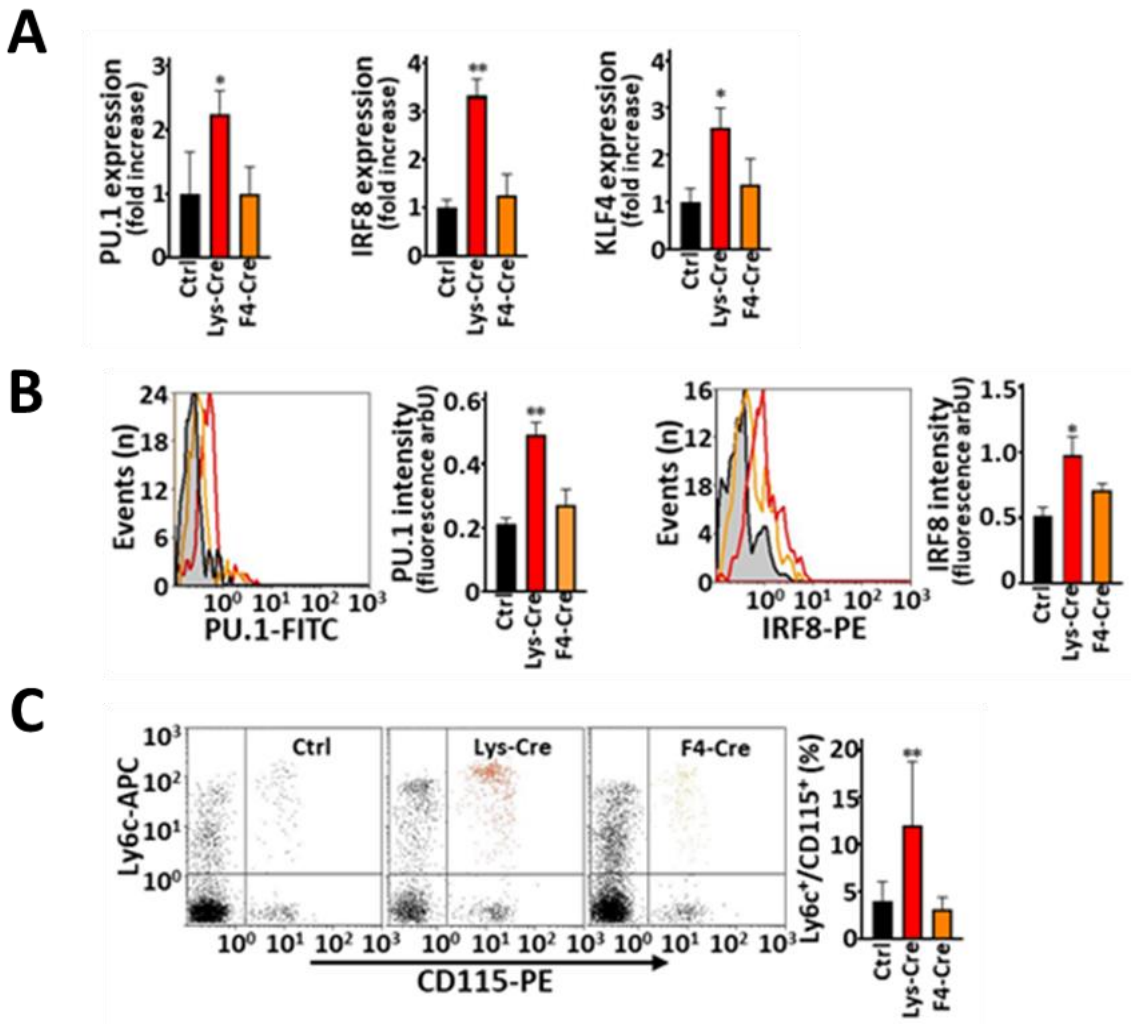

Figure 11. S1P1 overexpression in monocytes expands Ly6C^{hi} monocyte subset – **A**. PU.1, IRF8 and Klf4 mRNA expression levels (n = 5 for each group) were normalized to GAPDH and presented relative to S1pr1-KI. **B**. Intracellular and surface protein levels of PU.1 and IRF8 were analyzed by flow cytometry. Bar graphs show fluorescence intensity medians. **C**. Cell surface staining for Ly6C and CD115 analyzed by flow cytometry. Bar graphs represents % of Ly6c^{+}/CD115^{+} monocytes (n = 10 for each group). *p<0.05, **p<0.01 (Lys-Cre vs. Ctrl or F4-Cre vs. Ctrl).

Previous studies revealed that Ly6C^{hi} monocytes show altered expression of molecules involved in migration and adhesion to endothelial cells[239]. As shown in Figure 12A, monocytes obtained from *S1pr1-LysMCre* mice were characterized by an enhanced expression of CCR5 (receptor for regulated and normal T cell expressed and secreted, RANTES), but not CCR2 (receptor for monocyte chemoattractant protein-1, MCP-1) both at mRNA and protein levels. Consequently, these monocytes migrated more effectively towards RANTES but not MCP-1 as compared to control cells (Fig. 12B).

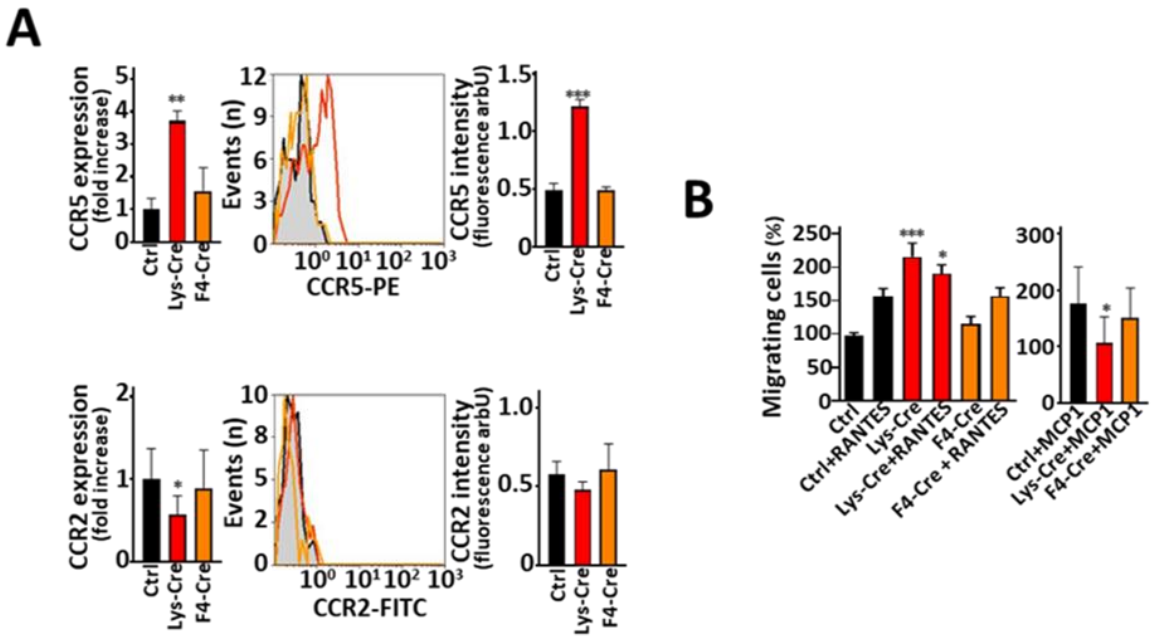

Figure 12. Evaluation of Ly6C^{hi} monocyte migration – **A**: CCR2 and CCR5 expression levels (n = 5 for each group). mRNA was normalized to GAPDH and presented relative to S1pr1-KI. Surface protein levels were analyzed by flow cytometry; Bar graphs show fluorescence intensity medians. **B**: Monocyte chemotaxis towards RANTES (5.0 ng/mL, left) or MCP-1 (10.0 ng/mL, right). Migrated cells in the basolateral compartment of Boyden chamber were stained and counted. Data from two experiments (n = 4 – 10 for each group). *p<0.05, **p<0.01, ***p<0.001 (Lys-Cre vs. Ctrl or F4-Cre vs. Ctrl).

With respect to adhesion-mediating molecules, monocytes from *S1pr1-LysMCre* mice showed increased expression of very late antigen 4 (VLA4) and P-selectin glycoprotein ligand-1 (PSGL-1; Fig. 13A). This was paralleled by increased binding of VCAM-1 and P-selectin, which are the partners for VLA4 and PSGL-1, respectively (Fig. 13B). Nevertheless, any differences in term of capacity of monocytes to bind ICAM-1 and to promote the relative expression of VLA1 were observed among the two experimental groups (Fig. 13C).

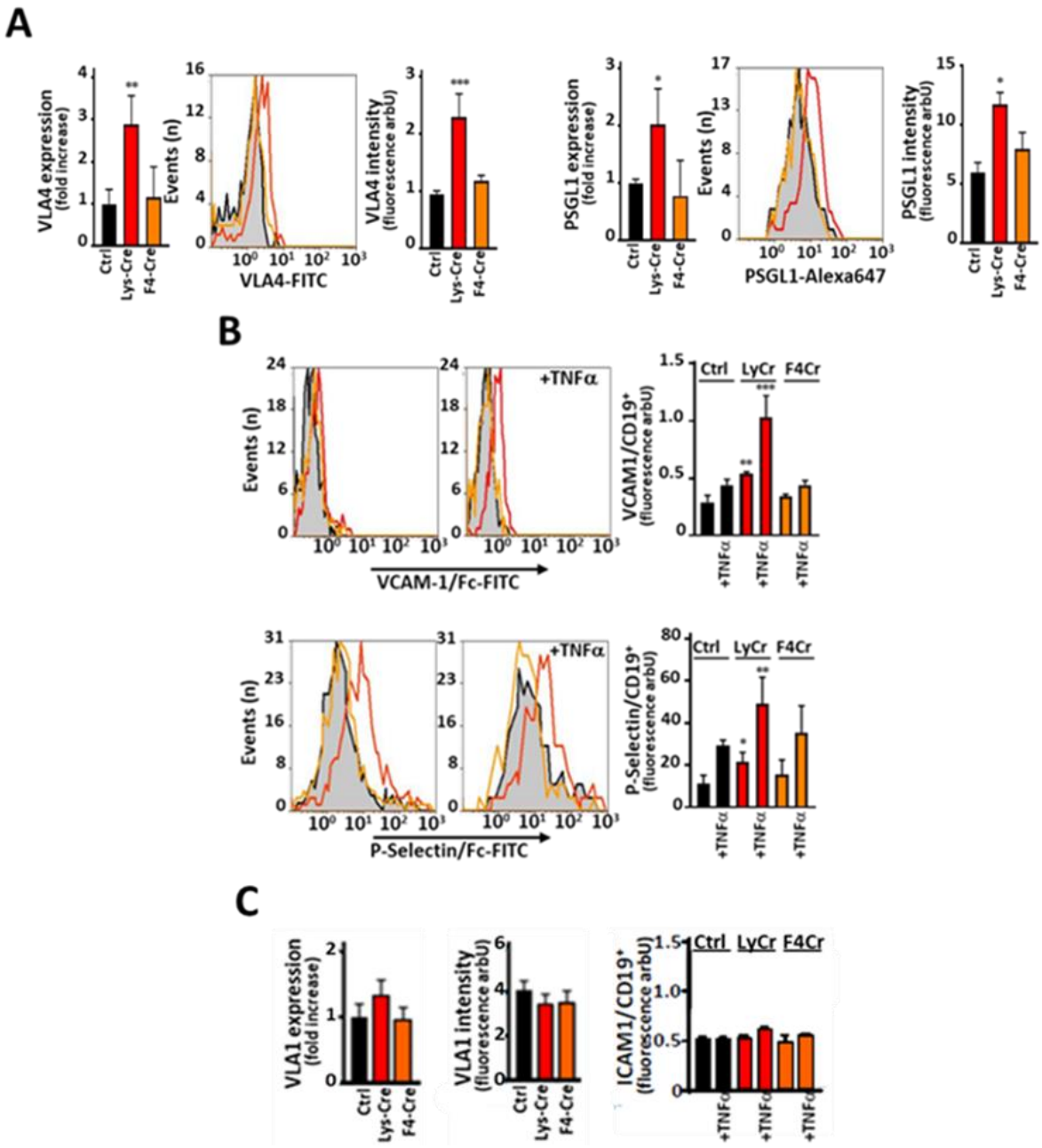

Figure 13. Evaluation of adhesion of Ly6C^{hi} monocyte– Monocytes were collected from either S1pr1-KI (Ctrl), S1pr1-LysMCre (Lys-Cre) or S1pr1-F4/80Cre (F4-Cre) mice fed Chow diet (ChD). **A**. VLA-4 and PSGL-1 expression levels (n = 5 for each group). **B**. Chimeric Fc/VCAM-1 and Fc/P-selectin binding to monocytes exposed for 4 h to TNFα. PE-conjugated antibody against human IgG1 was used for secondary staining (n= 4 for each group). **C**. VLA-1 expression levels (n=5) and chimeric Fc/ICAM-1 binding to monocytes after 4h to TNFα. PE-conjugated antibody against human IgG1 was used for secondary staining (n= 4 for each group). *p<0.05, **p<0.01, ***p<0.001 (Lys-Cre vs. Ctrl or F4-Cre vs. Ctrl).

In addition, an increased adhesion of *S1pr1-LysMCre* monocytes to bEnd.5 cells was observed when they were pretreated with TNFα(Fig. 14).

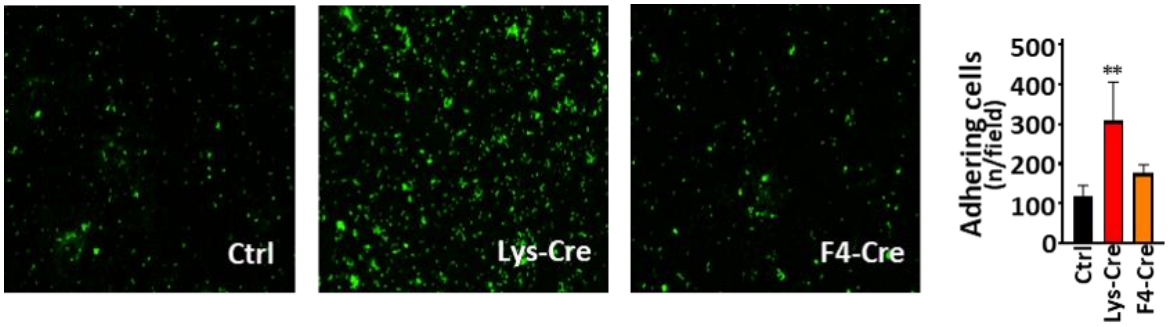

Figure 14. Evaluation of adhesion of Ly6C^{hi} monocyte– Monocytes were collected from either S1pr1-KI (Ctrl), S1pr1-LysMCre (Lys-Cre) or S1pr1-F4/80Cre (F4-Cre) mice fed Chow diet (ChD). bEnd.5 murine endothelial cells were stimulated with TNFα(50.0 ng/mL) for 4h. The adherence of calcein-loaded monocytes was evaluated under a fluorescence microscope. Data from two experiments (n=8 for each group). *p<0.05, **p<0.01, ***p<0.001 (Lys-Cre vs. Ctrl or F4-Cre vs. Ctrl).

22. $S1P_1$ overexpression in macrophages activates LXRα

In addition to IRF8- and PU.1-controlled genes, PM from *S1pr1-LysMCre* mice showed an increased expression of LXR-dependent genes (Fig. 15A). Therefore, we analyzed the effect of $S1P_1$ overexpression on LXR activity. We found elevated expression of LXRα and LXR target genes including ATP-binding cassette transporters A1 (ABCA1) and G1 (ABCG1), arginase 1 (Arg1) and IL-5 in PM from *S1pr1-LysMCre* and *S1pr1-F4/80Cre* mice (Figure 15A). In addition, expression of these genes was further upregulated in macrophages overexpressing $S1P_1$ upon treatment with LXR ligands desmosterol or 22-hydroxycholesterol with retinoic acid (22OH/RA, Fig. 15B).

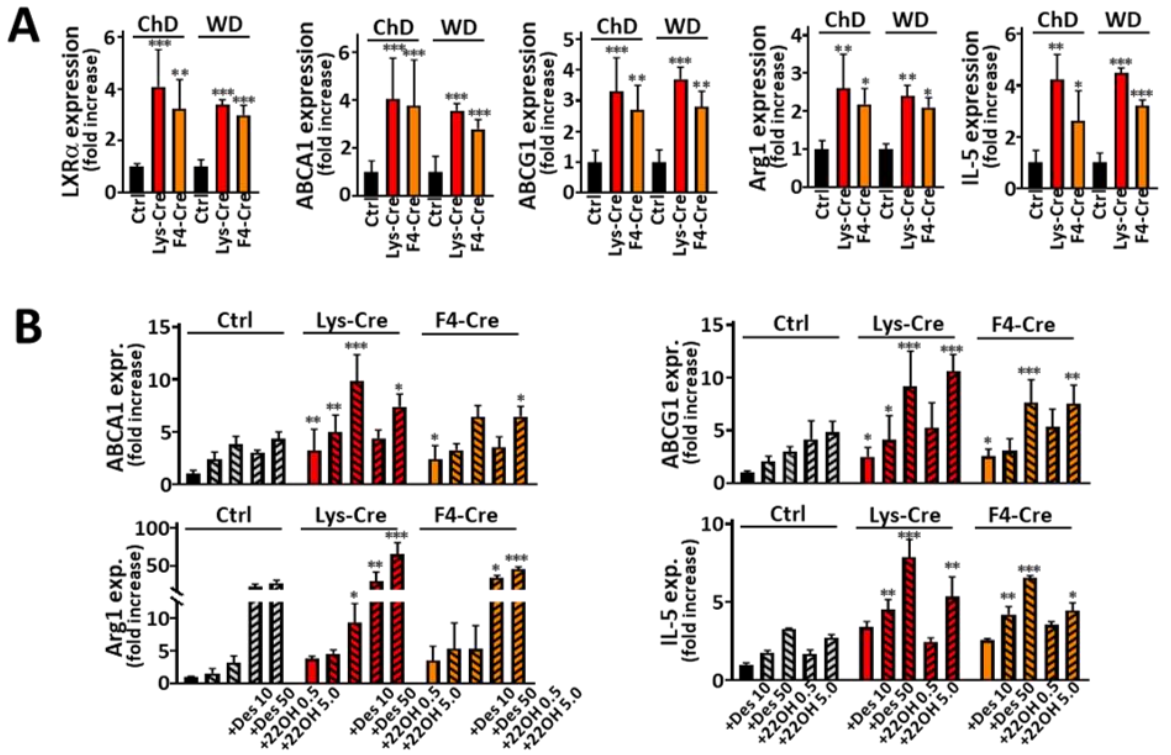

Figure 15. S1P$_1$ overexpression in macrophages enhances expression and activation of LXRα **and its target genes-** PM were collected from either *S1pr1-KI* (Ctrl n=10-12), *S1pr1-LysMCre* (Lys-Cre, n=9-12) or *S1pr1-F4/80Cre* (F4-Cre, n=10-12) fed Chow diet (ChD) or *Ldl-r*$^{-/-}$ mice transplanted with *S1pr1-KI* (n=10), *S1pr1-LysMCre* (n=9) or *S1pr1-F4/80Cre* (n=9) BM and fed Western diet (WD). **A.** Expression of LXRα and its targets analyzed by qPCR. mRNA was normalized to GAPDH and presented relative to *S1pr1-KI*. **B**. PM from ChD-fed mice were incubated for 24h in media with desmosterol (Des 10 or 50 µmol/L) or 22OH, 0.5 and 5.0 µg/mL/ 9cRA 10µM. LXR signature genes were analyzed by qPCR. Data from two experiments (n = 4 – 6 for each group). *p<0.05, **p<0.01, ***p<0.001 (Lys-Cre vs. Ctrl or F4-Cre vs. Ctrl).

Moreover, the expression of CD226 and CD244, two cell surface markers reflecting LXR activation, was upregulated in macrophages from *S1pr1-LysMCre* and *S1pr1-F4/80Cre* mice (Fig.16).

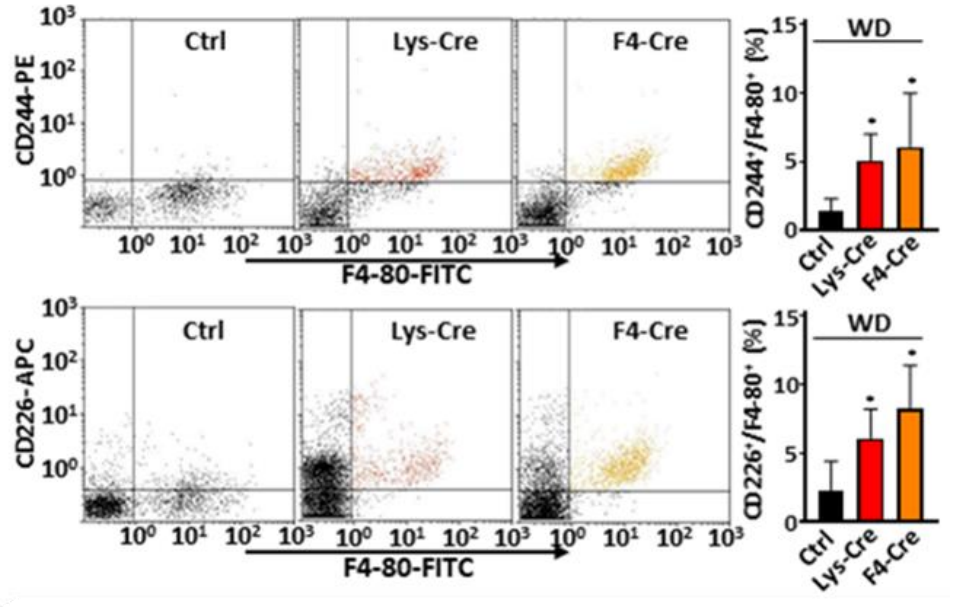

Figure 16: Additional phenotypic characterization of S1P1 overexpressing macrophages- Cell surface staining for LXR activity markers CD244 and CD226 was analyzed by flow cytometry. Shown are representative dot-blots and bar graphs representing % of $CD244^+/F4/80^+$ and $CD226^+/F4/80^+$ macrophages. n=10 for each group. *p<0.05(Lys-Cre vs. Ctrl or F4-Cre vs. Ctrl).

Because of the elevated LXR activity, $S1P_1$ overexpressing macrophages displayed increased cholesterol efflux to apoA-I or HDL, which are acceptor molecules interacting with ABCA1 and ABCG1, respectively (Fig.17).

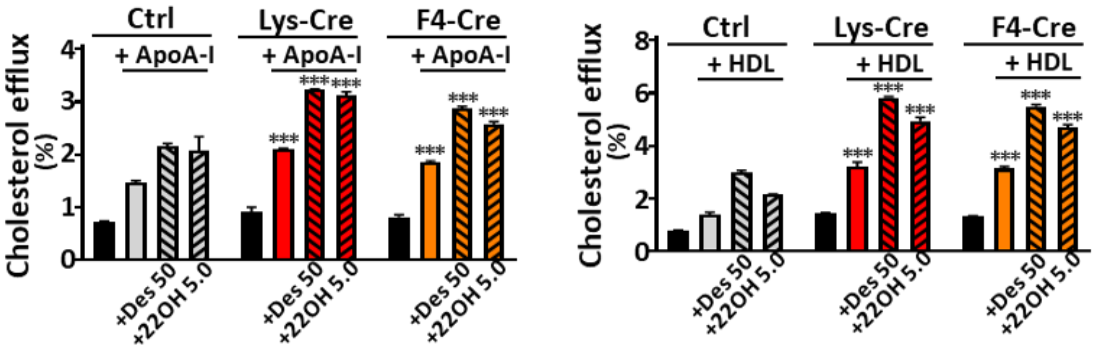

Figure 17: Evaluation of cholesterol efflux in macrophages overexpressing $S1P_1$- PM obtained from ChD-fed mice and loaded with [1,2-^{3}H]-cholesterol (n =3 for each group) were incubated for 4h in media with apoA-I (10.0 µg/mL) or HDL (12.5 µg/mL). Fractional efflux was calculated as ^{3}H-radioactivity present in the medium divided by the total radioactivity (medium plus cell).***p<0.001 (Lys-Cre vs. Ctrl or F4-Cre vs. Ctrl).

In addition, these cells secreted more IL-5 in response to desmosterol or 22OH/9cRA and elevated IL-5 levels were found in plasmas from *S1pr1-LysMCre* and *S1pr1-F4/80Cre* mice (Fig. 18).

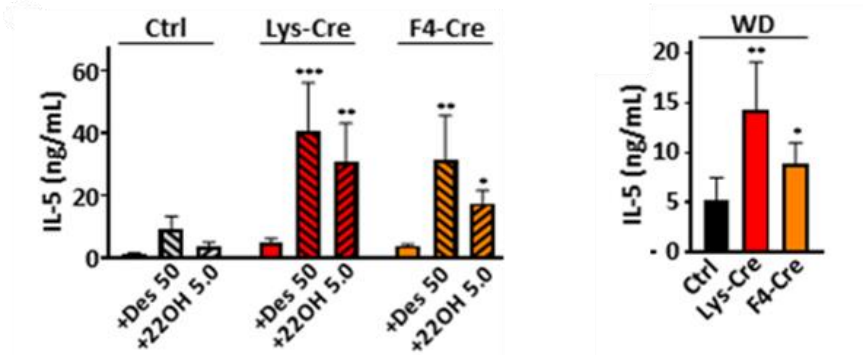

Figure 18: S1P₁ overexpression in macrophages enhances IL-5 secretion- PM established in cell culture were incubated for 24h in media containing desmosterol (Des, 50 µmol/L) or 22OH 5.0 µmol/L and 9cRA 10µM. IL-5 concentrations in cell media and plasmas from WD-fed mice were determined by ELISA. *p<0.05, **p<0.01, ***p<0.001 (Lys-Cre vs. Ctrl or F4-Cre vs. Ctrl).

23. $S1P_1$ overexpression in macrophages inhibits apoptosis and promotes efferocytosis

Since the expression of anti-apoptotic genes (Bcl6, MafB) was increased in $S1P_1$-overexpressing macrophages, we next examined the macrophage propensity to undergo endoplasmic reticulum (ER)-stress-induced apoptosis. To this purpose, as shown in Figure 19A and B respectively, the transmembrane phosphatidylserine shift and activity of the major executor caspase 3 were determined in PM after ER stress induction with thapsigargin/fucoidan or cholesterol loading. In addition, the caspase 12 activity (Fig. 19C) and the expression of CCAAT-enhancer-binding protein homologous protein CHOP (Fig.19D), which are induced by ER stress, were determined. As shown in Figure 19, all apoptosis indicators were attenuated in macrophages from *S1pr1-LysMCre* and *S1pr1-F4/80Cre* mice.

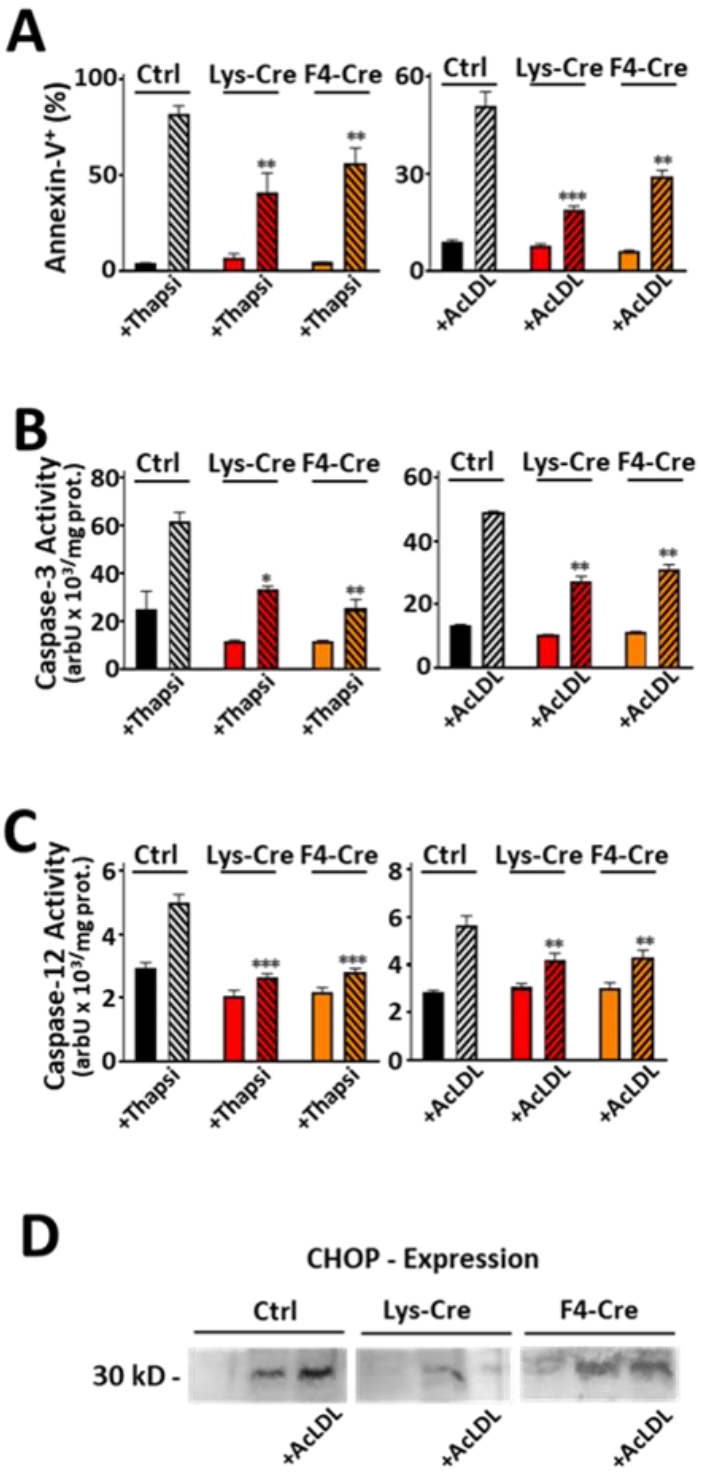

Figure 19. S1P$_1$ overexpression in macrophages inhibits ER-stress-dependent apoptosis - PM were collected from either *S1pr1-KI* (Ctrl, n=10-12), *S1pr1-LysMCre* (Lys-Cre, n=9-12) or *S1pr1-F4/80Cre* (F4-Cre, n=10-12) fed Chow diet (ChD) PM from ChD-fed mice were exposed for 24h to thapsigargin/fukoidan (Thapsi, 0.5 µmol/L and 25.0 µg/mL) or acetylated LDL (AcLDL, 100.0 µg/mL). Bar graphs show percentage of apoptotic (annexin-V-positive) cells (graph **A**) and caspase-3 activities (graph **B**). Data from two experiments (n = 5 – 6 for each group). Caspase-12 activities (graph **C**) and CHOP expression (picture **D**) in PM exposed to thapsigargin or AcLDL. Results representative for one experiment out of two. *p<0.05, **p<0.01, ***p<0.001 (Lys-Cre vs. Ctrl or F4-Cre vs. Ctrl).

Moreover, the tendency towards lower caspase-3 activity in $S1P_1$-overexpressing macrophages was reversed by Bcl6 inhibitor 79-6 or MafB inhibitor bortezomib (Figure 20).

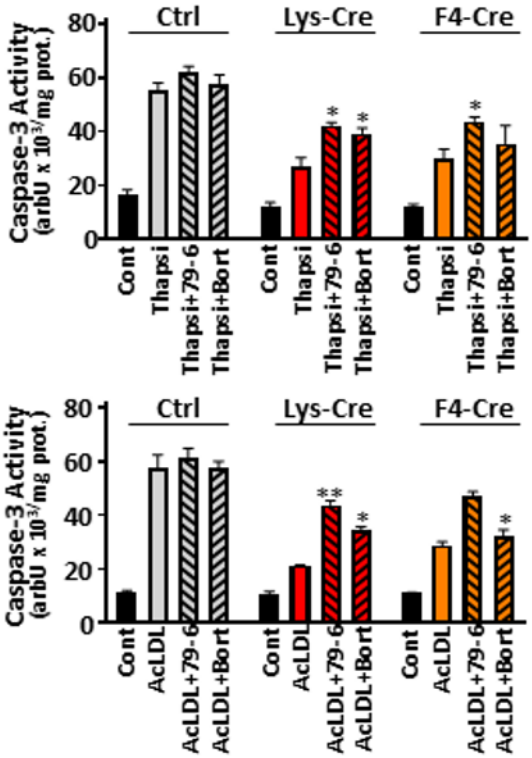

Figure 20. Effect of inhibitors of anti-apoptotic proteins on thapsigargin- or cholesterol-loading-induced caspase 3 activity - PM obtained from ChD-fed mice were established in cell culture and incubated for 30 min with 79-6 (50.0 µmol/L) or bortezomib (100 nmol/L) prior to adding thapsigargin/fukoidan (Thapsi, 0.5 µmol/L and fukoidan 25.0 µg/mL) or AcLDL (100.0 µg/mL) for 24h. Bar graphs show caspase-3 activities. Shown are results from 2 independent experiments in triplicates. * - $p<0.05$, ** - $p<0.01$ (thapsigargin vs. thapsigargin + inhibitor or AcLDL vs. AcLDL + inhibitor).

As the reduced propensity to undergo apoptosis is coupled to more effective efferocytosis, we subsequently examined, whether efferocytosis is altered in $S1P_1$-overexpressing macrophages. The results showed that the expression of MerTK and Axl1, receptors responsible for the apoptotic cell ingestion and controlled by LXR and MafB, respectively[126,240], was elevated in macrophages from *S1pr1-LysMCre* and *S1pr1-F4/80Cre* mice (Fig. 21A and B).

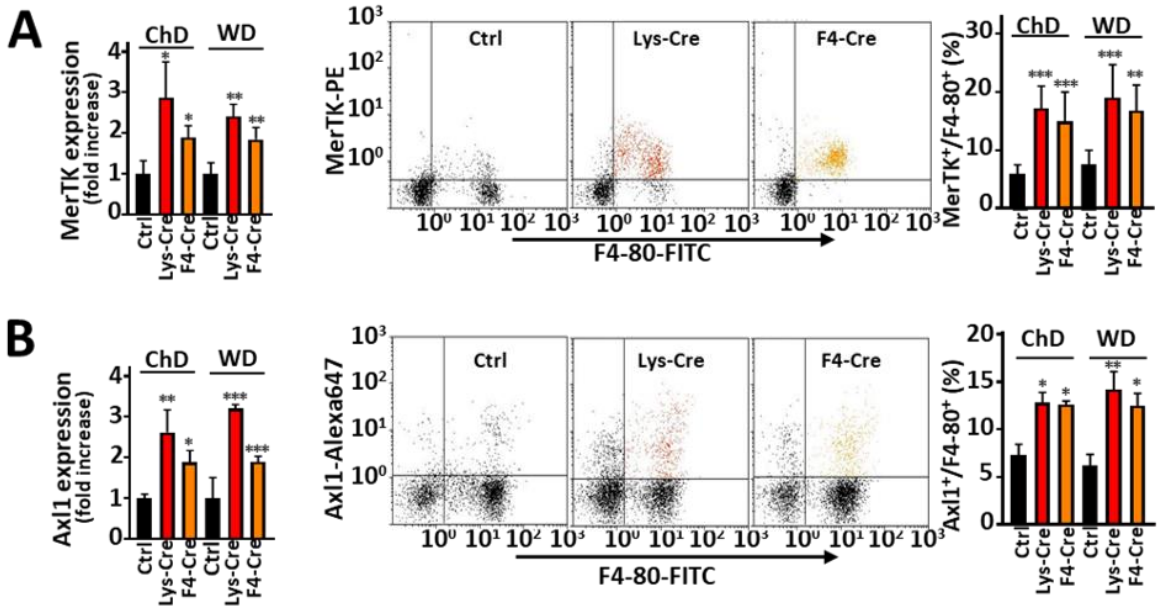

Figure 21. S1P$_1$ overexpression in macrophages enhances efferocytosis – **A** and **B** left graphics: Expression of efferocytosis receptor genes MerTK, and Axl-1 analyzed by qPCR. mRNA was normalized to GAPDH and presented relative to *S1pr1-KI*. Data from two experiments (n =4 – 6 for each group). **A** and **B** central dot-plots and right graphics: Cell surface staining for MerTK and Axl-1 analyzed by flow cytometry. Bar graphs represents percent MerTK$^+$/F4/80$^+$ and Axl-1$^+$/F4/80$^+$ macrophages. *p<0.05, **p<0.01, ***p<0.001 (Lys-Cre vs. Ctrl or F4-Cre vs. Ctrl).

In addition, both desmosterol and 22OH/9cRA augmented MerTK expression in these cells (Fig. 22A). Likewise, S1P$_1$ overexpression enhanced the expression of GAS6 acting as bridging molecule between MerTK and apoptotic cells (Fig. 22B).

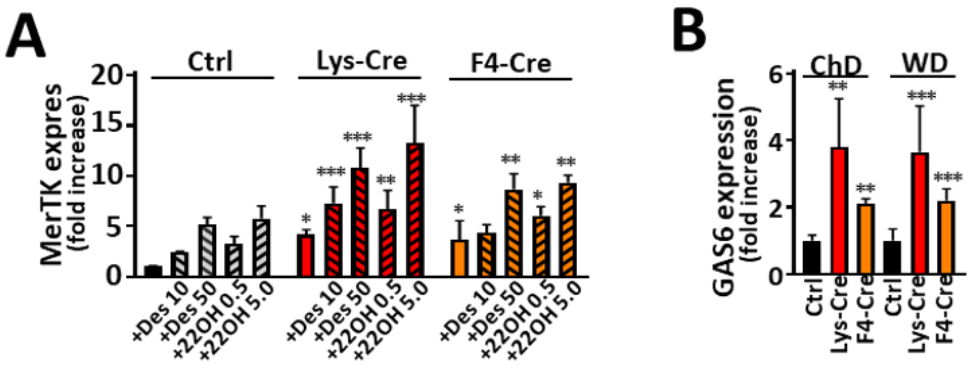

Figure 22*: *S1P1 overexpression enhanced the expression of MertK and GAS6 – **A**: MerTK expression in PM from ChD-fed mice incubated for 24 h with desmosterol (Des, 10 or 50 µmol/L) or 22-OH/9-cRA (22OH: 0.5 and 5.0 µg/Ml; 9cRA: 10µM). **B**. GAS6 expression in PM was analyzed by qPCR. mRNA was normalized to GAPDH and presented relative to *S1pr1-KI*. *p<0.05, **p<0.01, ***p<0.001 (Lys-Cre vs. Ctrl or F4-Cre vs. Ctrl).

Consequently, efferocytosis was enhanced in S1P$_1$-overexpressing macrophages both in the absence or presence of desmosterol as inferred from the increased ingestion of apoptotic

RAW264.7 cells (Fig. 23A). Next, it was investigated if $S1P_1$ overexpression affected apoptosis and efferocytosis in atherosclerotic lesions from *Ldl-r*$^{-/-}$ mice transplanted with S1pr1-KI, S1pr1-LysMCre or S1pr1-F4/80Cre BM. Fewer macrophages was detected with TUNEL-positive own nuclei, but more macrophages with TUNEL-positive ingested nuclei within aortic root lesions, pointing to attenuated apoptosis, but more efficient efferocytosis in *S1pr1-LysMCre* and *S1pr1-F4/80Cre* mice (Fig. 23B).

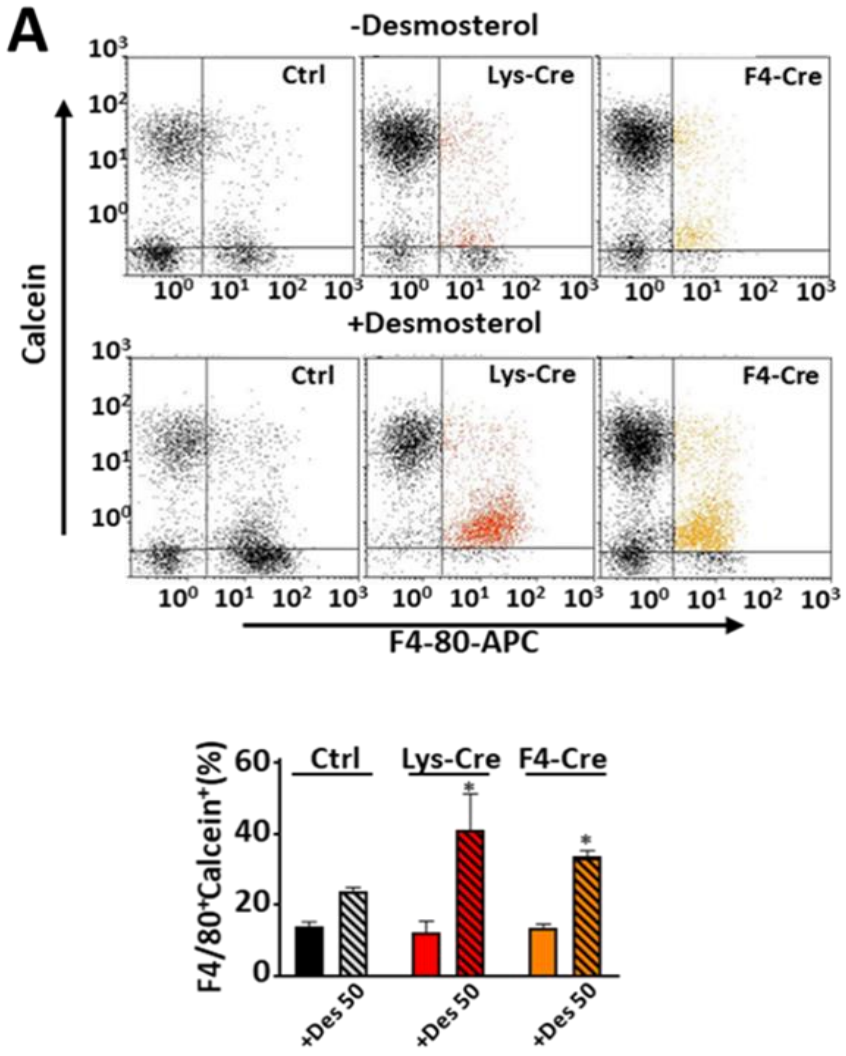

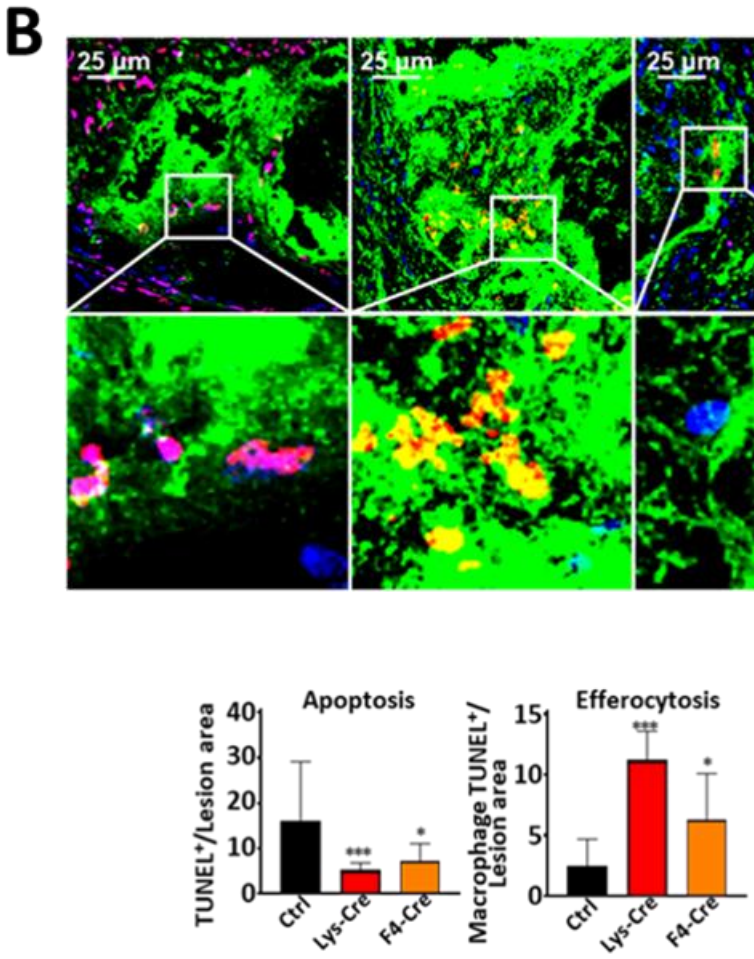

Figure 23. S1P$_1$ overexpression in macrophages inhibits ER-stress-dependent apoptosis and enhances efferocytosis - PM were collected from either *S1pr1-KI* (Ctrl, n=10-12), *S1pr1-LysMCre* (Lys-Cre, n=9-12) or *S1pr1-F4/80Cre* (F4-Cre, n=10-12) fed Chow diet (ChD) or *Ldl-r*$^{-/-}$ mice transplanted with *S1pr1-KI* (n=10), *S1pr1-LysMCre* (n=9) or *S1pr1-F4/80Cre* (n=9) BM and fed Western diet (WD). **A**: Flow cytometry dot-plots showing efferocytosis of apoptotic RAW264.7 cells by PM from ChD-fed mice incubated for 24h with desmosterol (50 µmol/L). RAW264.7 cells and PM were labeled with Calcein and anti-F4/80-FITC, respectively. Bar graph represents percent calcein$^+$/F4/80$^+$ macrophages (n = 5 for each group). **B**. Aortic root section images with apoptotic cells labeled by TUNEL (red), macrophages by anti-F4/80 (green), and nuclei by Hoechst (blue). Apoptotic cells appear violet (red on blue) and efferocytotic cells appear yellow (red on green). Bar-graph shows quantification of apoptotic and efferocytic cells. *p<0.05, **p<0.01, ***p<0.001 (Lys-Cre vs. Ctrl or F4-Cre vs. Ctrl).

24. $S1P_1$ signals in macrophages via protein kinases A (PKA) and AKT

Finally, the signaling pathways mediating the emergence of the anti-atherogenic phenotype were investigated in $S1P_1$-overexpressing macrophages. Since PU.1 and LXR activities are inversely and directly regulated by PKA as well as Akt and mechanistic target of rapamycin complex 1 (mTORC1)[241,242], respectively, the effect of S1P on the activation of these kinases was examined in PM. As shown in Figure 24A, the PKA activity and concentration of its upstream regulator cAMP were lower in PM from *S1pr1-LysMCre* and *S1pr1-F4/80Cre* mice and this effect was potentiated by exogenous S1P. Moreover, pre-incubating PM with the PKA activator DBcAMP suppressed the elevated PU.1 and IRF8 expression (Figure 24B).

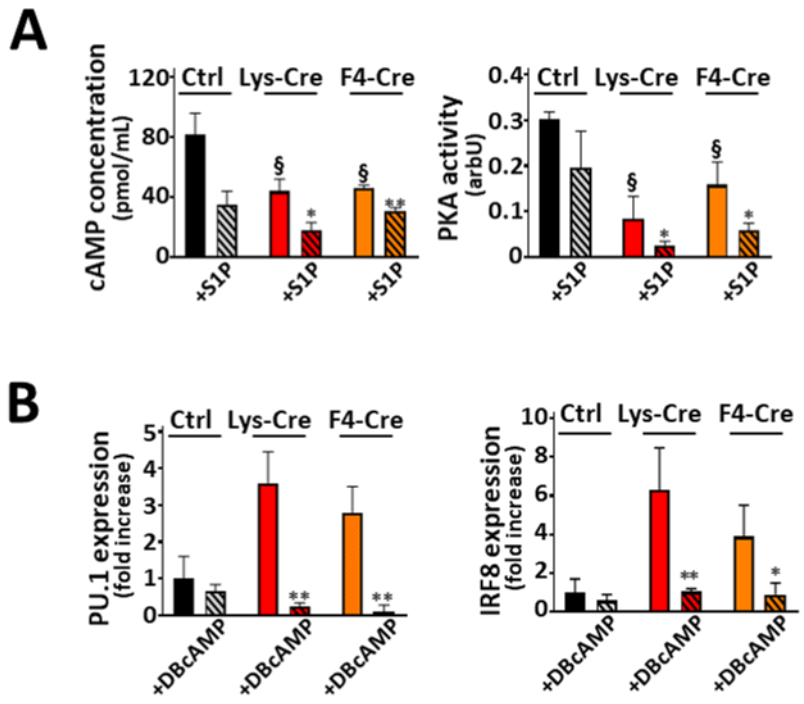

Figure 24: Evaluation of PKA activity- PM from *S1pr1-KI* (Ctrl, n = 3 - 5), *S1pr1-LysMCre* (Lys-Cre, n = 3 - 5) or *S1pr1-F4/80Cre* (F4-Cre, n = 3 - 5) fed Chow diet (ChD) were established in cell culture. **A.** Cells were exposed to S1P (1.0 µmol/L) for 2 h and intracellular cAMP levels and PKA activity were measured using EIA or Pep-Tag assay, respectively. **B.** PM were incubated with DbBcAMP (0.25 mmol/L) for 24h and PU.1 and IRF8 expressions were analyzed by qPCR. §p<0.1; *p<0.05, **p<0.01

Similarly, the elevated expression of LXR target genes ABCA1 and ABCG1 was abolished in PM pretreated with inhibitors of AKT (GSK690693) and mTORC1 (INK128). In addition, ABCA1 and ABCG1 expression was suppressed in the presence of bafilomycin (BAF) (Fig. 25), which indirectly inhibits Lamtor1, the scaffolding protein for mTORC1 activation and the element connecting the signaling between kinases Akt and mTORC1 and LXR[241].

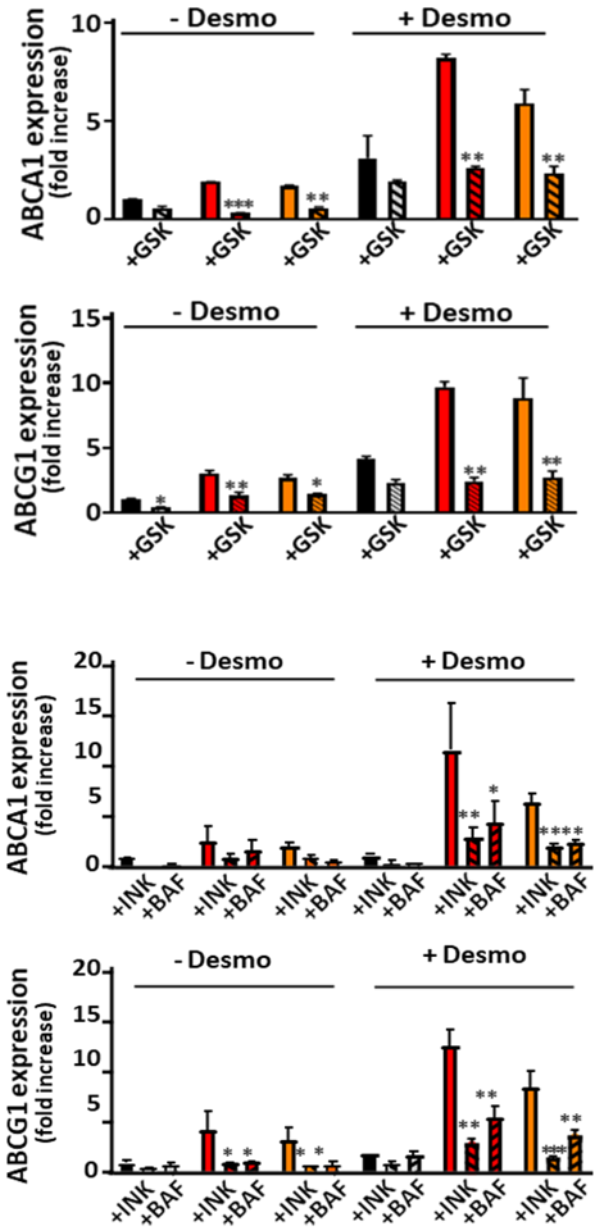

Figure 25: Investigation of the effect of S1P1 on the activation of kinases in macrophages- Cells were exposed for 30 min GSK690693 (10.0 µmol/L), INK128 (0.2 µmol/L) or bafilomycin (1.0 µmol/L) prior to incubation with desmosterol (50 µmol/L) for 24 h. ABCA1 and ABCG1 gene expressions were analyzed by qPCR. Shown are results from 2 independent experiments in duplicates. * - $p<0.05$, ** - $p<0.01$, *** - $p<0.001$ with vs. without treatment with activator/inhibitor.

By contrast, basal and S1P-stimulated Akt activities were increased in $S1P_1$-overexpressing macrophages (Figure 26A). Similarly, S1P treatment stimulated mTORC1 in macrophages from *S1pr1-LysMCre* and *S1pr1-F4/80Cre* mice, as indicated by the phosphorylation of its target p70S6 kinase (Fig. 26B). In contrast to Akt, STAT3 and STAT6 activities were unchanged in PM from $S1P_1$-overexpressing macrophages regardless of the presence or absence of S1P (Fig. 26C).

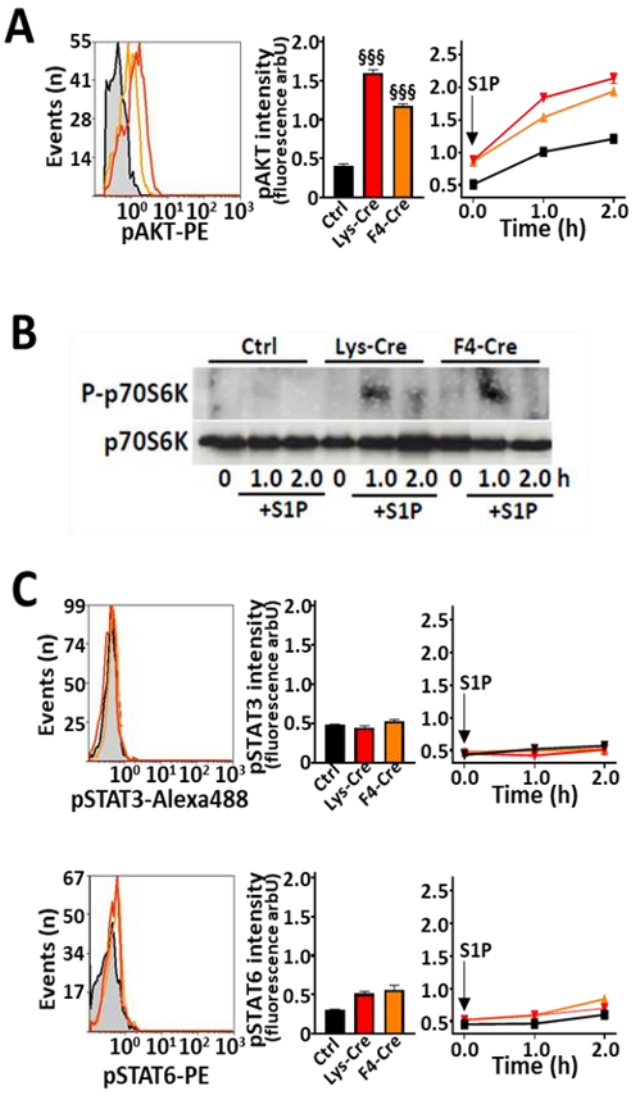

Figure 26: Investigation of $S1P_1$ signals in macrophages via AKT, STAT-3 and STAT-6 -. PM from *S1pr1-KI* (Ctrl, n = 3 - 5), *S1pr1-LysMCre* (Lys-Cre, n = 3 - 5) or *S1pr1-F4/80Cre* (F4-Cre, n = 3 - 5) fed Chow diet (ChD) were established in cell culture. **A**. and **C**. PM were analyzed for kinase activities or established in cell culture and exposed to S1P (1.0 µmol/L) for indicated times. Intracellular stainings for phospho-Akt (A graphics), phospho-STAT3 (C, upper graphics) and phospho-STAT6 (C, lower graphics) were analyzed by flow cytometry. Bar graphs show fluorescence intensity medians. **B**. For mTOR1 activity, PM lysates were probed with antibodies against total and phosphorylated (P)-p70S6 kinase. Blots are representative for two independent experiments. §§§ $p<0.001$ (Lys-Cre vs. Ctrl or F4-Cre vs. Ctrl).

Discussion

There is an abundant evidence *in vitro* supporting the notion that S1P, acting as a constituent of HDLs, exerts anti-atherogenic effects. By contrast, results of in vivo studies regarding the atheroprotective role of S1P are scarce and partially discrepant. In addition, S1P receptor subtypes mediating the potentially atheroprotective effects of S1P and the underlying molecular mechanisms still remain ambiguous. In particular, the use of pharmacological agonists to amplify S1P signaling in murine atherosclerosis models, was hampered by insufficient receptor specificity and poorly defined side effects[243]. Recently, a pronounced progression of atherosclerosis could be observed in mice with a deficiency of $S1P_1$ in endothelial[207] or myeloid cells[232,42]. However, the putative anti-atherogenic effects related to an increased signaling via S1P receptors expressed in cells relevant to the pathogenesis of atherosclerosis, such as macrophages, have not been as yet examined. Therefore, more specific approaches, focusing on the endogenous S1P signaling in selected cells became necessary to document beneficial effects in *vivo* of this sphingolipid on atherosclerosis.

To specifically address the putatively atheroprotective role of S1P receptor type-1 in macrophages, in the present study myeloid-specific $S1P_1$ knock-in transgenic mouse models were generated and used as donors in BM transplantation studies to produce $Ldl^{-/-}$ chimeras overexpressing $S1P_1$ in monocytes and macrophages (*S1pr1-LysMCre* mice) or macrophages only (*S1pr1-F4/80Cre* mice). Several pieces of evidence suggest that macrophages overexpressing $S1P_1$ protect against the development of atherosclerotic plaques in mice. First, the analysis of vascular lesions in brachiocephalic arteries and aortic roots showed a reduced plaque areas in both lines, even though the protective effects were much more pronounced in *S1pr1-LysMCre* than *S1pr1-F4/80Cre* mice. Second, $S1P_1$ overexpression attenuated necrotic core formation, which is dependent on the macrophage death rate and removal of apoptotic debris within plaques. Congruent with these results,

lower apoptosis levels, which correlated with an increased number of total and efferocytosis-positive macrophages were encountered in atherosclerotic lesions of both mice lines.

These findings, combined with the lower amount of collagen observed in the lesions of *S1pr1-LysMCre* mice, point to a slower advancement of atherosclerotic disease in chimeras overexpressing $S1P_1$ and for the first time provide a firm indication that the selective amplification of $S1P_1$-mediated signaling, contributes to the protection against the development of atherosclerosis in mice.

Although both the LysM and the F4/80 promoters direct the gene expression almost exclusively in the monocyte/macrophages lineages, as indicated in the source literature and confirmed in the present study using an in silico approach, the two $S1P_1$ overexpressing chimeras presented with two conspicuously distinct phenotypes. While *S1pr1-LysMCre* mice showed a pronounced reduction of atherosclerotic lesions combined with marked alterations in the peripheral blood counts(data not shown), the respective effects were less pronounced in *S1pr1-F4/80Cre* mice. Two putative explanations may account for this finding. First, the Cre expression directed by the F4/80 promoter was previously reported to be lower than the LysM promoter[244]. This observation has been recapitulated in the present study as approximately 20 – 50% weaker gene expressions, promoter occupancies and functional cell responses were noted in *S1pr1-F4/80Cre* as compared to *S1pr1-LysMCre* macrophages. Second, only *S1pr1-LysMCre* mice were able to overexpress $S1P_1$ in monocytes, resulting in elevated levels of PU.1 and IRF8 in these cells. These two transcription factors have a crucial role in the formation of the $Ly6C^{hi}$ monocytes, which are able to infiltrate inflammatory sites, including progressing plaques, and to dominate the monocytosis encountered in hypercholesterolemic animals[234,235]. Consistent with the evidence reported in literature[239], an expanded $Ly6C^{hi}$ monocyte population was observed in *S1pr1-LysMCre* mice in the present study and monocytes isolated from these animals

showed typical characteristics of Ly6C^{hi} cells including higher expression of proteins involved in chemotaxis and interaction with endothelial cells (CCR5, PSGL1, VLA4), an increased binding of P-selectin and VCAM-1, as well as a boosted migration towards RANTES and adhesion to TNFα-activated endothelial cells. These findings allow to assume that a high recruitment of $S1P_1$ overexpressing Ly6C^{hi} monocytes to atherosclerotic lesions is dependent on their enhanced capacity to migrate along the chemokine gradient. This characteristic of $S1P_1$ overexpressing monocytes, together with the reduced propensity to undergo apoptosis, likely accounts for the increased number of macrophages seen in plaques from *S1pr1-LysMCre* mice.

Ly6C^{hi} monocytes are conventionally considered pro-inflammatory, given that they are capable to differentiate in pro-inflammatory M1 macrophages after entering the inflamed tissue[236,245]. Nevertheless, in few instances Ly6C^{hi} monocytes were found to give rise to anti- rather than pro-inflammatory macrophages. For example, following to the recruitment of Ly6C^{hi} monocytes to allergic skin or injured myocardium, they tend to convert to anti-inflammatory M2 macrophages expressing typical surface markers and producing anti-inflammatory cytokines[150,151].

More importantly, in a recent study it has been demonstrated that the penetration of Ly6C^{hi} monocytes into atherosclerotic lesions and their differentiation to M2 macrophages is a pre-condition for the plaque regression[246]. Furthermore, it was demonstrated that a subset of Ly6C^{hi} monocytes characterized by a high expression of PU.1 was able to convert into anti-inflammatory monocyte-derived dendritic cells. Conversely, the pro-inflammatory M1 macrophages derived from Ly6C^{hi} monocytes showed a markedly lower expression levels of PU.1[247].

In parallel to the altering monocyte function, the $S1P_1$ overexpression also influences the functional phenotype of macrophages. The contribution of S1P-induced signaling to the

generation of the anti-inflammatory macrophages phenotype could be demonstrated in some previous studies, where the expression of M1 genes and inflammatory cytokines production in response to LPS[248] were both reduced in S1P-stimulated macrophages. Moreover, conventional markers defining the M2 phenotype, such as Ym1, Arg-1 and IL-10 were upregulated in these cells and this was explained either by a direct $S1P_1$ activation or the autocrine stimulation by IL-4[249]. In our study, we recap all these findings and extend them to define a novel functional phenotype observed in S1P exposed macrophages as a result of a concurrent activation of PU.1/IRF8 and LXRα. As it has been demonstrated previously, PU.1 acting in concert with additional transcriptions factors, such as IRF8, STAT6 or IRF4[250], is able to promote the expression of various M2 typical markers, including Arg-1, Ym-1 and Fizz-1 and also to shift macrophages in M2a phenotype, which is characterized by a high expression of MHCII and CD206 and an increased production of IL-1RA and IL-4[251,252]. Furthermore, PU.1 regulates the expression and activity of KLF4 and MafB, two transcription factors capable to promote M2a macrophage polarization[237,238]. In the present experimental setting, macrophages overexpressing $S1P_1$ displayed the typical characteristic of M2a, encompassing the enhanced expression of MHCII, CD206, IL-1RA and IL-4. However, these macrophages also showed the enhanced activity of LXR and the elevated expression of several LXR targets with known anti-atherogenic properties such as ABCA1 or ABCG1. Previously, several studies showed that the reprogramming macrophages towards the M2a phenotype down- rather than up-regulate LXRα-dependent gene expression[253,254]. In particular, after IL-4 treatment, M2a macrophages showed decreased cholesterol efflux capacity, owing to the reduced expression of LXRα and ABCA1[158]. In a marked contrast, the overexpression of $S1P_1$, which led to activation of LXRα, entailed the upregulation of different genes, including IL-5, ABCG1, ABCA1 and MerTK and thereby enhanced both the cholesterol efflux and the reversed cholesterol transport. In this way, the

simultaneous activation of PU.1/IRF8 and LXRα in $S1P_1$-overexpressing macrophages gave rise to an entirely novel functional macrophage phenotype bundling several anti-inflammatory and anti-atherogenic mechanisms **(Fig. 27)**.

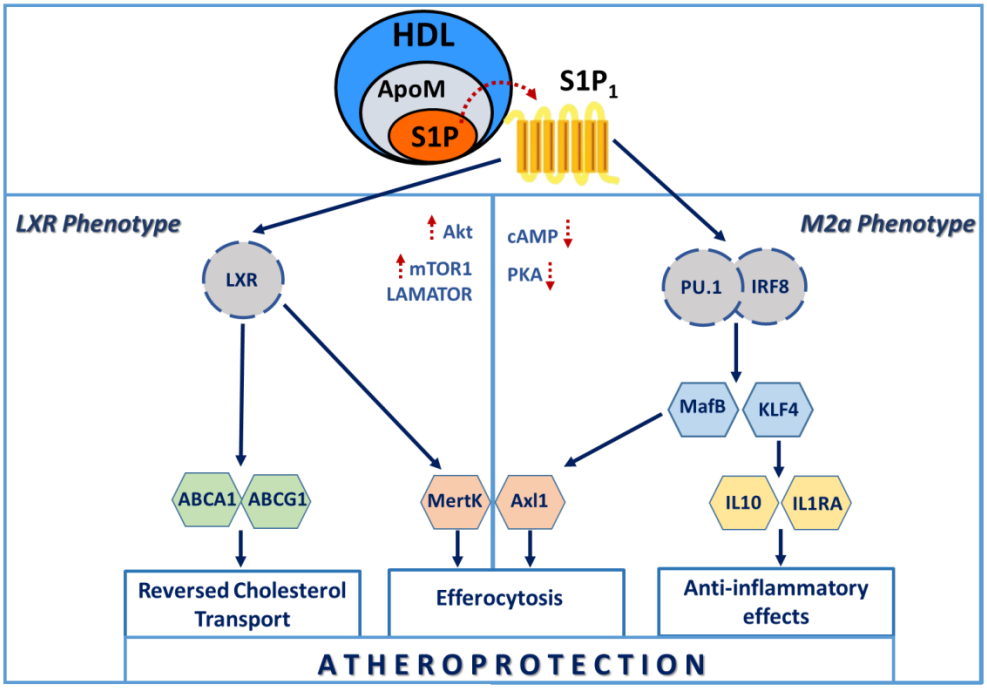

Figure 27. Molecular mechanisms underlying atheroprotective effects of S1P1 signaling on macrophages.

First, cells overexpressing $S1P_1$ acquired anti-inflammatory properties, including the increased secretion of cytokines such as IL-1RA, IL-10 and IL-5, through the enhanced expression of PU.1, MafB, KLF4 and LXRα. These anti-inflammatory properties likely help to resolve inflammation and protect against atherosclerosis. Moreover, due to an increase in the LXRα activity, $S1P_1$ overexpressing macrophages are able to upregulate the expression of two important cholesterol transporters (ABCA1 and ABCG1) and to improve cholesterol efflux capacity, which promotes the reverse cholesterol transport and consequently reduces the plaque cholesterol burden. In addition, the macrophage propensity to undergo ER-stress induced apoptosis, was attenuated though the increase expression of Bcl-6 and MafB. In this way, the macrophage survival within atherosclerotic lesions was enhanced in mouse models examined in the present study. Owing to the LXR and MafB dependent enhancement of the

expression of MertK and Axl-1, respectively, these macrophages could also clear in a more effective way the apoptotic cells, which is a process that decisively regulates the necrotic core formation and the late progression of atherosclerotic lesion. Taken together our, current findings support the idea that $S1P_1$ acts as master regulator of unique functional macrophage phenotype, unifying multiple atheroprotective mechanisms. The identification of this phenotype in *S1pr1-LysMCre* and, to a lesser extent, in *S1pr1-F4/80Cre* mice provides a consistent explanation for the attenuated plaque formation seen in these animals.

Our results provide new insights into the signaling pathways connecting $S1P_1$ with the molecular mechanism, which are implicated in the development of the atheroprotective phenotype in macrophages. $S1P_1$ linking to the trimeric G_i protein triggers several signaling cascades, which in addition to the conventional inhibition of cAMP, includes the activation of Akt and PI3K[255,256]. Accordingly, the drop in the intracellular cAMP concentration and PKA activity and an increased Akt activity, were noted in macrophages isolated from *S1pr1-LysMCre* and *S1pr1-F4/80Cre* mice. By contrast, STAT3 which is activated by $S1P_1$ in various tumor cell lines[257,258], remained latent in $S1P_1$-overexpressing macrophages. Furthermore, the activity of STAT6, which is involved in the development of M2 phenotype in macrophages exposed to IL-4[259], was not influenced by the $S1P_1$ expression[249].

Previous studies demonstrated a decreased PU.1 promoter binding in macrophages upon elevating intracellular cAMP levels and stimulating PKA activity[242,260]. Accordingly, the reversal of increased PU.1 and IRF8 expression could be observed in S1P1-overexpressing macrophages stimulated with cAMP mimetic DB-cAMP.

Although the effects of suppressing cAMP signaling on the atherosclerotic plaque development were not investigated to date, the present study suggests that the low level of cAMP coupled to the enhanced PU.1 and IRF8 expression in macrophages could account for the anti-inflammatory activity related to the macrophage phenotype and a consequent

reduction of atherosclerosis in *S1pr1-LysMCre* and *S1pr1-F4/80Cre* mice. Moreover, the Akt activation in macrophages was clearly linked to several anti-atherogenic effects. As an example, Akt was able to promote macrophage survival thought the inhibition of caspase-3 or to stimulate transcriptional activation of anti-apoptotic genes[261]. Consistently, macrophages isolated from LDL-related protein-1 deficient mice (*Lrp-1*$^{-/-}$), with a defective Akt activation, presented an impaired efferocytosis[262]. Finally, upregulation of Akt activity promotes the M2 macrophage polarization, whereas its attenuation gives rise to the M1 phenotype[263]. In this context, it is of interest how Akt is identified as a triggering component of the signaling pathway encompassing mTORC1, which is the lysosomal adapter protein Lamtor-1, and LXR, and culminating in the M2 macrophage polarization[241]. Consistent with these findings, we noted that the activation of LXR in $S1P_1$-overexpressing macrophages is dependent on the activation of Akt, mTORC1, and Lamtor-1, as it is abolished in the presence of respective inhibitors. Altogether, our present results and evidences of previous studies point to the role of Akt as an important mediator of the anti-atherogenic effect exerted by $S1P_1$ in macrophages.

In conclusion, the results of the present study document that the amplification of $S1P_1$-dependent signaling in monocytes and macrophages countervails the development of vascular lesion in a murine model of atherosclerosis. The underlying molecular mechanisms involve the emergence of a novel macrophage phenotype, in which the parallel activation of transcription factors PU.1/IRF8 and LXR coordinates several anti-atherogenic pathways including enhanced secretion of anti-inflammatory cytokines, cholesterol disposal and efferocytosis as well as reduced ER stress-induced apoptosis. Further investigations will be required to understand whether and to which extent the atheroprotective mechanisms of S1P identified here may contribute to the beneficial effect of this lysosphingolipid on cardiovascular risk inferred from observational studies in humans.

References

1. Bartke, N. & Hannun, Y. A. Bioactive sphingolipids: metabolism and function. *J. Lipid Res.* **50**, S91–S96 (2009).
2. Pralhada Rao, R. *et al.* Sphingolipid Metabolic Pathway: An Overview of Major Roles Played in Human Diseases. *J. Lipids* **2013**, 1–12 (2013).
3. Gault, C., Obeid, L. & Hannun, Y. An overview of sphingolipid metabolism: from synthesis to breakdown. *Adv Exp Med Biol* **688**, 1–23 (2010).
4. Futerman, A. H. & Hannun, Y. A. The complex life of simple sphingolipids. *EMBO Rep.* **5**, 1–6 (2004).
5. Hannun, Y. A. & Obeid, L. M. Principles of bioactive lipid signalling: Lessons from sphingolipids. *Nat. Rev. Mol. Cell Biol.* **9**, 139–150 (2008).
6. Proia, R. L., Hla, T., Proia, R. L. & Hla, T. Emerging biology of sphingosine-1-phosphate: its role in pathogenesis and therapy. *J. Clin. Invest* **125**, 1379–1387 (2013).
7. Le Stunff, H. *et al.* Recycling of sphingosine is regulated by the concerted actions of sphingosine-1-phosphate phosphohydrolase 1 and sphingosine kinase 2. *J. Biol. Chem.* **282**, 34372–34380 (2007).
8. Schwab, S. R. Lymphocyte Sequestration Through S1P Lyase Inhibition and Disruption of S1P Gradients. **1735**, 1735–1740 (2011).
9. Hla, T., Venkataraman, K. & Michaud, J. The vascular S1P gradient-Cellular sources and biological significance. *Biochim. Biophys. Acta - Mol. Cell Biol. Lipids* **1781**, 477–482 (2008).
10. Venkataraman, K. *et al.* Vascular endothelium as a contributor of plasma sphingosine 1-phosphate. *Circ. Res.* **102**, 669–676 (2008).
11. Mitra, P. *et al.* Role of ABCC1 in export of sphingosine-1-phosphate from mast cells. *Proc Natl Acad Sci U S A* **103**, 16394–9 (2006).
12. Takabe, K., Paugh, S. W., Milstien, S. & Spiegel, S. '. Inside-Out ' Signaling of Sphingosine-1-phosphate: Therapeutic targets. *Pharmacol Rev.* **60**, 181–195 (2008).
13. Vu, T. M. *et al.* Mfsd2b is essential for the sphingosine-1-phosphate export in erythrocytes and platelets. *Nature* **550**, 524–528 (2017).
14. Ito, K. *et al.* Lack of sphingosine 1-phosphate-degrading enzymes in erythrocytes. *Biochem. Biophys. Res. Commun.* **357**, 212–217 (2007).
15. Venkataraman, K. *et al.* Vascular endothelium as a contributor of plasma sphingosine 1-phosphate. *Circ. Res.* **102**, 669–676 (2008).
16. Deepa Jonnalagadda, Manjula Sunkara, Andrew J. Morris, and S. W. W. Granule-Mediated Release of Sphingosine-1-Phosphate by Activated Platelets. *Biochim Biophys Acta* **1841**, 1581–1589 (2014).
17. Kobayashi, N., Nishi, T., Hirata, T. & Kihara, A. Sphingosine 1-phosphate is released from the cytosol of rat platelets in a carrier-mediated manner. *J Lipid Res* **47**, (2006).
18. Anada, Y., Igarashi, Y. & Kihara, A. The immunomodulator FTY720 is phosphorylated and released from platelets. *Eur J Pharmacol* **568**, 106–111 (2007).
19. Sato, K. *et al.* Critical role of ABCA1 transporter in sphingosine 1-phosphate release from astrocytes. *J. Neurochem.* **103**, 2610–2619 (2007).
20. Nishi, T. *et al.* The Sphingolipid Transporter Spns2 Functions in Migration of Zebrafish Myocardial Precursors. *Science (80-.).* **323**, 524–527 (2008).
21. Murata, N. *et al.* Interaction of sphingosine 1-phosphate with plasma components, including lipoproteins, regulates the lipid receptor-mediated actions. *Biochem. J.* **352 Pt 3**, 809–15 (2000).
22. Christoffersen, C. & Nielsen, L. B. Apolipoprotein M: Bridging HDL and endothelial function. *Curr. Opin. Lipidol.* **24**, 295–300 (2013).
23. Karuna, R. *et al.* Plasma levels of sphingosine-1-phosphate and apolipoprotein M in patients with monogenic disorders of HDL metabolism. *Atherosclerosis* **219**, 855–863 (2011).
24. Christoffersen, C. *et al.* Endothelium-protective sphingosine-1-phosphate provided by HDL-associated apolipoprotein M. *Proc Natl Acad Sci U S A* **108**, 9613–9618 (2011).
25. Spiegel, S. & Milstien, S. The outs and the ins of sphingosine-1-phosphate in immunity. *Nat. Rev. Immunol.* **11**, 403–415 (2011).
26. Obinata, H. & Hla, T. Sphingosine 1-phosphate and inflammation. *Int. Immunol.* 1–9 (2019).

doi:10.1093/intimm/dxz037
27. Receptors, P. Lysophospholipid G Protein-coupled Receptors*. *J. Biol. Chem.* **1**, 3–7 (2004).
28. Chun, J., Hla, T., Lynch, K. R., Spiegel, S. & Moolenaar, W. H. International Union of Basic and Clinical Pharmacology . LXXVIII . Lysophospholipid. *Pharmacol. Rev.* **62**, 579–587 (2010).
29. Rosen, H. & Goetzl, E. J. Sphingosine 1-phosphate and its receptors: an autocrine and paracrine network. *Nat. Rev. Immunol.* **5**, 560–570 (2005).
30. Liu, Y. *et al.* Edg-1 , the G protein – coupled receptor for sphingosine-1-phosphate , is essential for vascular maturation. *J. Clin. Invest* **106**, 951–961 (2000).
31. Brinkmann, V. *et al.* The Immune Modulator FTY720 Targets Sphingosine 1-Phosphate Receptors *. *J. Biol. Chem.* **277**, 21453–21457 (2002).
32. Aoki, M., Aoki, H., Ramanathan, R., Hait, N. C. & Takabe, K. Sphingosine-1-Phosphate Signaling in Immune Cells and Inflammation: Roles and Therapeutic Potential. *Mediators Inflamm.* **2016**, 1–11 (2016).
33. Wang, F. *et al.* Sphingosine 1-Phosphate Stimulates Cell Migration through a G i -coupled Cell Surface Receptor. *J. Biol. Chem.* **274**, 35343–35350 (1999).
34. Garcia, J. G. N. *et al.* Sphingosine 1-phosphate promotes endothelial cell barrier integrity by Edg-dependent cytoskeletal rearrangement. *J. Clin. Invest* **108**, 689–701 (2001).
35. Lee, M. J. *et al.* Akt-mediated phosphorylation of the G protein-coupled receptor EDG-1 is required for endothelial cell chemotaxis. *Mol. Cell* **8**, 693–704 (2001).
36. Christopher Kable Means, Shigeki Miyamoto, J. C. and J. H. B. S1P1 receptor localization confers selectivity for Gi-mediated cAMP and contractile responses. *J. Biol. Chem.* **283**, 11954 –11963 (2008).
37. Pulli, I., Asghar, M. Y., Kemppainen, K. & Törnquist, K. Sphingolipid-mediated calcium signaling and its pathological effects. *BBA - Mol. Cell Res.* **1865**, 1668–1677 (2018).
38. Im, D.-S., Tomura, H., Tobo, M., Sato, K. & Okajima, F. Enhancement of sphingosine 1-phosphate-induced phospholipase C activation during G(0)-G(1) transition in rat hepatocytes. *J. Pharmacol. Sci.* **95**, 284–290 (2004).
39. Takashima, S. *et al.* G 12 / 13 and G q mediate S1P 2 -induced inhibition of Rac and migration in vascular smooth muscle in a manner dependent on Rho but not Rho kinase. *Cardiovasc. Res.* 689–697 (2008).
40. Sugimoto, N., Takuwa, N., Okamoto, H., Sakurada, S. & Takuwa, Y. Inhibitory and Stimulatory Regulation of Rac and Cell Motility by the G 12 / 13 -Rho and G i Pathways Integrated Downstream of a Single G Protein-Coupled Sphingosine-1-Phosphate Receptor Isoform. *Mol. Cell. Biol.* **23**, 1534–1545 (2003).
41. Park, S. & Im, D. Sphingosine 1-Phosphate Receptor Modulators and Drug Discovery. *Biomol Ther* **25**, 80–90 (2017).
42. Galvani, S. *et al.* HDL-bound sphingosine 1-phosphate acts as a biased agonist for the endothelial cell receptor S1P1 to limit vascular inflammation. *Sci sign* **8**, 1–26 (2016).
43. Benechet, A. P. *et al.* T cell-intrinsic S1PR1 regulates endogenous effector T-cell egress dynamics from lymph nodes during infection. *Proc. Natl. Acad. Sci. U. S. A.* **113**, 2182–2187 (2016).
44. Ku, D. N., Giddens, D. P., Zarins, C. K. & Glagov, S. Pulsatile flow and atherosclerosis in the human carotid bifurcation. Positive correlation between plaque location and low oscillating shear stress. *Arteriosclerosis* **5**, 293–302 (1985).
45. Lepley, D., Paik, J. H., Hla, T. & Ferrer, F. The G protein-coupled receptor S1P2 regulates Rho/Rho kinase pathway to inhibit tumor cell migration. *Cancer Res.* **65**, 3788–3795 (2005).
46. Skoura, A. *et al.* Sphingosine-1-phosphate receptor-2 function in myeloid cells regulates vascular inflammation and atherosclerosis. *Arterioscler. Thromb. Vasc. Biol.* **31**, 81–85 (2011).
47. Shimizu, T. *et al.* Sphingosine 1-phosphate receptor 2 negatively regulates neointimal formation in mouse arteries. *Circ. Res.* **101**, 995–1000 (2007).
48. Okamoto, H. *et al.* Inhibitory regulation of Rac activation, membrane ruffling, and cell migration by the G protein-coupled sphingosine-1-phosphate receptor EDG5 but not EDG1 or EDG3. *Mol. Cell. Biol.* **20**, 9247–61 (2000).
49. Das, A., Lenz, S. M., Awojoodu, A. O. & Botchwey, E. A. Abluminal stimulation of sphingosine 1-phosphate receptors 1 and 3 promotes and stabilizes endothelial sprout formation. *Tissue Eng. Part A* **21**, 202–213 (2015).
50. Murakami, A. *et al.* Sphingosine 1-phosphate (S1P) regulates vascular contraction via S1P3 receptor: investigation based on a new S1P3

receptor antagonist. *Mol. Pharmacol.* **77**, 704–713 (2010).
51. Murakami, K. *et al.* Knock out of S1P3 receptor signaling attenuates inflammation and fibrosis in bleomycin-induced lung injury mice model. *PLoS One* **9**, e106792 (2014).
52. Nofer, J. R. *et al.* Suppression of endothelial cell apoptosis by high density lipoproteins (HDL) and HDL-associated lysosphingolipids. *J. Biol. Chem.* **276**, 34480–34485 (2001).
53. Keul, P. *et al.* Sphingosine-1-phosphate receptor 3 promotes recruitment of monocyte/macrophages in inflammation and atherosclerosis. *Circ. Res.* **108**, 314–323 (2011).
54. Pyne, S. & Pyne, N. J. Sphingosine 1-phosphate signalling in mammalian cells. *Biochem. J.* **402**, 385–402 (2000).
55. Ghosh, T. K., Bian, J. & Gill, D. L. Intracellular Calcium Release Mediated by Sphingosine Derivatives Generated in Cells. *Science (80-.).* **248**, 1653–1656 (1990).
56. Alvarez, S. E. *et al.* Sphingosine-1-phosphate is a missing cofactor for the E3 ubiquitin ligase TRAF2. *Nature* **465**, 1084–1088 (2010).
57. Xia, P. *et al.* Sphingosine kinase interacts with TRAF2 and dissects tumor necrosis factor-alpha signaling. *J. Biol. Chem.* **277**, 7996–8003 (2002).
58. P. Puneet, C.T. Yap, A. J. M. SphK1 regulates proinflammatory responses associated with endotoxin and polymicrobial sepsis. *Science (80-.).* **328**, 1290–1294 (2010).
59. Hait, N. C. *et al.* Regulation of Histone Acetylation in the Nucleus by Sphingosine-1- Phosphate. *Science (80-.).* **325**, 1254–1257 (2009).
60. Gartel, A. L. & Tyner, A. L. The role of the cyclin-dependent kinase inhibitor p21 in apoptosis. *Mol. Cancer Ther.* **1**, 639–49 (2002).
61. Strub, G. M. *et al.* Sphingosine-1-phosphate produced by sphingosine kinase 2 in mitochondria interacts with prohibitin 2 to regulate complex IV assembly and respiration. *FASEB J.* **25**, 600–612 (2011).
62. Zhang, H. *et al.* Sphingosine-l-Phosphate, a Novel Lipid, Involved in Cellular Proliferation. **114**, (1991).
63. Kleuser, B., Cuvillier, O. & Spiegel, S. 1Alpha,25-dihydroxyvitamin D3 inhibits programmed cell death in HL-60 cells by activation of sphingosine kinase. (1998).
64. Obeid, L. M., Linardic, C. M., Karolak, L. A. & Hannun, Y. A. Programmed Cell Death Induced by Ceramide. *Science (80-.).* **259**, 1769–1771 (1993).
65. Spiegel, S. & Milstien, S. Sphingosine-1-phosphate: an enigmatic signalling lipid. **4**, (2003).
66. Cuvillier, O., Pirianov, G., Kleuser, B., Vanek, P. G., Coso, O. A., Gutkind, J. S., & Spiegel, S. Suppression of Ceramide-Mediated Programmed Cell Death by Shingosine 1 phosphate.pdf. (1996).
67. Fyrst, H. & Saba, J. D. An update on sphingosine-1-phosphate and other sphingolipid mediators. *Nat. Chem. Biol.* **6**, 489–497 (2011).
68. Michaud, J., Im, D., Hla, T. & Alerts, E. Inhibitory Role of Sphingosine 1-Phosphate Receptor 2 in Macrophage Recruitment during Inflammation. *J. Immunol* (2019). doi:10.4049/jimmunol.0901586
69. Jenne, C. N. *et al.* T-bet – dependent S1P 5 expression in NK cells promotes egress from lymph nodes and bone marrow. *JEM* **206**, 2469–2481 (2009).
70. Allende, M. L. *et al.* Sphingosine-1-phosphate Lyase Deficiency Produces a Pro-inflammatory Response While Impairing Neutrophil. *J. Biol. Chem.* **286**, 7348–7358 (2011).
71. Lewis, N. D. *et al.* Circulating Monocytes are Reduced by Sphingosine-1-Phosphate Receptor Modulators Independently of S1P3. *J. Immunol* **190**, 3533–3540 (2013).
72. Sadahira, Y., Ruan, F., Hakomori, S. & Igarashi, Y. Sphingosine 1-phosphate, a specific endogenous signaling molecule controlling cell motility and tumor cell invasiveness. *Proc. Natl. Acad. Sci. U. S. A.* **89**, 9686–90 (1992).
73. Lee, M. *et al.* Vascular Endothelial Cell Adherens JunctionAssembly and Morphogenesis Inducedby Sphingosine-1-Phosphate. *Cell* **99**, 301–312 (1999).
74. Takuwa, Y., Okamoto, Y., Yoshioka, K. & Takuwa, N. Sphingosine-1-phosphate signaling in physiology and diseases. *BioFactors* **38**, 329–337 (2012).
75. Kono, M. *et al.* The Sphingosine-1-phosphate Receptors S1P1, S1P2, and S1P3 Function Coordinately during Embryonic Angiogenesis. *J. Biol. Chem.* **279**, 29367–29373 (2004).
76. Igarashi, J. & Michel, T. Sphingosine-1-phosphate and modulation of vascular tone. *Cardiovasc. Res.* **82**, 212–220 (2009).
77. Lorenz, J. N., Arend, L. J., Robitz, R., Paul, R. J. & MacLennan, A. J. Vascular dysfunction in S1P2 sphingosine 1-phosphate receptor knockout mice. *Americ*

J. Physiol. - Regul. Integr. Comp. Physiol. **292**, 440–446 (2007).
78. Pyne, N. J., El Buri, A., Adams, D. R. & Pyne, S. Sphingosine 1-phosphate and cancer. *Nat Rev Cancer* **10**, 489–503. (2010).
79. Anelli, V., Gault, C. R., Snider, A. J., Obeid, L. M. & Sp, S.--phosphate. Role of sphingosine kinase-1 in paracrine / transcellular angiogenesis and lymphangiogenesis in vitro. *FASEB J.* 4–6 (2010). doi:10.1096/fj.09-150540
80. Lee, H. *et al.* STAT3-induced S1PR1 expression is crucial for persistent STAT3 activation in tumors. *Nat. Med.* **16**, 1–9 (2010).
81. Visentin, B. *et al.* Validation of an anti-sphingosine-1-phosphate antibody as a potential therapeutic in reducing growth , invasion , and angiogenesis in multiple tumor lineages. *Cancer Cell* 225–238 (2006). doi:10.1016/j.ccr.2006.02.023
82. Liang, J. *et al.* Sphingosine-1-phosphate links persistent STAT3 activation, chronic intestinal inflammation, and development of colitis-associated cancer. *Cancer Cell* **23**, 107–120 (2013).
83. Antoon, J. W. *et al.* Pharmacological inhibition of sphingosine kinase isoforms alters estrogen receptor signaling in human breast cancer. *J. Mol. Endocrinol.* **46**, 205–216 (2011).
84. Pettus, B. J. *et al.* The sphingosine kinase 1/sphingosine-1-phosphate pathway mediates COX-2 induction and PGE2 production in response to TNF-alpha. *FASEB J. Off. Publ. Fed. Am. Soc. Exp. Biol.* **17**, 1411–1421 (2003).
85. Billich, A. *et al.* Basal and induced sphingosine kinase 1 activity in A549 carcinoma cells: function in cell survival and IL-1beta and TNF-alpha induced production of inflammatory mediators. *Cell. Signal.* **17**, 1203–1217 (2005).
86. Kulakowska, A. *et al.* Intrathecal increase of sphingosine 1-phosphate at early stage multiple sclerosis. *Neurosci. Lett.* **477**, 149–152 (2010).
87. Kitano, M. *et al.* Sphingosine 1-phosphate/sphingosine 1-phosphate receptor 1 signaling in rheumatoid synovium: regulation of synovial proliferation and inflammatory gene expression. *Arthritis Rheum.* **54**, 742–753 (2006).
88. Hohlfeld, R. *et al.* A Placebo-Controlled Trial of Oral Fingolimod in Relapsing Multiple Sclerosis. *N. Engl .J. Med.* 387–401 (2010).
89. Scott, F. L. *et al.* Ozanimod (RPC1063) is a potent sphingosine-1-phosphate receptor-1 (S1P 1) and receptor-5 (S1P 5) agonist with autoimmune disease-modifying activity. *Br. J. Pharmacol.* **173**, 1778–1792 (2016).
90. Rasche, L. & Paul, F. Ozanimod for the treatment of relapsing remitting multiple sclerosis. *Expert Opin. Pharmacother.* **19**, 2073–2086 (2018).
91. Dumitrescu, L., Constantinescu, C. S. & Tanasescu, R. Expert Opinion on Pharmacotherapy Siponimod for the treatment of secondary progressive multiple sclerosis. *Expert Opin. Pharmacother.* **20**, 143–150 (2019).
92. Pérez-jeldres, T. *et al.* Targeting Cytokine Signaling and Lymphocyte Traffic via Small Molecules in Inflammatory Bowel Disease : JAK Inhibitors and S1PR Agonists. *Front. Pharmacol.* **10**, 1–15 (2019).
93. Fleischmann, R. Novel small-molecular therapeutics for rheumatoid arthritis. *Curr. Opin. Rheumato.* 335–341 (2012). doi:10.1097/BOR.0b013e32835190ef
94. Weber, C. & Noels, H. Atherosclerosis: current pathogenesis and therapeutic options. *Nat. Med.* **17**, 1410–1422 (2011).
95. Santos-Gallego, C. G., Giannarelli, C. & Badimon, J. J. Experimental models for the investigation of high-density lipoprotein-mediated cholesterol efflux. *Curr. Atheroscler. Rep.* **13**, 266–276 (2011).
96. Lusis, A. Atherosclerosis. *Nature* **407**, 233–241 (2000).
97. Soeki, T. & Sata, M. Inflammatory Biomarkers and Atherosclerosis. *Int. Heart J.* **57**, 134–139 (2016).
98. Albert, M. A. Inflammatory biomarkers, race/ethnicity and cardiovascular disease. *Nutr. Rev.* **65**, S234-8 (2007).
99. Goldstein, J. A. Relation of number of complex coronary lesions to serum C-reactive protein levels and major adverse cardiovascular events at one year. *Am. J. Cardiol.* **96**, 56–60 (2005).
100. Zakynthinos, E. & Pappa, N. Inflammatory biomarkers in coronary artery disease. *J. Cardiol.* **53**, 317–333 (2009).
101. Lorenzatti, A. J. & Servato, M. L. New evidence on the role of inflammation in CVD risk. *Curr. Opin. Cardiol.* **34**, 418–423 (2019).
102. Barton, M., Minotti, R. & Haas, E. Inflammation and atherosclerosis. *Circulation research* **101**, 750–751 (2007).
103. Pant, S. *et al.* Inflammation and

atherosclerosis--revisited. *J. Cardiovasc. Pharmacol. Ther.* **19**, 170–178 (2014).
104. Ross, R. The pathogenesis of atherosclerosis: a perspective for the 1990s. *Nature* **362**, 801–809 (1993).
105. Taleb, S. Inflammation in atherosclerosis. *Arch. Cardiovasc. Dis.* **109**, 708–715 (2016).
106. Haidari, M. *et al.* Increased oxidative stress in atherosclerosis-predisposed regions of the mouse aorta. *Life Sci.* **87**, 100–110 (2010).
107. Cybulsky, M. I. & Jongstra-Bilen, J. Resident intimal dendritic cells and the initiation of atherosclerosis. *Curr. Opin. Lipidol.* **21**, 397–403 (2010).
108. Kzhyshkowska, J., Neyen, C. & Gordon, S. Role of macrophage scavenger receptors in atherosclerosis. *Immunobiology* **217**, 492–502 (2012).
109. Glass, C. K. & Witztum, J. L. Atherosclerosis: the road ahead. *Cell* **104**, 503–516 (2001).
110. Wang, W. *et al.* Oxidized low-density lipoprotein inhibits nitric oxide-mediated coronary arteriolar dilation by up-regulating endothelial arginase I. *Microcirculation* **18**, 36–45 (2011).
111. Kockx, M. M. *et al.* Apoptosis and related proteins in different stages of human atherosclerotic plaques. *Circulation* **97**, 2307–2315 (1998).
112. Wang, B. Y. *et al.* Regression of atherosclerosis: role of nitric oxide and apoptosis. *Circulation* **99**, 1236–1241 (1999).
113. Liu, J. *et al.* Reduced macrophage apoptosis is associated with accelerated atherosclerosis in low-density lipoprotein receptor-null mice. *Arterioscler. Thromb. Vasc. Biol.* **25**, 174–179 (2005).
114. Bhatia, V. K. *et al.* Complement C1q reduces early atherosclerosis in low-density lipoprotein receptor-deficient mice. *Am. J. Pathol.* **170**, 416–426 (2007).
115. Libby, P. Mechanisms of acute coronary syndromes and their implications for therapy. *N. Engl. J. Med.* **368**, 2004–2013 (2013).
116. Moore, K. J. & Tabas, I. Macrophages in the pathogenesis of atherosclerosis. *Cell* **145**, 341–355 (2011).
117. Clarke, M. C. H. & Bennett, M. R. Cause or consequence: what does macrophage apoptosis do in atherosclerosis? *Arteriosclerosis, thrombosis, and vascular biology* **29**, 153–155 (2009).
118. Lutgens, E. *et al.* Biphasic pattern of cell turnover characterizes the progression from fatty streaks to ruptured human atherosclerotic plaques. *Cardiovasc. Res.* **41**, 473–479 (1999).
119. Crisby, M. *et al.* Cell death in human atherosclerotic plaques involves both oncosis and apoptosis. *Atherosclerosis* **130**, 17–27 (1997).
120. Tabas, I. Macrophage death and defective inflammation resolution in atherosclerosis. *Nat. Rev. Immunol.* **10**, 36–46 (2010).
121. Schrijvers, D. M., De Meyer, G. R. Y., Kockx, M. M., Herman, A. G. & Martinet, W. Phagocytosis of apoptotic cells by macrophages is impaired in atherosclerosis. *Arterioscler. Thromb. Vasc. Biol.* **25**, 1256–1261 (2005).
122. Tabas, I. Consequences and Therapeutic Implications of Macrophage Apoptosis in Atherosclerosis The Importance of Lesion Stage and Phagocytic Efficiency. *Arter. Thromb Vasc Biol.* (2005). doi:10.1161/01.ATV.0000184783.04864.9f
123. Fredman, G. *et al.* An imbalance between specialized pro-resolving lipid mediators and pro-inflammatory leukotrienes promotes instability of atherosclerotic plaques. *Nat. Commun.* **7**, 12859 (2016).
124. Ishimoto, Y., Ohashi, K., Mizuno, K. & Nakano, T. Promotion of the uptake of PS liposomes and apoptotic cells by a product of growth arrest-specific gene, gas6. *J. Biochem.* **127**, 411–417 (2000).
125. Ait-Oufella, H. *et al.* Defective mer receptor tyrosine kinase signaling in bone marrow cells promotes apoptotic cell accumulation and accelerates atherosclerosis. *Arterioscler. Thromb. Vasc. Biol.* **28**, 1429–1431 (2008).
126. A-Gonzalez, N. *et al.* Apoptotic cells promote their own clearance and immune tolerance through activation of the nuclear receptor LXR. *Immunity* **31**, 245–258 (2009).
127. Tontonoz, P. & Mangelsdorf, D. J. Liver X receptor signaling pathways in cardiovascular disease. *Mol. Endocrinol.* **17**, 985–993 (2003).
128. Ross, R. Atherosclerosis--an inflammatory disease. *N. Engl. J. Med.* **340**, 115–126 (1999).
129. Roos, A. *et al.* Mini-review: A pivotal role for innate immunity in the clearance of apoptotic cells. *Eur. J. Immunol.* **34**, 921–929 (2004).
130. Seimon, T. & Tabas, I. Mechanisms and consequences of macrophage apoptosis in atherosclerosis. *J. Lipid Res.* S382–S387 (2009).
131. Tabas, I. Macrophage apoptosis in atherosclerosis: consequences on plaque

progression and the role of endoplasmic reticulum stress. *Antioxid. Redox Signal.* **11**, 2333–2339 (2009).
132. Hansson, G. K., Libby, P. & Tabas, I. Inflammation and plaque vulnerability. *J. Intern. Med.* **278**, 483–493 (2015).
133. Hafiane, A. Vulnerable Plaque , Characteristics , Detection , and Potential Therapies. *J Cardiovasc Dev Dis* **6**, 26 (2019).
134. Bentzon, J. F., Otsuka, F., Virmani, R. & Falk, E. Mechanisms of plaque formation and rupture. *Circ. Res.* **114**, 1852–1866 (2014).
135. Watson, K. E. *et al.* TGF-beta 1 and 25-hydroxycholesterol stimulate osteoblast-like vascular cells to calcify. *J. Clin. Invest.* **93**, 2106–2113 (1994).
136. Hjortnaes, J. *et al.* Arterial and aortic valve calcification inversely correlates with osteoporotic bone remodelling: a role for inflammation. *Eur. Heart J.* **31**, 1975–1984 (2010).
137. Naghavi, M. *et al.* From vulnerable plaque to vulnerable patient: a call for new definitions and risk assessment strategies: Part I. *Circulation* **108**, 1664–1672 (2003).
138. Sillesen, H. *et al.* Carotid plaque burden as a measure of subclinical atherosclerosis: comparison with other tests for subclinical arterial disease in the High Risk Plaque BioImage study. *JACC. Cardiovasc. Imaging* **5**, 681–689 (2012).
139. Hansson, G. K. & Hermansson, A. The immune system in atherosclerosis. *Nat. Immunol.* **12**, 204–212 (2011).
140. Ley, K., Miller, Y. I. & Hedrick, C. C. Monocyte and macrophage dynamics during atherogenesis. *Arterioscler. Thromb. Vasc. Biol.* **31**, 1506–1516 (2011).
141. Barringhaus, K. G. *et al.* Alpha4beta1 integrin (VLA-4) blockade attenuates both early and late leukocyte recruitment and neointimal growth following carotid injury in apolipoprotein E (-/-) mice. *J. Vasc. Res.* **41**, 252–260 (2004).
142. Watanabe, T. & Fan, J. Atherosclerosis and inflammation mononuclear cell recruitment and adhesion molecules with reference to the implication of ICAM-1/LFA-1 pathway in atherogenesis. *Int. J. Cardiol.* **66 Suppl 1**, S45–53; discussion S55 (1998).
143. Rolin, J. & Maghazachi, A. A. Implications of chemokines, chemokine receptors, and inflammatory lipids in atherosclerosis. *J. Leukoc. Biol.* **95**, 575–585 (2014).
144. Combadiere, C. *et al.* Combined inhibition of CCL2, CX3CR1, and CCR5 abrogates Ly6C(hi) and Ly6C(lo) monocytosis and almost abolishes atherosclerosis in hypercholesterolemic mice. *Circulation* **117**, 1649–1657 (2008).
145. Hansson, G. K. & Libby, P. The immune response in atherosclerosis: a double-edged sword. *Nat. Rev. Immunol.* **6**, 508–519 (2006).
146. Geissmann, F. *et al.* Development of monocytes, macrophages, and dendritic cells. *Science* **327**, 656–661 (2010).
147. Swirski, F. K. *et al.* Ly-6Chi monocytes dominate hypercholesterolemia-associated monocytosis and give rise to macrophages in atheromata. *J. Clin. Invest.* **117**, 195–205 (2007).
148. Tacke, F. *et al.* Monocyte subsets differentially employ CCR2, CCR5, and CX3CR1 to accumulate within atherosclerotic plaques. *J. Clin. Invest.* **117**, 185–194 (2007).
149. Auffray, C., Sieweke, M. H. & Geissmann, F. Blood monocytes: development, heterogeneity, and relationship with dendritic cells. *Annu. Rev. Immunol.* **27**, 669–692 (2009).
150. Nahrendorf, M. *et al.* The healing myocardium sequentially mobilizes two monocyte subsets with divergent and complementary functions. *J. Exp. Med.* **204**, 3037–3047 (2007).
151. Egawa, M. *et al.* Inflammatory monocytes recruited to allergic skin acquire an anti-inflammatory M2 phenotype via basophil-derived interleukin-4. *Immunity* **38**, 570–580 (2013).
152. Rahman, K. *et al.* Inflammatory Ly6C hi monocytes and their conversion to M2 macrophages drive atherosclerosis regression Find the latest version : Inflammatory Ly6C hi monocytes and their conversion to M2 macrophages drive atherosclerosis regression. *J Clin Invest* **127**, 2904–2915 (2017).
153. Woollard, K. J. & Geissmann, F. Monocytes in atherosclerosis: subsets and functions. *Nat. Rev. Cardiol.* **7**, 77–86 (2010).
154. Smith, J. D. *et al.* Decreased atherosclerosis in mice deficient in both macrophage colony-stimulating factor (op) and apolipoprotein E. *Proc. Natl. Acad. Sci. U. S. A.* **92**, 8264–8268 (1995).
155. Taylor, P. R. & Gordon, S. Monocyte heterogeneity and innate immunity. *Immunity* **19**, 2–4 (2003).
156. Murray, P. J. *et al.* Macrophage activation and polarization: nomenclature and experimental guidelines. *Immunity* **41**, 14–

20 (2014).
157. Adamson, S. & Leitinger, N. Phenotypic modulation of macrophages in response to plaque lipids. *Curr. Opin. Lipidol.* **22**, 335–342 (2011).
158. Chinetti-Gbaguidi, G. *et al.* Human atherosclerotic plaque alternative macrophages display low cholesterol handling but high phagocytosis because of distinct activities of the PPARgamma and LXRalpha pathways. *Circ. Res.* **108**, 985–995 (2011).
159. Stoger, J. L. *et al.* Distribution of macrophage polarization markers in human atherosclerosis. *Atherosclerosis* **225**, 461–468 (2012).
160. Ohta, H. *et al.* Disruption of tumor necrosis factor-alpha gene diminishes the development of atherosclerosis in ApoE-deficient mice. *Atherosclerosis* **180**, 11–17 (2005).
161. Kirii, H. *et al.* Lack of interleukin-1beta decreases the severity of atherosclerosis in ApoE-deficient mice. *Arterioscler. Thromb. Vasc. Biol.* **23**, 656–660 (2003).
162. Mantovani, A. & Sozzani, S. Macrophage polarization: tumor-associated macrophages as a paradigm for polarized M2 mononuclear phagocytes. *Trends Immunol.* **23**, 549–555 (2002).
163. Bobryshev, Y. V, Nikiforov, N. G., Elizova, N. V & Orekhov, A. N. Macrophages and Their Contribution to the Development of Atherosclerosis. *Results Probl Cell Differ*. 273–298 (2017). doi:10.1007/978-3-319-54090-0
164. Moore, K. J., Sheedy, F. J. & Fisher, E. A. Macrophages in atherosclerosis: a dynamic balance. *Nat. Rev. Immunol.* **13**, 709–721 (2013).
165. Martinez, F. O., Sica, A., Mantovani, A. & Locati, M. Macrophage activation and polarization. *Front. Biosci.* **13**, 453–461 (2008).
166. Pilling, D., Galvis-Carvajal, E., Karhadkar, T. R., Cox, N. & Gomer, R. H. Monocyte differentiation and macrophage priming are regulated differentially by pentraxins and their ligands. *BMC Immunol.* **18**, 30 (2017).
167. Zizzo, G., Hilliard, B. A., Monestier, M. & Cohen, P. L. Efficient clearance of early apoptotic cells by human macrophages requires M2c polarization and MerTK induction. *J. Immunol.* **189**, 3508–3520 (2012).
168. Ferrante, C. J. *et al.* The adenosine-dependent angiogenic switch of macrophages to an M2-like phenotype is independent of interleukin-4 receptor alpha (IL-4Ralpha) signaling. *Inflammation* **36**, 921–931 (2013).
169. Liberale, L., Dallegri, F., Montecucco, F. & Carbone, F. Pathophysiological relevance of macrophage subsets in atherogenesis. *Thromb. Haemost.* **117**, 7–18 (2017).
170. Finn, A. V *et al.* Hemoglobin directs macrophage differentiation and prevents foam cell formation in human atherosclerotic plaques. *J. Am. Coll. Cardiol.* **59**, 166–177 (2012).
171. Boyle, J. J. Heme and haemoglobin direct macrophage Mhem phenotype and counter foam cell formation in areas of intraplaque haemorrhage. *Curr. Opin. Lipidol.* **23**, 453–461 (2012).
172. Boyle, J. J. *et al.* Activating transcription factor 1 directs Mhem atheroprotective macrophages through coordinated iron handling and foam cell protection. *Circ. Res.* **110**, 20–33 (2012).
173. Kadl, A. *et al.* Identification of a novel macrophage phenotype that develops in response to atherogenic phospholipids via Nrf2. *Circ. Res.* **107**, 737–746 (2010).
174. Gill, N. *et al.* The immunophenotype of decidual macrophages in acute atherosis. *Am. J. Reprod. Immunol.* **81**, e13098 (2019).
175. Colin, S., Chinetti-Gbaguidi, G. & Staels, B. Macrophage phenotypes in atherosclerosis. *Immunol. Rev.* **262**, 153–66 (2014).
176. Erbel, C. *et al.* Prevalence of M4 macrophages within human coronary atherosclerotic plaques is associated with features of plaque instability. *Int. J. Cardiol.* **186**, 219–225 (2015).
177. Shin, H. J. & McCullough, P. A. Focus on lipids: high-density lipoprotein cholesterol and its associated lipoproteins in cardiac and renal disease. *Nephron. Clin. Pract.* **127**, 158–164 (2014).
178. von Eckardstein, A., Nofer, J. R. & Assmann, G. High density lipoproteins and arteriosclerosis. Role of cholesterol efflux and reverse cholesterol transport. *Arterioscler. Thromb. Vasc. Biol.* **21**, 13–27 (2001).
179. Rothblat, G. H. & Phillips, M. C. High-density lipoprotein heterogeneity and function in reverse cholesterol transport. *Curr. Opin lipidol* **21**, 229–238 (2010).
180. Tall, A. R. Cholesterol efflux pathways and other potential mechanisms involved in the athero-protective effect of high density lipoproteins. *J. Intern. Med.* **263**, 256–273 (2008).
181. Nofer, J. R. & Assmann, G.

Atheroprotective effects of high-density lipoprotein-associated lysosphingolipids. *Trends Cardiovasc. Med.* **15**, 265–271 (2005).
182. Ma, L. *et al.* Ht31, a protein kinase A anchoring inhibitor, induces robust cholesterol efflux and reverses macrophage foam cell formation through ATP-binding cassette transporter A1. *J. Biol. Chem.* **286**, 3370–3378 (2011).
183. Nofer, J.-R. *et al.* Apolipoprotein A-I activates Cdc42 signaling through the ABCA1 transporter. *J. Lipid Res* **47**, 794–803 (2006).
184. Tang, C., Liu, Y., Kessler, P. S., Vaughan, A. M. & Oram, J. F. The macrophage cholesterol exporter ABCA1 functions as an anti-inflammatory receptor. *J. Biol. Chem.* **284**, 32336–32343 (2009).
185. Liu, D. *et al.* Human apolipoprotein A-I induces cyclooxygenase-2 expression and prostaglandin I-2 release in endothelial cells through ATP-binding cassette transporter A1. *Am J. Physiol. Cell physiol* **301**, C739-48 (2011).
186. Kimura, T. *et al.* Role of scavenger receptor class B type I and sphingosine 1-phosphate receptors in high density lipoprotein-induced inhibition of adhesion molecule expression in endothelial cells. *J. Biol. Chem.* **281**, 37457–37467 (2006).
187. Nofer, J.-R. *et al.* High density lipoprotein-associated lysosphingolipids reduce E-selectin expression in human endothelial cells. *Biochem Biophys Res Comm* **310**, 98–103 (2003).
188. Cockerill, G. W. *et al.* Elevation of plasma high-density lipoprotein concentration reduces interleukin-1-induced expression of E-selectin in an in vivo model of acute inflammation. *Circulation* **103**, 108–112 (2001).
189. Fuller, M. *et al.* The effects of diet on occlusive coronary artery atherosclerosis and myocardial infarction in scavenger receptor class B, type 1/low-density lipoprotein receptor double knockout mice. *Arter. Thromb Vasc Biol* **34**, 2394–2403 (2014).
190. Tabet, F. *et al.* HDL-transferred microRNA-223 regulates ICAM-1 expression in endothelial cells. *Nat commun* **5**, 3292 (2014).
191. Mineo, C. & Shaul, P. W. Role of high-density lipoprotein and scavenger receptor B type I in the promotion of endothelial repair. *Trends Cardiovas Med.* **17**, 156–161 (2007).
192. Seetharam, D. *et al.* High-density lipoprotein promotes endothelial cell migration and reendothelialization via scavenger receptor-B type I. *Circ Res* **98**, 63–72 (2006).
193. Argraves, K. M. & Argraves, W. S. HDL serves as a S1P signaling platform mediating a multitude of cardiovascular effects. *J Lipid Res* **48**, 2325–2333 (2007).
194. Argraves, K. M. *et al.* High density lipoprotein-associated sphingosine 1-phosphate promotes endothelial barrier function. *J. Biol. Chem.* **283**, 25074–25081 (2008).
195. Duenas, A. I. *et al.* Selective attenuation of Toll-like receptor 2 signalling may explain the atheroprotective effect of sphingosine 1-phosphate. *Cardiovasc. Res.* **79**, 537–544 (2008).
196. Nofer, J. R. *et al.* FTY720, a synthetic sphingosine 1 phosphate analogue, inhibits development of atherosclerosis in low-density lipoprotein receptor-deficient mice. *Circulation* **115**, 501–508 (2007).
197. Potí, F. *et al.* KRP-203, sphingosine 1-phosphate receptor type 1 agonist, ameliorates atherosclerosis in LDL-R-/- mice. *Arterioscler. Thromb. Vasc. Biol.* **33**, 1505–1512 (2013).
198. Murphy, A. J., Chin-Dusting, J. P. F., Sviridov, D. & Woollard, K. J. The anti inflammatory effects of high density lipoproteins. *Curr. Med. Chem.* **16**, 667–675 (2009).
199. Blaho, V. A. & Hla, T. An update on the biology of sphingosine 1-phosphate receptors. *J Lipid Res* **55**, 1596–1608 (2014).
200. Christoffersen, C., Bartels, E. D., Aarup, A., Nielsen, L. B. & Pedersen, T. X. ApoB and apoM - New aspects of lipoprotein biology in uremia-induced atherosclerosis. *Eur. J. Pharmacol.* **816**, 154–160 (2017).
201. Argraves, K. M. *et al.* S1P, dihydro-S1P and C24:1-ceramide levels in the HDL-containing fraction of serum inversely correlate with occurrence of ischemic heart disease. *Lipids Health Dis.* **10**, 70 (2011).
202. Poti, F. *et al.* KRP-203, sphingosine 1-phosphate receptor type 1 agonist, ameliorates atherosclerosis in LDL-R-/- mice. *Arterioscler. Thromb. Vasc. Biol.* **33**, 1505–1512 (2013).
203. Nofer, J.-R. *et al.* FTY720, a synthetic sphingosine 1 phosphate analogue, inhibits development of atherosclerosis in low-density lipoprotein receptor-deficient mice. *Circulation* **115**, 501–508 (2007).
204. Keul, P. *et al.* The sphingosine-1-phosphate analogue FTY720 reduces atherosclerosis in apolipoprotein E-

deficient mice. *Arterioscler. Thromb. Vasc. Biol.* **27**, 607–613 (2007).
205. Bot, M. *et al.* Hematopoietic Sphingosine 1-Phosphate Lyase Deficiency Decreases Atherosclerotic Lesion Development in LDL-Receptor Deficient Mice. *PLoS One* **8**, 1–13 (2013).
206. Feuerborn, R. *et al.* Elevating Endogenous Sphingosine-1-Phosphate (S1P) Levels Improves Endothelial Function and Ameliorates Atherosclerosis in Low Density Lipoprotein Receptor-Deficient (LDL-R−/−) Mice. *Thromb. Haemost.* **118**, 1470–1480 (2018).
207. Gonzalez, L., Qian, A. S., Tahir, U., Yu, P. & Trigatti, B. L. Sphingosine-1-phosphate receptor 1, expressed in myeloid cells, slows diet-induced atherosclerosis and protects against macrophage apoptosis in ldlr KO mice. *Int. J. Mol. Sci.* **18**, 1–22 (2017).
208. Kimura, T. *et al.* High-density lipoprotein stimulates endothelial cell migration and survival through sphingosine 1-phosphate and its receptors. *Arterioscler. Thromb. Vasc. Biol.* **23**, 1283–1288 (2003).
209. Nofer, J. R. *et al.* HDL induces NO-dependent vasorelaxation via the lysophospholipid receptor S1P3. *J. Clin. Invest.* **113**, 569–581 (2004).
210. Kimura, T. *et al.* Mechanism and role of high density lipoprotein-induced activation of AMP-activated protein kinase in endothelial cells. *J. Biol. Chem.* **285**, 4387–4397 (2010).
211. Tolle, M. *et al.* HDL-associated lysosphingolipids inhibit NAD(P)H oxidase-dependent monocyte chemoattractant protein-1 production. *Arterioscler. Thromb. Vasc. Biol.* **28**, 1542–1548 (2008).
212. Cooney, M. T. *et al.* HDL cholesterol protects against cardiovascular disease in both genders, at all ages and at all levels of risk. *Atherosclerosis* **206**, 611–616 (2009).
213. Fisher, E. A., Feig, J. E., Hewing, B., Hazen, S. L. & Smith, J. D. High-density lipoprotein function, dysfunction, and reverse cholesterol transport. *Arterioscler. Thromb. Vasc. Biol.* **32**, 2813–2820 (2012).
214. Barter, P. J., Puranik, R. & Rye, K.-A. New insights into the role of HDL as an anti-inflammatory agent in the prevention of cardiovascular disease. *Curr. Cardiol. Rep.* **9**, 493–498 (2007).
215. Yvan-Charvet, L., Wang, N. & Tall, A. R. Role of HDL, ABCA1, and ABCG1 transporters in cholesterol efflux and immune responses. *Arterioscler. Thromb. Vasc. Biol.* **30**, 139–143 (2010).
216. Westerterp, M. *et al.* ATP-binding cassette transporters, atherosclerosis, and inflammation. *Circ. Res.* **114**, 157–170 (2014).
217. Okajima, F., Sato, K. & Kimura, T. Anti-atherogenic actions of high-density lipoprotein through sphingosine 1-phosphate receptors and scavenger receptor class B type I. *Endocr. J.* **56**, 317–334 (2009).
218. Nofer, J. R. High-density lipoprotein, sphingosine 1-phosphate, and atherosclerosis. *J. Clin. Lipidol.* **2**, 4–11 (2008).
219. Egom, E. E., Mamas, M. A. & Soran, H. HDL quality or cholesterol cargo: What really matters - Spotlight on sphingosine-1-phosphate-rich HDL. *Curr. Opin. Lipidol.* **24**, 351–356 (2013).
220. Sattler, K. J. E. *et al.* Sphingosine 1-phosphate levels in plasma and HDL are altered in coronary artery disease. *Basic Res. Cardiol.* **105**, 821–832 (2010).
221. Duong, C. Q. *et al.* Expression of the lysophospholipid receptor family and investigation of lysophospholipid-mediated responses in human macrophages. *Biochim. Biophys. Acta - Mol. Cell Biol. Lipids* **1682**, 112–119 (2004).
222. Clausen, B. E., Burkhardt, C., Reith, W., Renkawitz, R. & Forster, I. Conditional gene targeting in macrophages and granulocytes using LysMcre mice. *Transgenic Res.* **8**, 265–277 (1999).
223. Schaller, E. *et al.* Inactivation of the F4/80 glycoprotein in the mouse germ line. *Mol. Cell. Biol.* **22**, 8035–8043 (2002).
224. Ishibashi, S. *et al.* Hypercholesterolemia in low density lipoprotein receptor knockout mice and its reversal by adenovirus-mediated gene delivery. *J. Clin. Invest.* **92**, 883–893 (1993).
225. Burkhardt, R. *et al.* Cosegregation of aortic root atherosclerosis and intermediate lipid phenotypes on chromosomes 2 and 8 in an intercross of C57BL/6 and BALBc/ByJ low-density lipoprotein receptor-/- mice. *Arterioscler. Thromb. Vasc. Biol.* **31**, 775–784 (2011).
226. Schindelin, J. *et al.* Fiji: an open-source platform for biological-image analysis. *Nat. Methods* **9**, 676–682 (2012).
227. Thorp, E., Cui, D., Schrijvers, D. M., Kuriakose, G. & Tabas, I. Mertk receptor mutation reduces efferocytosis efficiency and promotes apoptotic cell accumulation and plaque necrosis in atherosclerotic lesions of apoe-/- mice. *Arterioscler.*

Thromb. Vasc. Biol. **28**, 1421–1428 (2008).
228. Kallio, M. A. *et al.* Chipster: user-friendly analysis software for microarray and other high-throughput data. *BMC Genomics* **12**, 507 (2011).
229. Smyth, G. K. Linear models and empirical bayes methods for assessing differential expression in microarray experiments. *Stat. Appl. Genet. Mol. Biol.* **3**, (2004).
230. Zhou, Y. *et al.* Metascape provides a biologist-oriented resource for the analysis of systems-level datasets. *Nat. Commun.* **10**, 1523 (2019).
231. Heng, T. S. P. & Painter, M. W. The Immunological Genome Project: networks of gene expression in immune cells. *Nat immunol* **9**, 1091–1094 (2008).
232. Feuerborn, R. *et al.* Elevating Endogenous Sphingosine-1-Phosphate (S1P) Levels Improves Endothelial Function and Ameliorates Atherosclerosis in Low Density Lipoprotein Receptor-Deficient (LDL-R-/-) Mice. *Thromb. Haemost.* **118**, 1470–1480 (2018).
233. Tjaden, K. *et al.* Low density lipoprotein interferes with intracellular signaling of monocytes resulting in impaired chemotaxis and enhanced chemokinesis. *Int. J. Cardiol.* **255**, 160–165 (2018).
234. Kurotaki, D. *et al.* Essential role of the IRF8-KLF4 transcription factor cascade in murine monocyte differentiation. *Blood* **121**, 1839–1849 (2013).
235. Feinberg, M. W. *et al.* The Kruppel-like factor KLF4 is a critical regulator of monocyte differentiation. *EMBO J.* **26**, 4138–4148 (2007).
236. Vlacil, A.-K., Schuett, J., Schieffer, B. & Grote, K. Variety matters: Diverse functions of monocyte subtypes in vascular inflammation and atherogenesis. *Vascul. Pharmacol.* **113**, 9–19 (2019).
237. Liao, X. *et al.* Kruppel-like factor 4 regulates macrophage polarization. *J. Clin. Invest.* **121**, 2736–2749 (2011).
238. Kim, H. The transcription factor MafB promotes anti-inflammatory M2 polarization and cholesterol efflux in macrophages. *Sci. Rep.* **7**, 7591 (2017).
239. Huo, Y. & Xia, L. P-selectin glycoprotein ligand-1 plays a crucial role in the selective recruitment of leukocytes into the atherosclerotic arterial wall. *Trends Cardiovasc. Med.* **19**, 140–145 (2009).
240. Sato, M. *et al.* MafB enhances efferocytosis in RAW264.7 macrophages by regulating Axl expression. *Immunobiology* **223**, 94–100 (2018).
241. Kimura, T. *et al.* Polarization of M2 macrophages requires Lamtor1 that integrates cytokine and amino-acid signals. *Nat commun* **7**, 13130 (2016).
242. Zaslona, Z., Scruggs, A. M., Peters-Golden, M. & Huang, S. K. Protein kinase A inhibition of macrophage maturation is accompanied by an increase in DNA methylation of the colony-stimulating factor 1 receptor gene. *Immunology* **149**, 225–237 (2016).
243. Poti, F. *et al.* Effect of sphingosine 1-phosphate (S1P) receptor agonists FTY720 and CYM5442 on atherosclerosis development in LDL receptor deficient (LDL-R(-)/(-)) mice. *Vascul. Pharmacol.* **57**, 56–64 (2012).
244. Abram, C. L., Roberge, G. L., Hu, Y. & Lowell, C. A. Comparative analysis of the efficiency and specificity of myeloid-Cre deleting strains using ROSA-EYFP reporter mice. *J. Immunol. Methods* **408**, 89–100 (2014).
245. Tacke, F. & Randolph, G. J. Migratory fate and differentiation of blood monocyte subsets. *Immunobiology* **211**, 609–618 (2006).
246. Rahman, K. *et al.* Inflammatory Ly6Chi monocytes and their conversion to M2 macrophages drive atherosclerosis regression. *J. Clin. Invest* **127**, 2904–2915 (2017).
247. Menezes, S. *et al.* The Heterogeneity of Ly6C(hi) Monocytes Controls Their Differentiation into iNOS(+) Macrophages or Monocyte-Derived Dendritic Cells. *Immunity* **45**, 1205–1218 (2016).
248. Hughes, J. E. *et al.* Sphingosine-1-phosphate induces an antiinflammatory phenotype in macrophages. *Circ. Res.* **102**, 950–958 (2008).
249. Park, S.-J. *et al.* Sphingosine 1-phosphate induced anti-atherogenic and atheroprotective M2 macrophage polarization through IL-4. *Cell Signal* **26**, 2249–2258 (2014).
250. Czimmerer, Z. *et al.* Extensive and functional overlap of the STAT6 and RXR cistromes in the active enhancer repertoire of human CD14+ monocyte derived differentiating macrophages. *Mol cell endocrinol* **471**, 63–74 (2018).
251. Pourcet, B. *et al.* LXRα regulates macrophage arginase 1 through PU.1 and interferon regulatory factor 8. *Circ. Res.* **109**, 492–501 (2011).
252. Qian, F. *et al.* The transcription factor PU.1 promotes alternative macrophage polarization and asthmatic airway inflammation. *J. Mol. Cell Biol.* **7**, 557–567 (2015).

253. Martinez, F. O. *et al.* Genetic programs expressed in resting and IL-4 alternatively activated mouse and human macrophages: similarities and differences. *Blood* **121**, e57-69 (2013).
254. Czimmerer, Z. *et al.* The Transcription Factor STAT6 Mediates Direct Repression of Inflammatory Enhancers and Limits Activation of Alternatively Polarized Macrophages. *Immunity* **48**, 75–90.e6 (2018).
255. Marciniak, A., Camp, S. M., Garcia, J. G. N. & Polt, R. An update on sphingosine-1-phosphate receptor 1 modulators. *Bioorganic Med. Chem. Lett.* **28**, 3585–3591 (2018).
256. Cannavo, A. *et al.* Sphingosine kinases and sphingosine 1-phosphate receptors: Signaling and actions in the cardiovascular system. *Front. Pharmacol.* **8**, 1–12 (2017).
257. Nagahashi, M. *et al.* Sphingosine-1-phosphate in chronic intestinal inflammation and cancer. *Adv. Biol. Regul.* **54**, 112–120 (2014).
258. Liang, J. *et al.* Sphingosine-1-phosphate links persistent STAT3 activation, chronic intestinal inflammation, and development of colitis-associated cancer. *Cancer Cell* **23**, 107–120 (2013).
259. Kang, K. *et al.* Adipocyte-derived Th2 cytokines and myeloid PPARdelta regulate macrophage polarization and insulin sensitivity. *Cell metab* **7**, 485–495 (2008).
260. Park, S. Y. *et al.* Suppression of PU.1-linked TLR4 expression by cilostazol with decrease of cytokine production in macrophages from patients with rheumatoid arthritis. *Br. J. Pharmacol.* **168**, 1401–1411 (2013).
261. Linton, M. F., Moslehi, J. J. & Babaev, V. R. Akt Signaling in Macrophage Polarization, Survival, and Atherosclerosis. *Int. J. Mol. Sci.* **20**, (2019).
262. Yancey, P. G. *et al.* Macrophage LRP-1 controls plaque cellularity by regulating efferocytosis and Akt activation. *Arterioscler. Thromb. Vasc. Biol.* **30**, 787–795 (2010).
263. Linton, M. F. *et al.* Macrophage Apoptosis and Efferocytosis in the Pathogenesis of Atherosclerosis. *Circ. J.* **80**, 2259–2268 (2016).